SECRET
SECURITY INFORMATION
AEC RESEARCH AND DEVELOPMENT REPORT

MARTIN MARIETTA ENERGY SYSTEMS LIBRARIES
3 4456 0360911 0

ORNL-1147
Reactors-Research and Power

DECLASSIFIED
CLASSIFICATION CHANGED TO:
BY AUTHORITY OF DOE/OC 12-8-87
BY: Ann Lackerman Date 8/1/88

RESEARCH AND DEVELOPMENT REPORT
LABORATORY RECORDS
1954

THE UNIT SHIELD EXPERIMENTS

AT THE

BULK SHIELDING FACILITY

CENTRAL RESEARCH LIBRARY
DOCUMENT COLLECTION
LIBRARY LOAN COPY
DO NOT TRANSFER TO ANOTHER PERSON
If you wish someone else to see this document, send in name with document and the library will arrange a loan.

OAK RIDGE NATIONAL LABORATORY
OPERATED BY
CARBIDE AND CARBON CHEMICALS COMPANY
A DIVISION OF UNION CARBIDE AND CARBON CORPORATION
UCC
POST OFFICE BOX P
OAK RIDGE, TENNESSEE

SECRET
SECURITY INFORMATION

SECRET
SECURITY INFORMATION

ORNL-1147

This document consists of 202 pages. No. 9 of 173 copies. Series A.

Contract No. W-7405, eng 26

PHYSICS DIVISION

THE UNIT SHIELD EXPERIMENTS AT THE BULK SHIELDING FACILITY

J. L. Meem
H. E. Hungerford

DATE ISSUED: APR 30 1952

OAK RIDGE NATIONAL LABORATORY
operated by
CARBIDE AND CARBON CHEMICALS COMPANY
A Division of Union Carbide and Carbon Corporation
Post Office Box P
Oak Ridge, Tennessee

RESTRICTED DATA

This document contains restricted data as defined in the Atomic Energy Act of 1946. Its transmittal or the disclosure of its contents in any manner to an unauthorized person is prohibited.

MARTIN MARIETTA ENERGY SYSTEMS LIBRARIES
3 4456 0360911 0

SECRET
SECURITY INFORMATION

INTERNAL DISTRIBUTION

1. G. T. Felbeck (C&CCC)
2-3. Chemistry Library
4. Physics Library
5. Biology Library
6. Health Physics Library
7. Metallurgy Library
8-9. Training School Library
10. Reactor Experimental Engineering Library
11-14. Central Files
15. C. E. Center
16. C. E. Larson
17. W. B. Humes (K-25)
18. W. D. Lavers (Y-12)
19. A. M. Weinberg
20. E. H. Taylor
21. A. H. Snell
22. F. C. VonderLage
23. R. C. Briant
24. J. A. Swartout
25. S. C. Lind
26. F. L. Steahly
27. A. Hollaender
28. M. T. Kelley
29. K. Z. Morgan
30. J. S. Felton
31. A. S. Householder
32. C. S. Harrill
33. C. E. Winters
34. D. S. Billington
35. J. H. Buck
36. D. W. Cardwell
37. E. M. King
38. E. O. Wollan
39. J. A. Lane
40. L. D. Roberts
41. R. N. Lyon
42. W. C. Koehler
43. W. K. Ergen
44. E. P. Blizard
45. M. E. Rose
46. P. M. Reyling
47. D. D. Cowen
48. G. H. Clewett
49. J. L. Meem
50. F. C. Maienschein
51. R. G. Cochran
52. H. E. Hungerford
53. L. B. Holland
54. E. B. Johnson
55. C. E. Clifford
56. H. L. F. Endlund
57. A. P. Fraas
58. F. K. McGowan
59. F. J. Muckenthaler
60. F. H. Murray
61. R. H. Ritchie
62. A. Simon
63. E. D. Shipley
64-81. Central Files (O.P.)

EXTERNAL DISTRIBUTION

82-91. Argonne National Laboratory
92. Armed Forces Special Weapons Project (Sandia)
93-100. Atomic Energy Commission, Washington
101. Battelle Memorial Institute
102-104. Brookhaven National Laboratory
105. Bureau of Ships
106-111. Carbide and Carbon Chemicals Company (Y-12 Area)
112. Chicago Patent Group
113. Chief of Naval Research
114-118. duPont Company
119-121. General Electric Company, Oak Ridge
122-125. General Electric Company, Richland
126. Hanford Operations Office
127-130. Idaho Operations Office
131. Iowa State College
132-135. Knolls Atomic Power Laboratory
136-138. Los Alamos
139. Massachusetts Institute of Technology (Kaufmann)
140-141. Mound Laboratory
142. National Advisory Committee for Aeronautics
143-144. New York Operations Office
145-146. North American Aviation, Inc.
147. Patent Branch, Washington
148. Savannah River Operations Office
149-150. University of California Radiation Laboratory
151-154. Westinghouse Electric Corporation
155-157. Wright Air Development Center
158-172. Technical Information Service, Oak Ridge
173. H. K. Ferguson Co.

RESTRICTED DATA
This document contains restricted data as defined in the Atomic Energy Act of 1946. Its transmittal or the disclosure of its contents in any manner to an unauthorized person is prohibited.

SECRET
SECURITY INFORMATION

SECRET

PERSONNEL PARTICIPATING IN THE UNIT SHIELD EXPERIMENTS

In Charge:	J. L. Meem
Design:	J. P. Gill*
	A. S. Kitzes*
	J. L. Meem

EXPERIMENTAL MEASUREMENTS:

Gamma Radiation Measurements:	L. H. Ballweg, USAF*
	J. P. Gill
	H. E. Hungerford
Thermal Neutrons, Foil Measurements:	E. B. Johnson
	M. P. Haydon
	G. M. McCammon
Thermal Neutrons, Counter Measurements:	H. E. Hungerford
Fast Neutron Dosimetry:	R. G. Cochran
	H. E. Hungerford
Analysis and Calculations:	H. E. Hungerford
	J. L. Meem
Consultant:	E. P. Blizard

Reactor Engineers:	Laboratory Technicians	Instrument Technicians
L. B. Holland	K. Honeycutt	A. Gilmore*
K. Henry	D. J. Kirby	J. Groover*
J. K. Leslie	R. M. Simmons	S. B. DeHart
J. L. Meem		J. Miniard

* No longer with group

RESTRICTED DATA

This document contains restricted data as defined in the Atomic Energy Act of 1946. Its transmittal or the disclosure of its contents in any manner to an unauthorized person is prohibited.

SUMMARY

Experiments have been performed on a unit shield mockup based on the Lid Tank optimization which was used by the ANP Shielding Board. Attenuation of neutrons and gamma rays from the Bulk Shielding Reactor through the shield have been measured. For a 200-megawatt reactor in the shape of a 3-ft right square cylinder and with a tolerance of 1 r/hr at the crew position 50 ft away, the Shielding Board predicted a shield weight of 134,000 lb. The present experiments give a weight of 127,600 lb for the shield. This is the minimum weight for the lead spacing used. An additional reduction in weight is indicated if more boron is added to the water and the lead spacing is reoptimized.

Included as appendices are data on the attenuation of neutrons and gamma rays through a water shield and an iron-water shield.

TABLE OF CONTENTS

		Page
I.	Description of the Experiments	11
	A. Introduction	11
	B. Procedure	12
	C. The Reactor	13
	D. Detectors	18
	1. Thermal Neutron Detectors	18
	2. Fast Neutron Detector	18
	3. Gamma Radiation Detectors	19
	E. Unit Shield Mockup	20
II.	Experimental Measurements on the Unit Shield	27
	A. General	27
	B. Results	29
	C. A Note on Power Normalization	32
III.	Calculations of Aircraft Reactor Shield Weight	37
	A. Shield Weight Calculations for Crew Tolerance of 1r/hr and 1/4r/hr.	37
	1. Specifications	37
	2. Leakage from the Aircraft Reactor	40
	3. Leakage from the Unit Shield Reactor	41
	4. The Dosage Unit, D	42
	5. The Allowed Dosage at Surface of Shield	43
	6. The Proper Thickness, t, of the Unit Shield	44
	7. Evaluation of Shield Weights	45

TABLE OF CONTENTS (Cont'd)

		Page
III.	Calculations of Aircraft Reactor Shield Weight (Cont'd)	
	B. Variation of Shield Weight with Shield Thickness	51
	C. Effects of Boration of Water Upon Shield Weights	53
	D. Errors in the Estimation of Shield Weights	58
IV.	Conclusions and Observations	60

APPENDICES

		Page
A.	Tables of Experimental Data for the Unit Shield Experiments	62
B.	The Effectiveness of the Boron Solution	81
C.	Power Calculations for the Unit Shield Reactor	88
D.	Calculations of Leakage from the Bulk Shielding Reactor	103
E.	Thermal Neutron Measurements in Water at the Bulk Shielding Facility	117
F.	Centerline Foil Measurements of Thermal Neutron Intensities in Water at the Bulk Shielding Facility	131
G.	Fast Neutron Dosimeter Measurements in Water at the Bulk Shielding Facility	139
H.	Gamma Ray Measurements in Water at the Bulk Shielding Facility	146
I.	Thermal Neutron Measurements behind an Iron-Water Shield at the Bulk Shielding Facility	151
J.	Fast Neutron Dosimeter Measurements behind an Iron-Water Shield at the Bulk Shielding Facility	161
K.	Gamma Ray Measurements behind an Iron-Water Shield at the Bulk Shielding Facility	166
L.	Preliminary Results on the Determination of Thermal Neutron Flux in Water	169
M.	A Proportional Counter Method of Measuring the Fast Neutron Dose	172
N.	Calibration of the Fast Neutron Dosimeter used at the Bulk Shielding Facility	180
O.	Fast Neutron Measurements at the Bulk Shielding Facility	188
P.	Center of Detection Calculations for Neutron Counters and Ion Chambers	199

LIST OF ILLUSTRATIONS

Fig.	Title	Page
1-1	Bulk Shielding Facility, Isometric Layout	13
1-2	Photograph of Pool, Showing Reactor and Instrument Bridges	14
1-3	Photograph of Assembled Reactor	16
1-4	Fuel Assembly Arrangement - Test #2 Critical Experiments - Bulk Shielding Facility Reactor	17
1-5	Unit Shield Mockup, Bulk Shielding Facility	21
1-6	Shield Details, Unit Shield Mockup	22
1-7	Photograph of the Nine Lead Hemispheres Before Mounting	23
1-8	Photograph of the Unit Shield Mockup Installed in Pool	25
2-1	Radial Traverses Around the Unit Shield, and the Shielding of Reactor with Concrete Blocks to Prevent Streaming	30
2-2	Radial Traverse Around the Unit Shield Mockup to Determine Amount of Gamma Streaming at Theoretical Edge of Shield	31
2-3	Gamma Radiation Intensity Curves for the Unit Shield Experiments	32
2-4	Thermal Neutron Flux Curves for the Unit Shield Experiments	33
2-5	Fast Neutron Dosage Curves for the Unit Shield Experiments	34
3-1	The Unit Shield Reactor	39
3-2	Experimental and Allowed Dosage Curves for the Unit Shield Mockup, Illustrating the Method of Obtaining the Required Shield Thicknesses	46

		Page
3-3	Dependence of the Weight of the Unit Shield upon its Thickness for Tolerance Radiation Dosages	52
3-4	Variation of Shield Weight with Boron Concentration (Based upon Shield No. 2)	57
B-1	γ-Intensities as a Function of Boron Concentration, Experimental Data	86
B-2	Gamma Flux Ratios as a Function of Boron Concentration - Extrapolation of Experimental Data	87
C-1	Power Distribution Through the Bulk Shielding Reactor	101
C-2	Thermal Neutron Flux Distribution Through the Bulk Shielding Reactor	102
D-1	North Face of Reactor, with Dimensions and Positions Marked	105
D-2	Comparison of Thermal Neutron Traverses Along X-Axis in Magnitude and Shape for the Water Reflected and Unit Shield Reactors	107
D-3	Illustration of the Method of Obtaining the Power Function P(Z) for Each Row of Fuel Elements for the Leakage Calculations	109
D-4	Power Per Unit Distance, P(Z), in Reactor, Watts/cm (Distribution by Rows)	110
E-1	Bulk Shielding Facility Method of Obtaining Centerline Measurements	119
E-2	Bulk Shielding Facility Method of Finding Z Position of Counters	122
E-3	Thermal Neutron Centerline Measurements in 100% Water	123

		Page
F-1	Bulk Shielding Facility Foil Data - Experiment 1, Centerline Measurements of Saturated Activities of Foils - 100% Water	137
F-2	Bulk Shielding Facility Foil Data - Experiment 1, Neutron Centerline Measurements, 100% Water	138
G-1	Experiment 1 - Fast Neutron Dosimeter Centerline Measurements	145
H-1	Gamma Attenuation in 100% Water, Experiment 1	150
I-I	Bulk Shielding Facility Iron Shield Arrangement for Experiment 2	159
I-2	Experiment 2 - Thermal Neutron Centerline Measurements Behind 17-in Iron Shield	160
J-1	Experiment 2 - Fast Neutron Dosage Measurements Behind 17-in Iron Shield	165
K-1	Experiment 2 - Iron-Water Test, Centerline Gamma Radiation Measurements	168
M-1	Sketch of Dosimeter Counter	175
M-2	Block Diagram of Apparatus for Dosimeter	176
M-3a	Relative Counts per Unit Flux versus Integral Pulse Height Settings	178
M-3b	Relative Dose per Unit Flux versus Neutron Energy	178
N-1	Bulk Shielding Facility Linearity Test of Integrator, Low Counting Rates	183
N-1a	Bulk Shielding Facility Linearity Test of Integrator, High Counting Rates	184
N-2	Air Calibration for Dosimeter Using a Po-Be Source	185
O-1	Bulk Shielding Facility Fast Neutron Data	196
O-2	U^{238} Fission Counter Voltage Dependence	197
O-3	U^{238} Counter Calibration in Large Pool	198

I. DESCRIPTION OF THE EXPERIMENTS

A. Introduction

For the better part of the year 1950, the effort of the group operating the Lid Tank at the X-10 pile was devoted to measuring materials suitable for a minimum weight shield for an aircraft reactor. The trend of study was toward determining the optimum configuration of a "unit shield." The unit shield is defined as a one-piece shield which not only protects the crew of an airplane during flight but also reduces the radiation from the reactor sufficiently to enable a maintenance crew to service the airplane on the ground within a short time after the airplane has landed and the reactor has been shut down.

The first approach to such a shield is one in which both neutron and gamma radiations are shielded equally in all directions. The "ideal" unit shield is then a spherical shield around a spherical reactor. The departure from this ideal shield to a shield around a reactor in the form of a right square cylinder will not be very radical. Therefore for simplicity the work at the Lid Tank was directed toward developing the optimum configuration for an ideal unit shield. The results of the Lid Tank study to determine the optimum spacing of the lead in a laminated lead-water shield were used by the ANP Shielding Board[1] as a basis for the design of a unit shield.

---

(1) A list of references will be found at the end of this report.

Since the weight of the shield is of extreme importance in proving the feasibility of the nuclear powered airplane, it was decided that an independent measurement on a mockup of a unit shield should be made with the Bulk Shielding Reactor. The mockup should be spherical and should utilize the optimum configuration as determined by the Lid Tank.

This report describes the experiments made upon a unit shield mockup and contains an estimate of the weight of the unit shield for a 200-megawatt aircraft reactor 3.8 ft in diameter, using the experimental data obtained.

B. Procedure

The Bulk Shielding Facility has been described by Breazeale.[2] A reactor is suspended in a large pool of water as shown schematically in Fig. 1-1. Figure 1-2 is a photograph of the pool showing the reactor and instrument bridges. The procedure was to erect a shielding sample next to the reactor and measure the attenuation of neutron and gamma rays with suitable detectors behind the shield. Two preliminary experiments were performed prior to the measurement of the unit shield. The first was the determination of the attenuation of neutrons and gamma rays through the water in the pool, and the second was a measurement through water and about 17 in of iron. The results of Experiments 1 and 2 have been described in preliminary memoranda but have not received wide publication. For this reason and also because the data are interesting as a basis of comparison with the present experiments, the memoranda are included in Appendices E through K.

SECRET

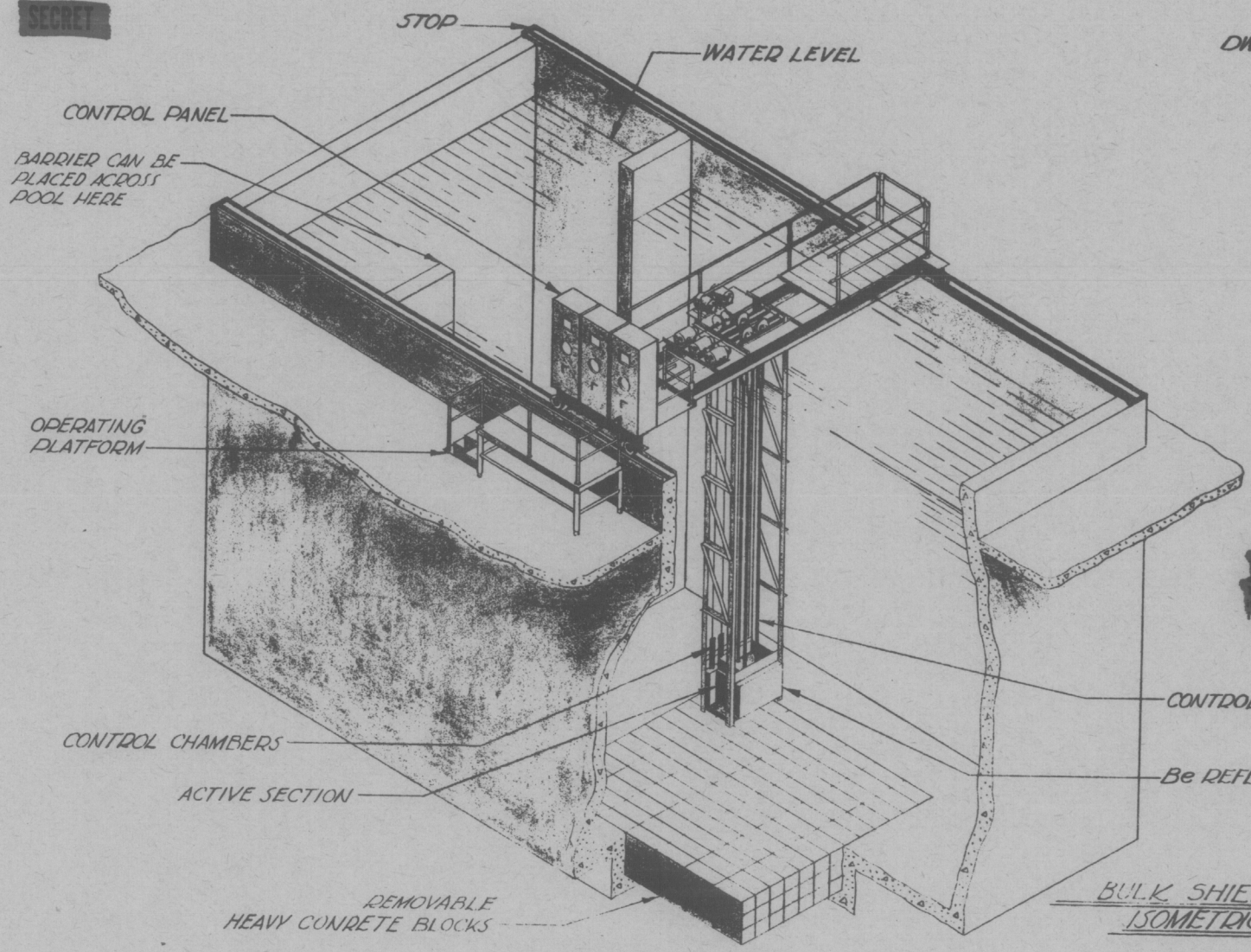

DWG. #8332

RESTRICTED DATA

This document contains restricted data as defined in the Atomic Energy Act of 1946. Its transmittal or the disclosure of its contents in any manner to an unauthorized person is prohibited.

SECRET

BULK SHIELDING FACILITY
ISOMETRIC LAYOUT

NOT TO SCALE

FIG. 1-1

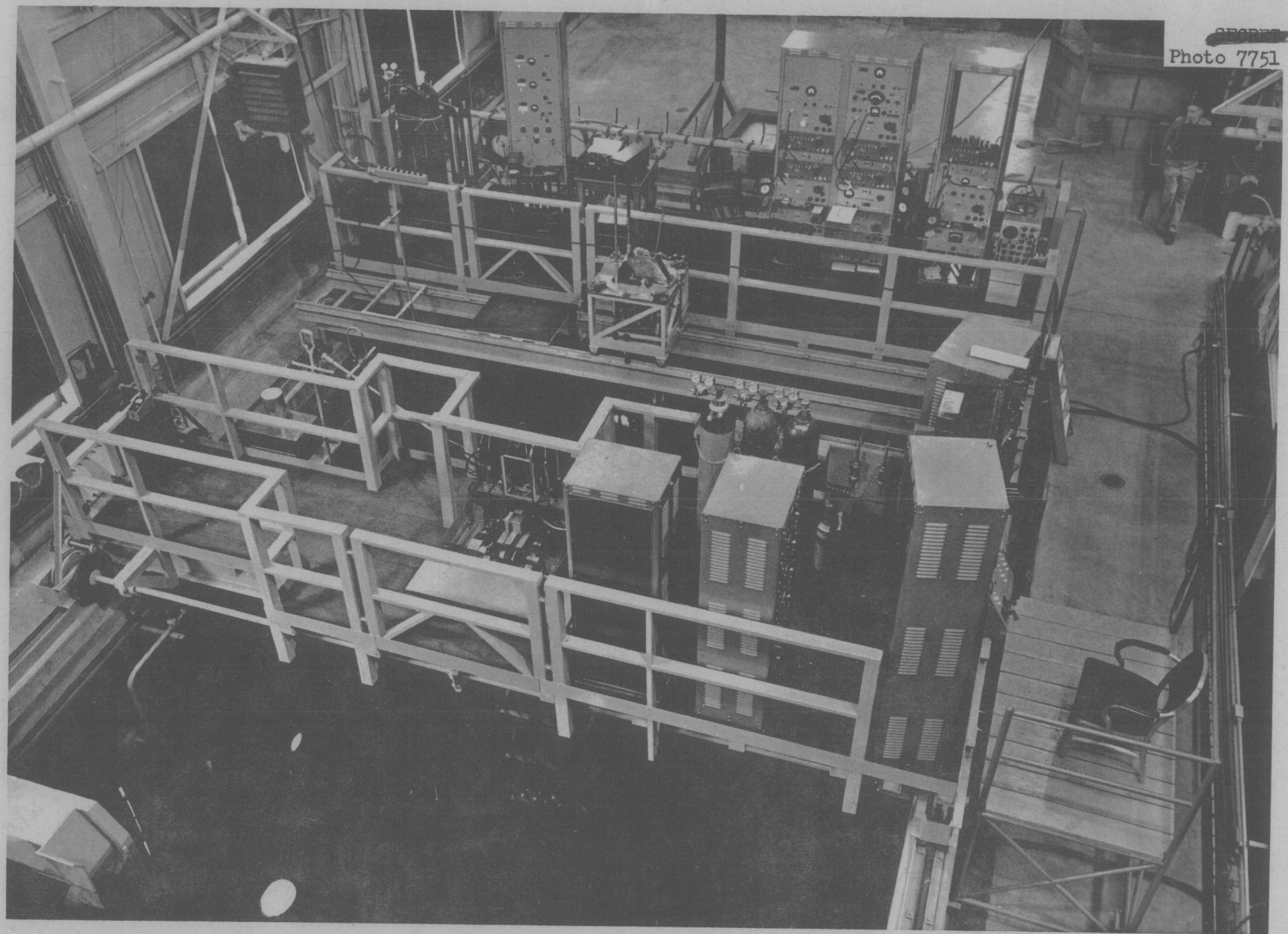

Fig. 1-2 Photograph of Pool, Showing Reactor and Instrument Bridges

C. The Reactor

Details of the construction and operation of the Bulk Shielding Reactor are given in Ref. 1. The reactor was made up of 25 fuel elements, each approximately 36 in. high and 3 by 3 in. in cross section. Only the central 24 in. of each fuel element contained fissionable material. The total critical mass was 3.2 kg of U^{235}. Figure 1-3 is a photograph of the assembled reactor and Fig. 1-4 is a plan view of the loading pattern. Since the fuel elements can be moved around in the grid plate, the reactor can be made critical with various loadings. In the loading used in these experiments, the reactor was reflected on all sides but one by the water of the pool (see Fig. 1-4). On the rear side away from the face from which shielding measurements were made, there was a beryllium oxide reflector on which the control chambers for the reactor were mounted.

A determination of the power distribution of the reactor from measurements of the neutron flux distribution has been made by Meem and Johnson.(3) In the present shield test it was found that placing the shield mockup next to the face of the reactor altered the power distribution in the front row of fuel elements relative to the rest of the reactor. A correction for this effect is described later.

For the measurements described in this report the power of the reactor was varied at will so as to provide a desirable counting rate for the detector in use during a particular run. All measurements were then normalized to a power of 1 watt. It was found that a given power setting of the reactor could be repeated within a precision of a few per cent. The absolute value of the power of the reactor is discussed in Ref. 3.

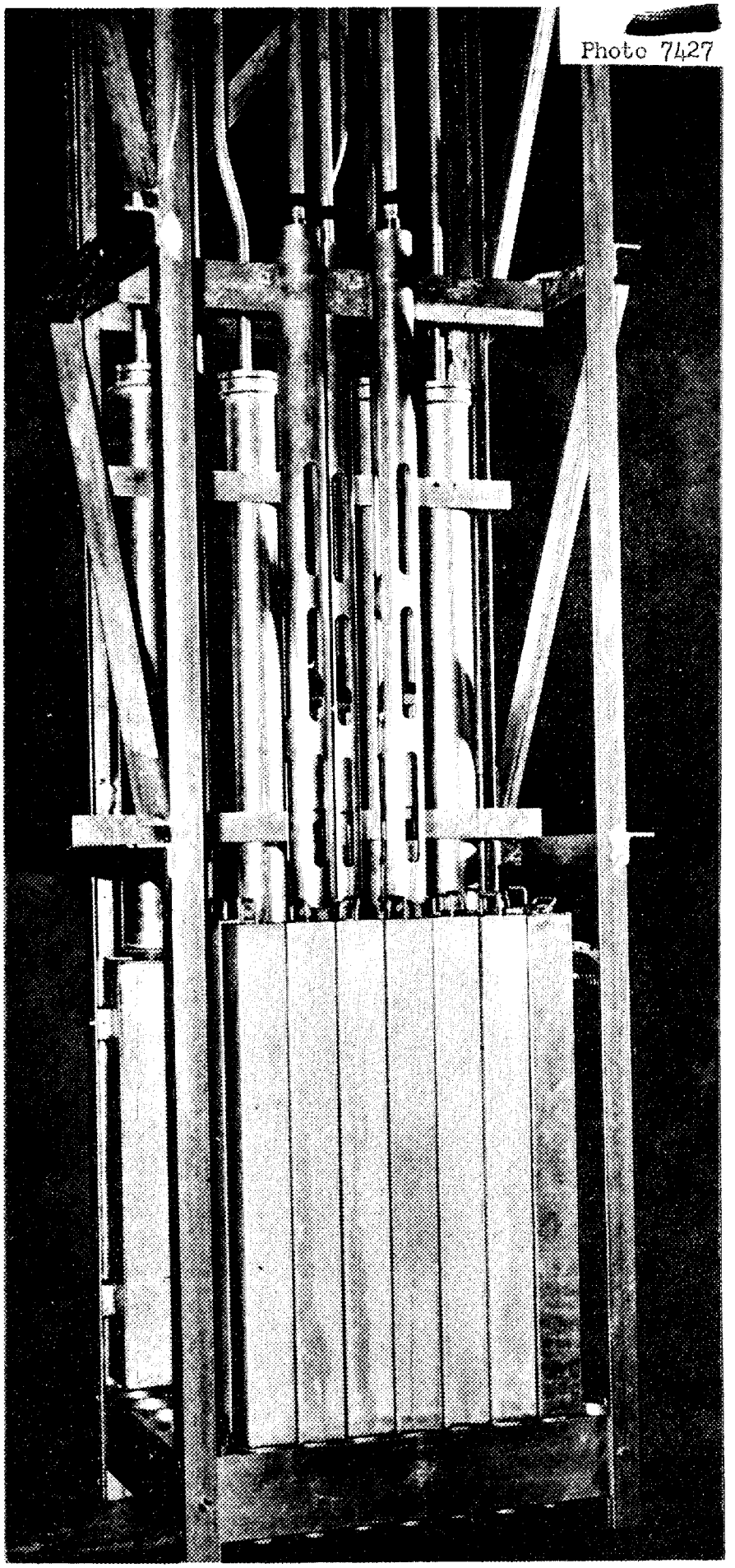

Fig. 1-3 Photograph of Assembled Reactor

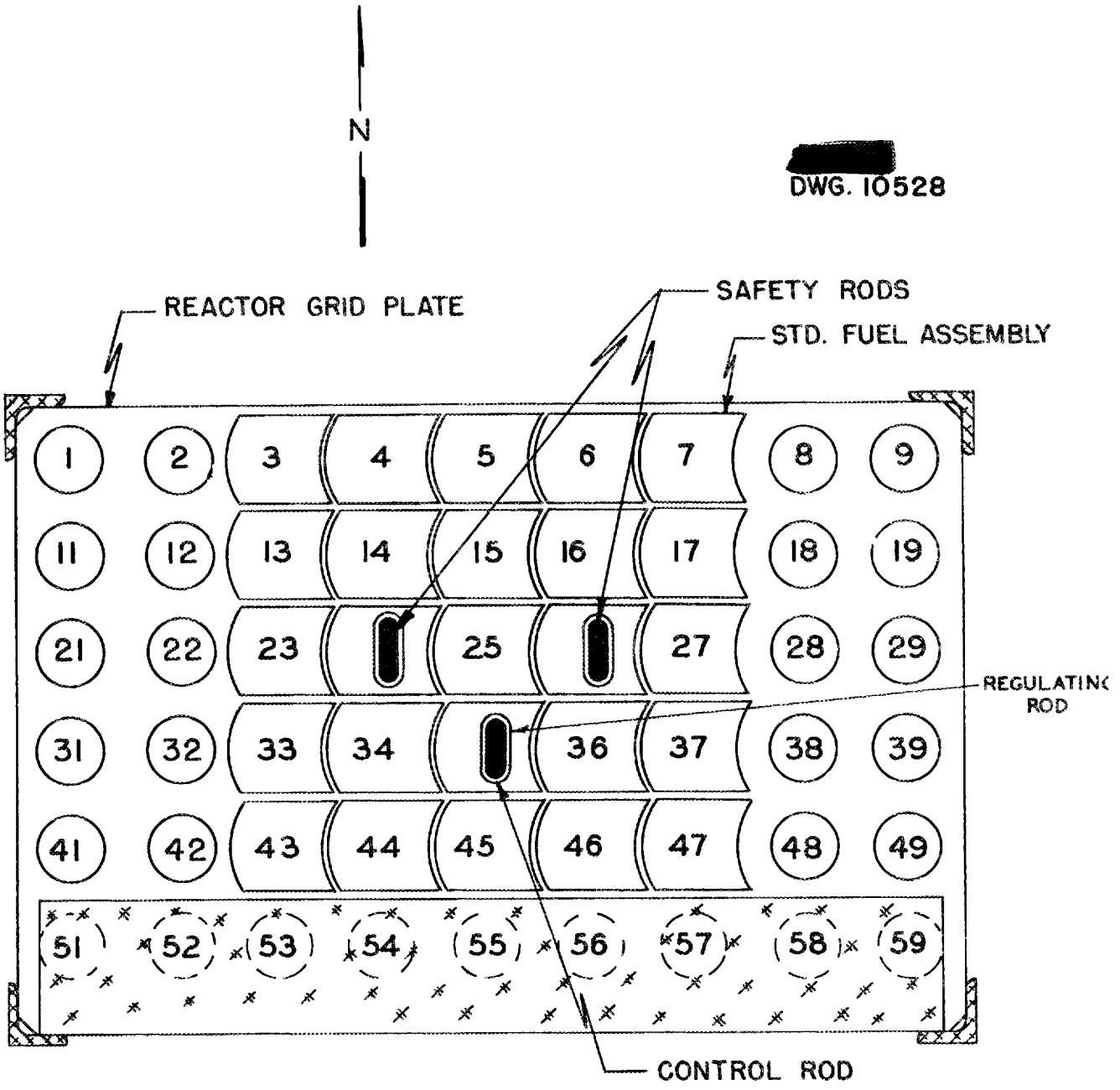

NOTE: BeO REFLECTOR ONE SIDE
WATER REFLECTOR THREE SIDES

FIG. 1-4

FUEL ASSEMBLY ARRANGEMENT – TEST No. 2

CRITICAL EXPERIMENTS – BULK SHIELDING FACILITY REACTOR

D. Detectors

Three types of measurements were made in these experiments: (1) thermal-neutron flux, (2) fast-neutron dosage, and (3) gamma-ray dosage.

1. Thermal-Neutron Detectors

Both U^{235} fission chambers and boron trifluoride counters were used for thermal-neutron measurements as described in Appendix E. The method of locating a counter with respect to the reactor is also described in this appendix. It was possible to reproduce the position of a detector within a millimeter. To obtain the absolute value of the thermal-neutron flux as measured with the above counters, some of the experimental points were also measured with indium foils as described in Appendix F. All measurements with the counters were then normalized against the foil measurements. Because the calibration of the foils was done in a graphite pile and the exposures were made in water, it was necessary to increase the water values by 22%. The basis for this correction is described in Appendix L.

2. Fast-Neutron Detectors

The procedure for measuring fast-neutron dosage is outlined in Appendix G. A fast-neutron dosimeter of the integrating type, which simulates the dosage effect of fast neutrons, has been developed by Hurst (see Appendix M). The calibration of the instrument used in these experiments is described in Appendix N. It was determined that the probable error of the measurements with the dosimeter was within $\pm 30\%$.

Fast neutrons were measured by two other independent means in water as a check on the measurements obtained by the dosimeter. The first set of measurements was made with a U^{238} fast fission counter, and the other by using pressed sulfur as a threshold detector. The results of these measurements are described in Appendix O.

3. Gamma-Radiation Detectors

Gamma-ray dosage was measured with graphite-wall ionization chambers. One of these chambers was designed and constructed very carefully and was used as a standard chamber. When this chamber was used to measure the gamma rays from a radium source obtained from the National Bureau of Standards, the experimental results agreed with the calculated values within 1%. This accuracy was better than the probable error of the constants available for the calculation. All other ionization chambers were then calibrated against the standard chamber. The precision of the gamma-ray measurements listed in this report should be well within 5%, both in reproducibility and absolute magnitude. The construction and calibration of the ionization chambers has been described in detail by Ballweg and Meem.(4)

In making shielding measurements under water it becomes important to determine the center of detection of the instrument used. For a counter on the order of 10 to 20 centimeters in diameter the radiation received at the front of the counter is greater than that at the rear. The calculation of the centers of detection for the various instruments was done by Hungerford and is included in Appendix O.

E. Unit Shield Mockup

Figure 1-5 shows the unit shield mockup installed in the pool and Fig. 1-6 shows the important dimensions. The shield is a mockup of that described in the Shielding Board Report. The mockup consists of the following items in the order listed: 1 in. of iron a 7-in. air space, 2 in. of iron, and nine 1-in. layers of lead separated by varying thicknesses of borated water. The purpose of the air void is to simulate a spherical reactor. Table 1-1 gives the detailed specifications.

The 2-in. steel hemisphere, a mild steel casting, was welded to the 1-3/4-in. steel supporting plate and tested under 25 psi for air leaks. The lead hemispheres were fabricated by forming 1-in. sheet lead into "orange peel" sections over wooden forms and then burning the sections together. A photograph of these sections before mounting is shown in Fig. 1-7. These hemispherical shells were fastened to the supporting plate with 3/8-in. lag screws. After each lead shell was secured in place, 1-in. holes were drilled in the top and bottom of the shell to permit filling with borated water. The dashed curve in Fig. 1-6 denotes the outer boundary of the water layer of the ideal spherical shield. This imaginary surface was 27 in. beyond the last lead layer.

As shown in the sketches, the hemispherical lead shells were mounted inside a large aluminum tank filled with borated water. On the outside of this tank was the normal water of the pool. It can be shown that beyond about 12 in. outside the last lead layer the gamma production from neutrons in the water becomes negligible; therefore boration of the water was unnecessary in the outer regions of the shield. The tank was

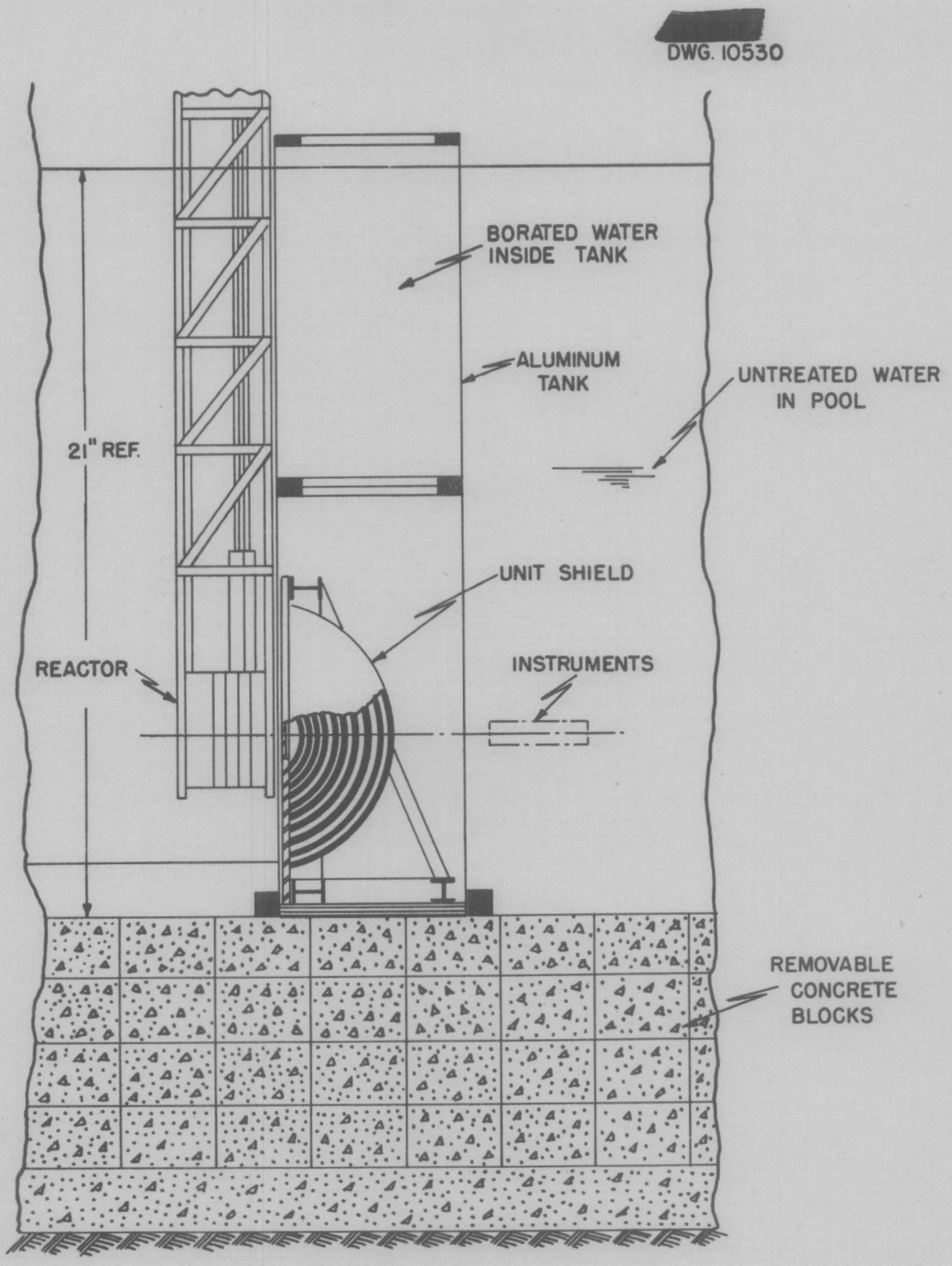

FIG. 1-5
UNIT SHIELD MOCK-UP
BULK SHIELDING FACILITY

SECRET

DWG. 10531

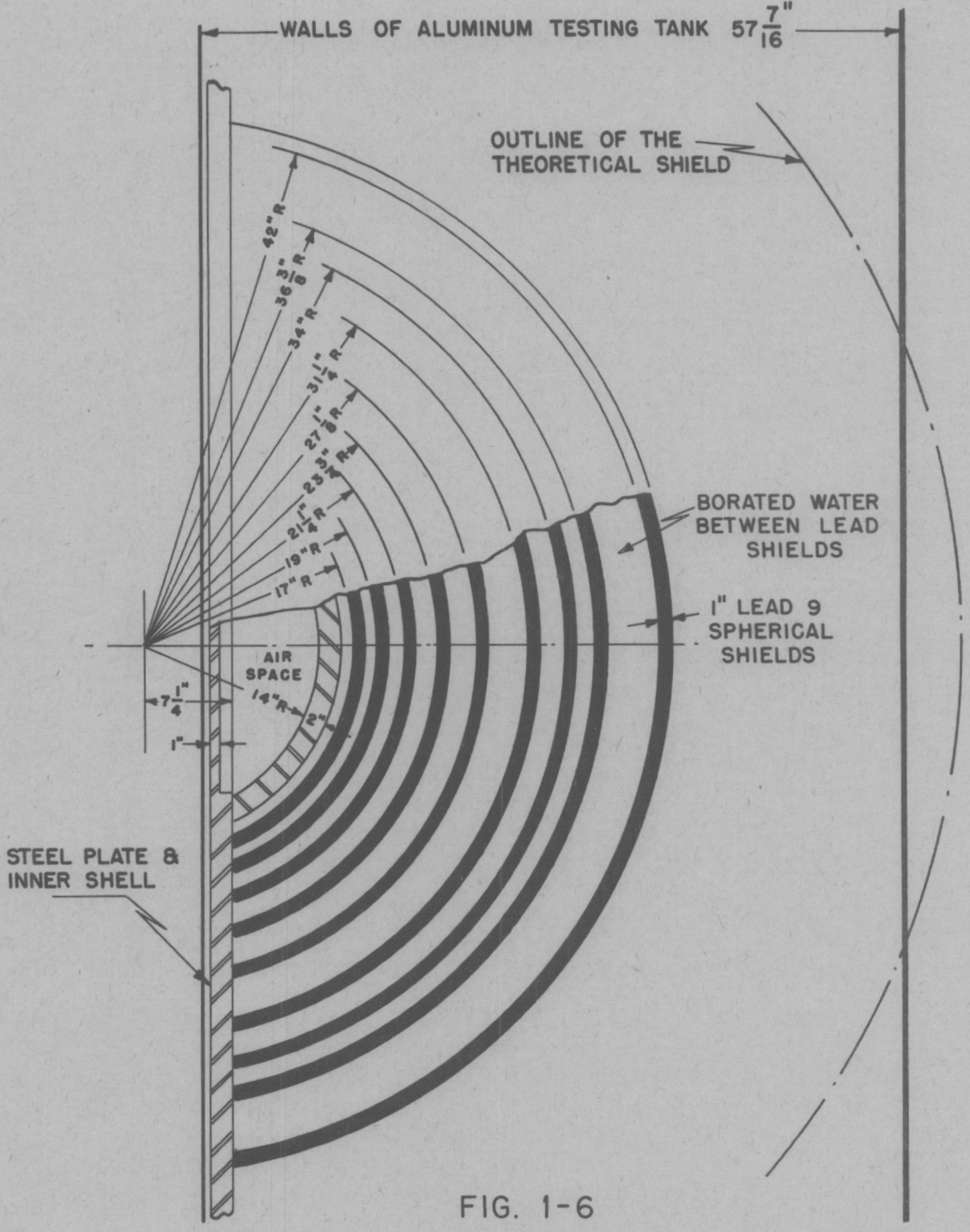

FIG. 1-6

SHIELD DETAILS

UNIT SHIELD MOCK UP BULK SHIELDING FACILITY

Fig. 1-7 Photograph of the Nine Lead Hemispheres Before Mounting

constructed so that the borated water extended 20 in. beyond the last lead layer. The final 7 in. of water for the shield was just the pool water itself, and the shield boundary was merely an imaginary surface in the pool.

Figure 1-8 is a photograph of the assembled mockup before installation of the aluminum tank.

Fig. 1-8 Photograph of the Unit Shield Mockup Installed in Pool

TABLE 1-1

The Unit Shield Mockup

Composition as Designed for the Unit Shield Experiments at

The Bulk Shielding Facility

Layer	Material	Inner Radius (in.)	Inner Radius (cm.)	Thickness (cm.)
1*	Iron	13	33.0	7.62
3	Lead	17	43.2	2.54
5	Lead	19	48.3	2.54
7	Lead	21-1/4	54.0	2.54
9	Lead	23-3/4	60.3	2.54
11	Lead	27-1/8	68.9	2.54
13	Lead	31-1/4	79.4	2.54
15	Lead	34	86.4	2.54
17	Lead	36-3/8	92.4	2.54
19	Lead	42	106.7	2.54

* The iron layer was divided into a 1-in. flat layer and a 2-in. spherical layer of 14 in. inner radius, as shown in Fig. 2-6, to form an airspace. The intervening layers consisted of water or borated water.

II. EXPERIMENTAL MEASUREMENTS ON THE UNIT SHIELD

A. General

The measurements behind the unit shield mockup comprised two separate experiments, designated as Bulk Shielding Facility Experiments 3 and 4. Experiment 3 consisted of measurements in pure water behind the lead hemispheres along the centerline, with water filling the spaces between the hemispheres. For Experiment 4 the shield was encased in an aluminum tank as shown in Fig. 2-5. The tank was filled with water of various boron concentrations, which permeated the spaces between the hemispheres. The presence of the tank made it impossible for instruments to approach the last lead shell closer than 48.6 cm.

With the exception of two gamma-ray traverses around the periphery of the shield, all measurements for Experiments 3 and 4 were made along the reactor centerline. Table 2-1 summarizes the type of measurements made and detectors used in the experiments.

TABLE 2-1

Detectors Used for Various Measurements in

Experiments 3 and 4

TYPE OF MEASUREMENT	DETECTOR USED	
	EXPT. 3	EXPT. 4
Thermal-neutron flux	Indium foils	
	3-in. fission counter	3-in. fission counter
	8-in. BF_3 counter	8-in. BF_3 counter
	12-in BF_3 double chamber counter	12-in BF_3 double chamber counter
		12-in BF_3 single chamber counter
Fast-neutron dosage	Fast-neutron dosimeter	Fast-neutron dosimeter
Gamma-ray dosage	Standard 50-cc 10^{12} ionization chamber	
	900-cc 10^{10} ionization chamber	
	900-cc 10^{12} ionization chamber	900-cc 10^{12} ionization chamber
		G-M counter

B. Results

Before making the centerline measurements it was necessary to determine whether streaming from around the sides of the shield would affect these measurements. Accordingly, a horizontal gamma-ray traverse with an ion chamber was made around the shield in unborated water at a radius of 175 cm, as shown in Fig. 2-1. The results of this traverse indicated that there was some streaming at large angles. A concrete block shield was then erected around the reactor (see Fig. 2-1) and another traverse was made. The traverses showed that within an angle of 30° on each side of the centerline there was negligible effect from streaming. These traverses are shown in Fig. 2-2 plotted from the data of Table I in Appendix A.

The centerline measurements in unborated water (Experiment 3) are shown in Figs. 2-3, 2-4, and 2-5. The data are given in Tables 2, 3, and 4 of Appendix A. The data of Experiment 3 have been normalized to a power of 1 watt as determined from the power calibration of the water-reflected reactor.[3]

After installation of the aluminum tank around the shield, it was filled with borated water of various concentrations (Experiment 4), and gamma-ray centerline measurements were made behind the tank. As shown in Fig. 2-3, the boron concentrations tested were 0.0, 0.1, 0.2, and 0.4% by weight. It was difficult to dissolve additional B_2O_3 in the water beyond a boron concentration of 0.4%; therefore heavier concentrations were not tested. Thermal-neutron and dosimeter measurements were made at the 0.4% concentration as shown in Figs. 2-4 and 2-5.

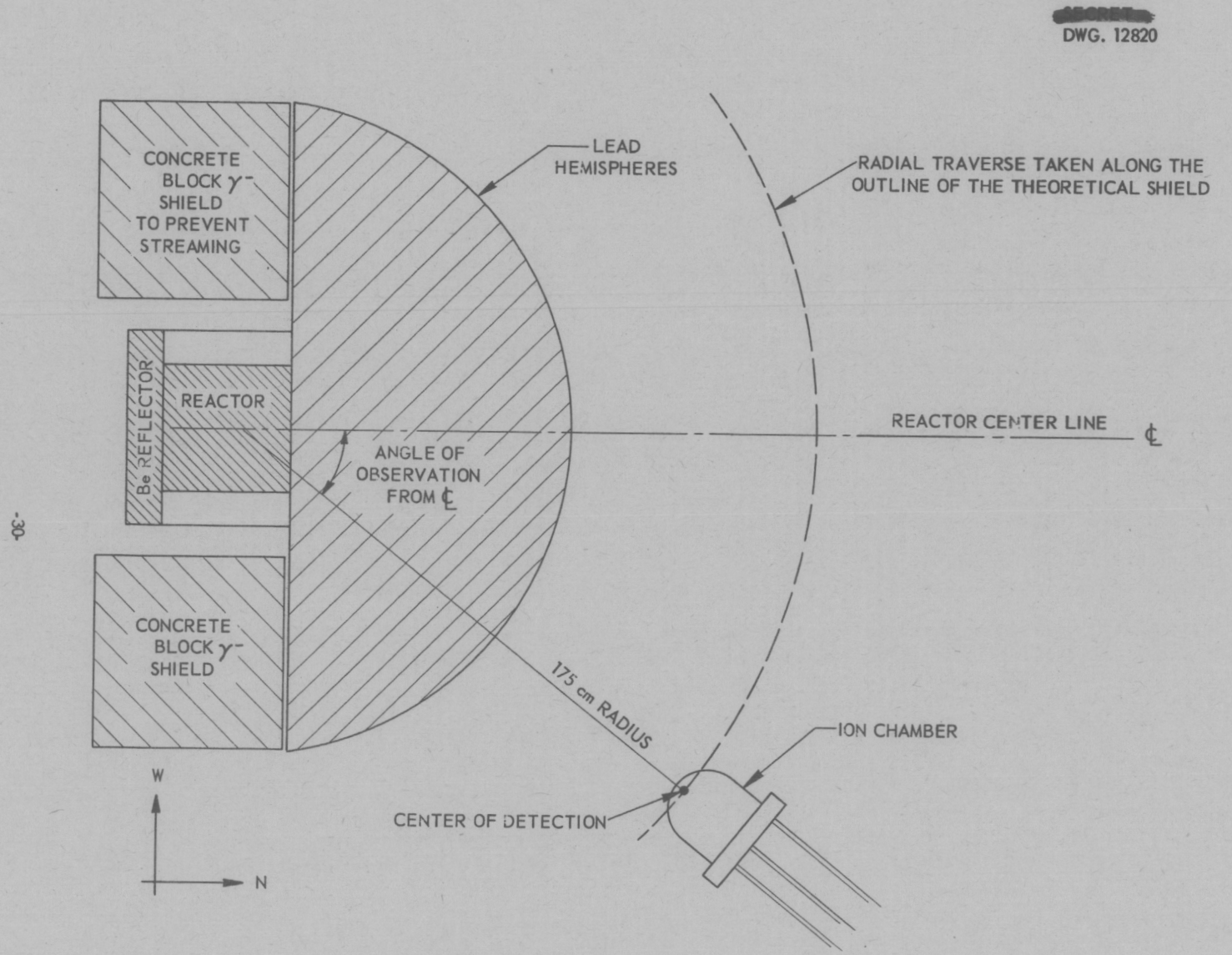

FIG. 2-1 BULK SHIELDING FACILITY – ILLUSTRATING THE RADIAL TRAVERSES AROUND THE UNIT SHIELD AND THE SHIELDING OF REACTOR WITH CONCRETE BLOCKS, TO PREVENT STREAMING

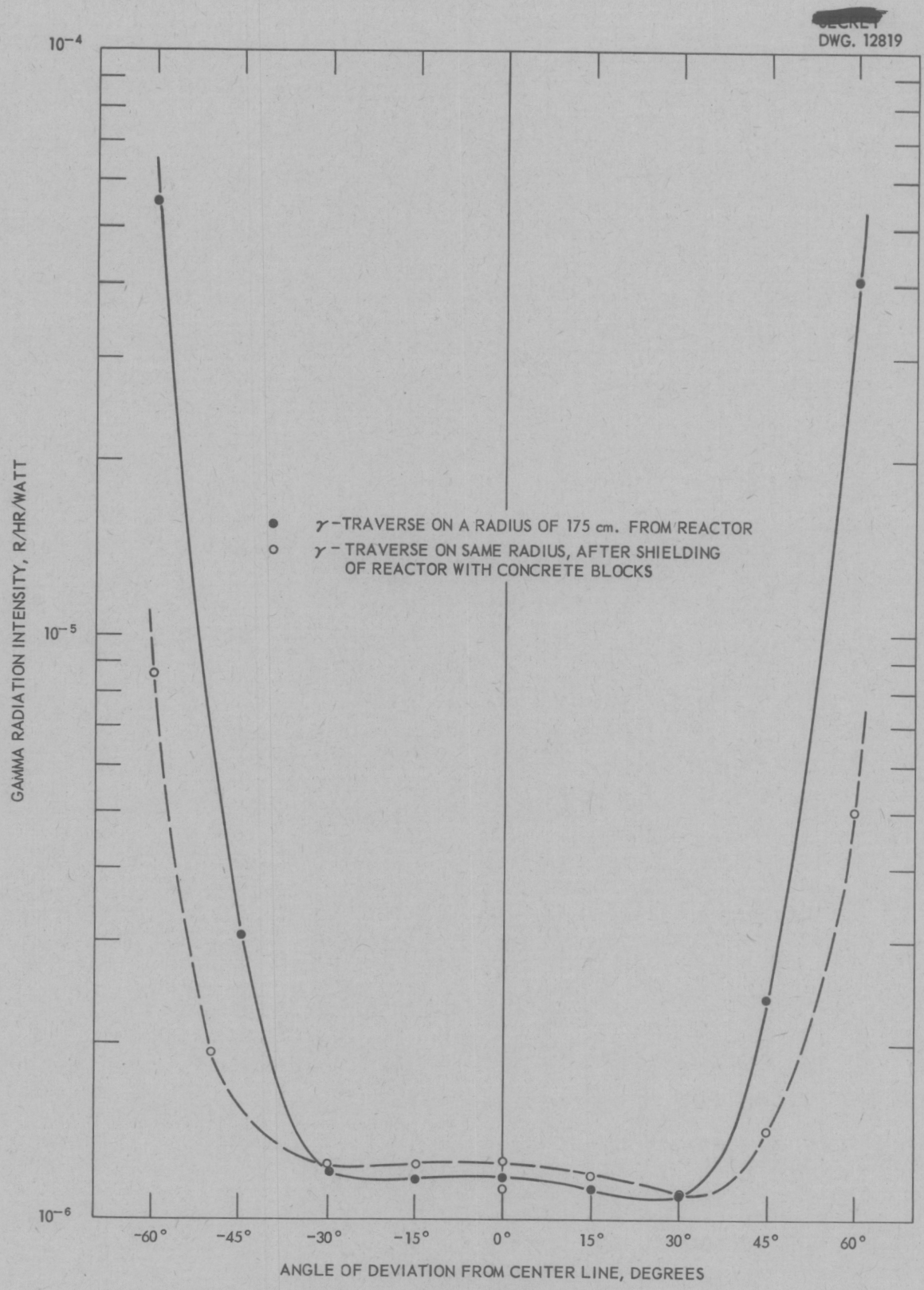

FIG. 2-2 BULK SHIELDING FACILITY – RADIAL TRAVERSE AROUND THE UNIT SHIELD MOCK-UP TO DETERMINE AMOUNT OF GAMMA STREAMING AT THEORETICAL EDGE OF SHIELD

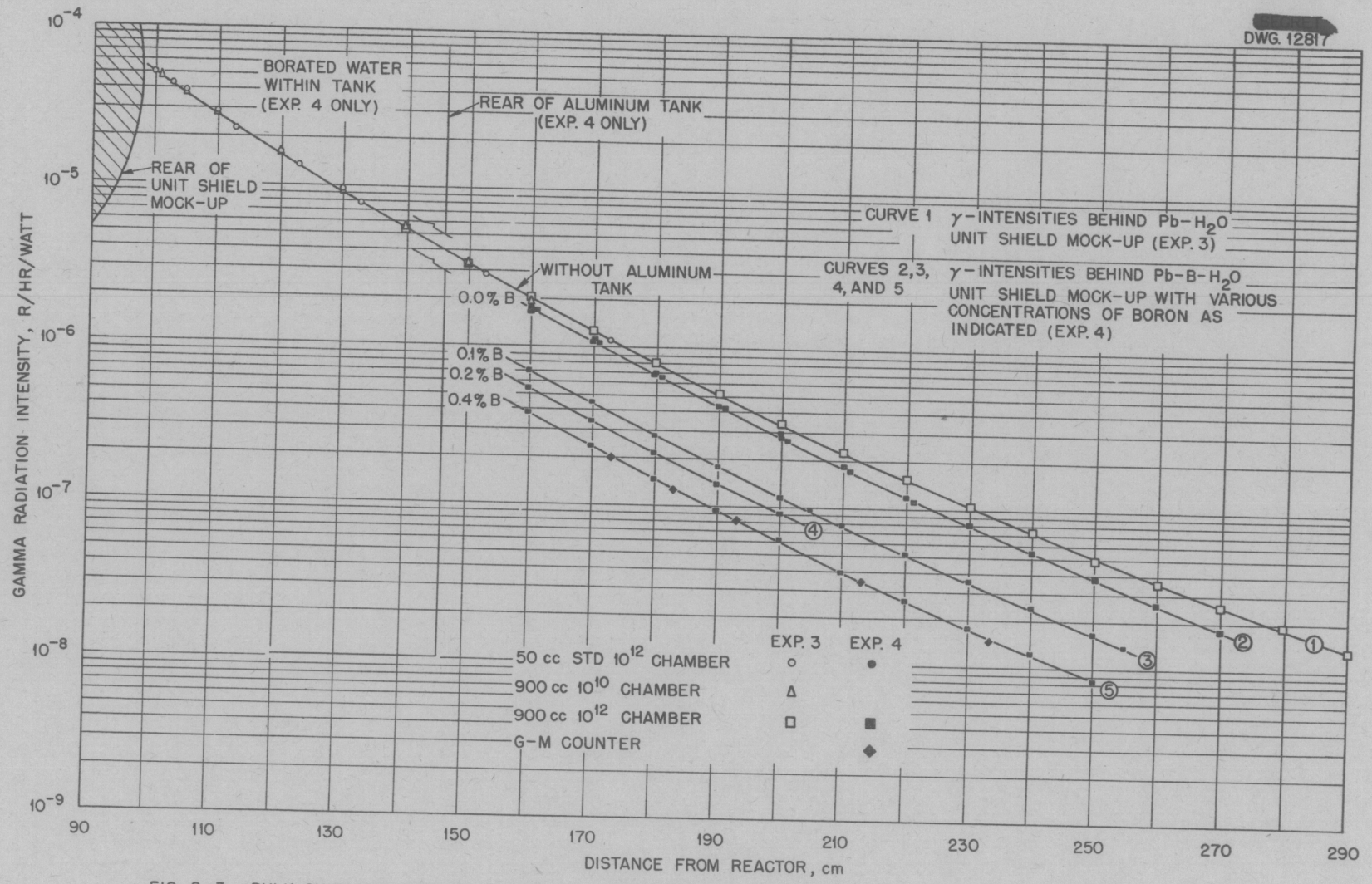

FIG. 2-3 BULK SHIELDING FACILITY- GAMMA RADIATION INTENSITY CURVES FOR THE UNIT SHIELD EXPERIMENTS

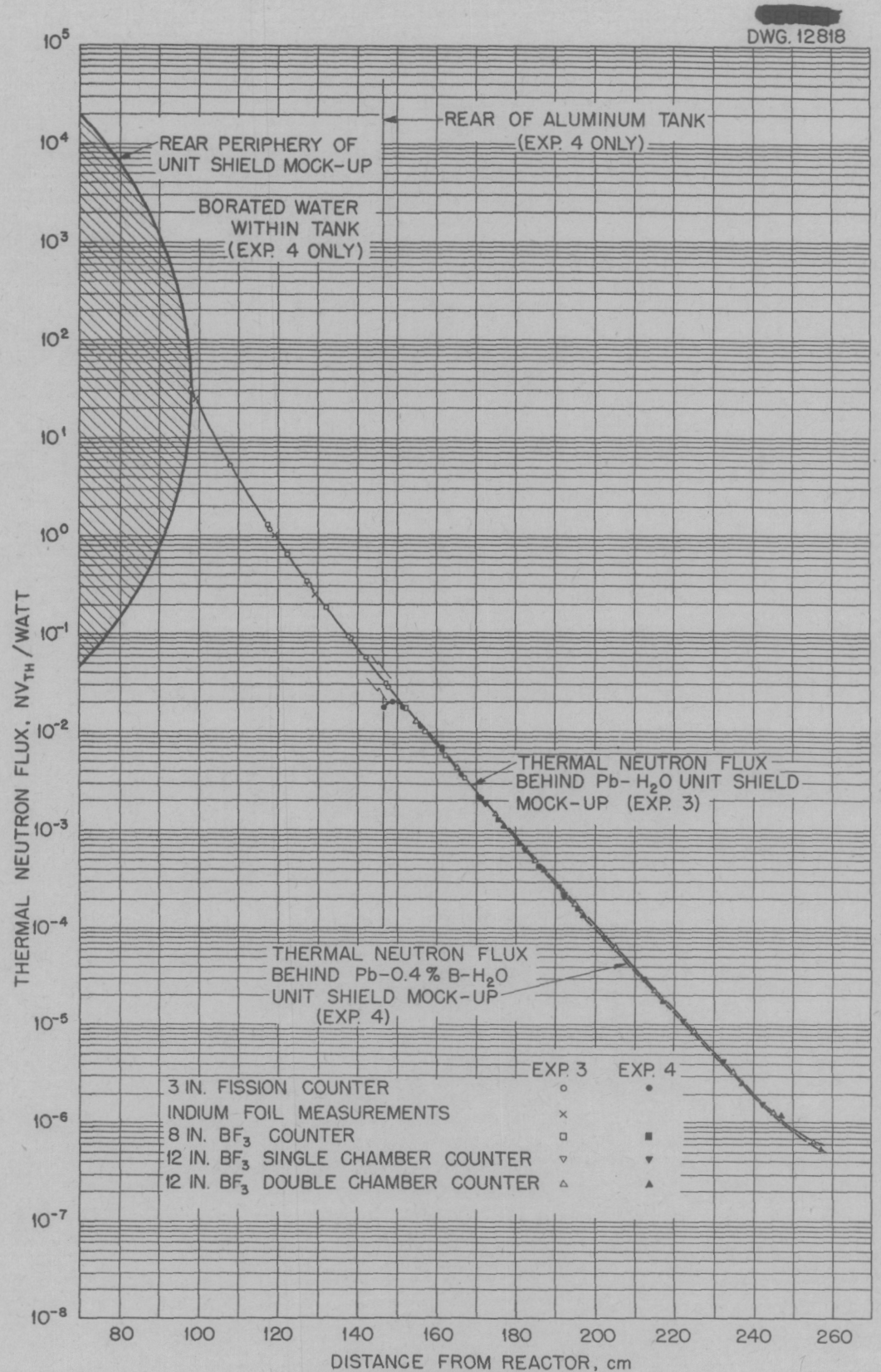

FIG. 2-4 BULK SHIELDING FACILITY- THERMAL NEUTRON FLUX CURVES FOR THE UNIT SHIELD EXPERIMENTS

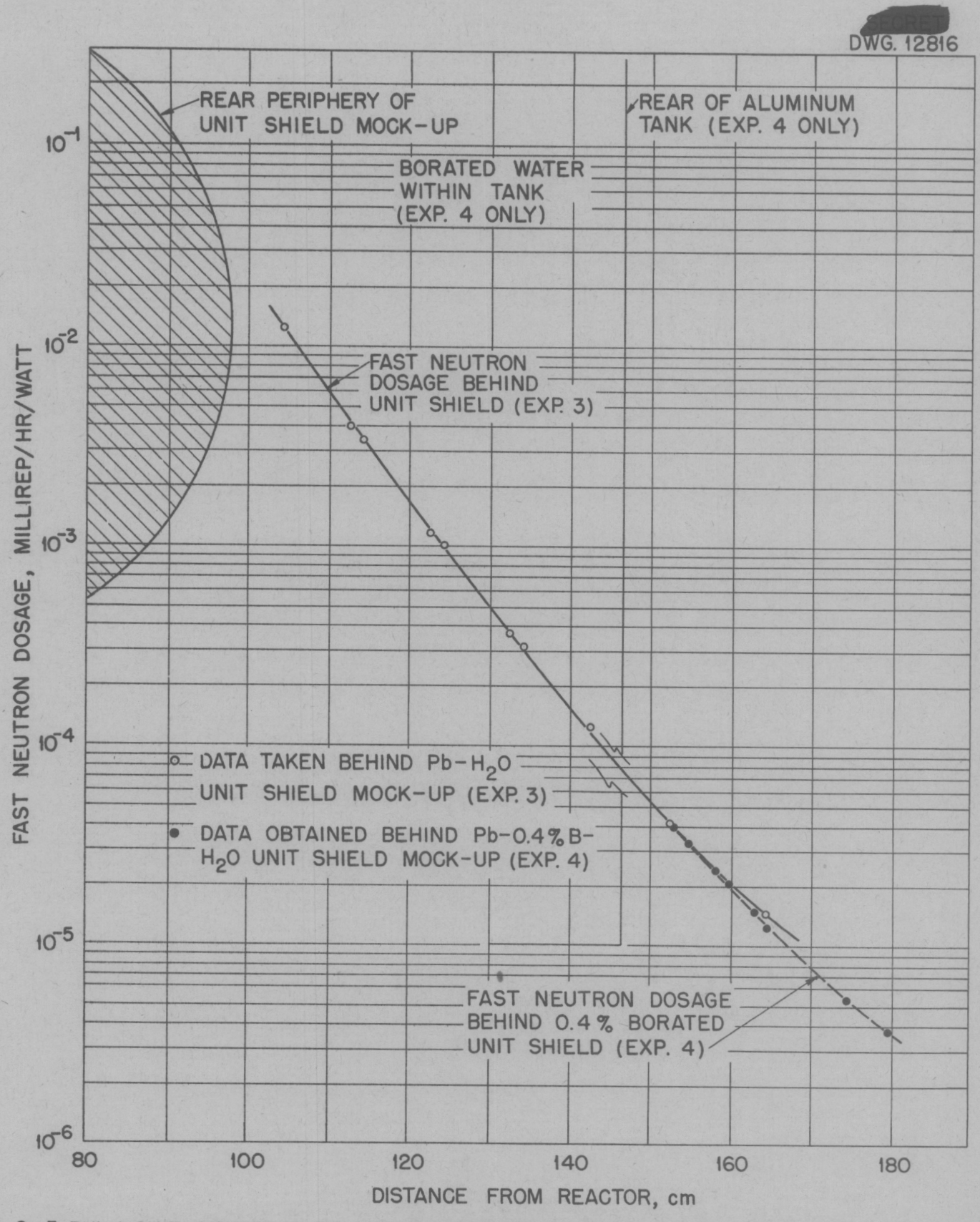

FIG. 2-5 BULK SHIELDING FACILITY – FAST NEUTRON DOSAGE CURVES FOR THE UNIT SHIELD EXPERIMENTS

The data obtained in Experiment 4 were normalized to a power of 1 watt according to the power calibration of the unit shield reactor as described in Appendix C. The data are tabulated in Appendix A, Tables 5, 6, and 7.

A more complete discussion of the boron problem is given in Appendix B.

C. A Note on Power Normalization

The nominal power of "1 watt" has been shown to be*

1. 0.738 watts for the water-reflected reactor, and

2. 0.715 watts for the reactor in place against the borated-water shield.

A new determination of the power of the reactor in its position against the borated-water shield became necessary when discrepancies in the data between Experiments 3 and 4 became evident. As noted in Appendix C, the new power determination gave a power about 3% lower for the reactor in its position against the borated shield than the power determined previously. Calculations of the leakage, as shown in Appendix D, in the two cases showed a lowering of the leakage of high-energy neutrons by approximately 7-1/2% when the reactor was against the borated-water shield.

When the appropriate power corrections were applied the discrepancies were accounted for. To illustrate, the 7% discrepancy between the thermal-neutron curves of Experiments 3 and 4 can be accounted for by the difference in the leakage values for the two reactors.

Since there seemed to be no effect upon the reactor due to the presence of the shield itself during Experiment 3, the original power correction factors were assumed to be valid.

---

* See Reference 3 and Appendix C.

The power corrections used in the preparation of the data of these experiments were:

No boron	- 0.738
0.1% boron	- 0.732
0.2% boron	- 0.726
0.4% boron	- 0.715

III. CALCULATION OF AIRCRAFT REACTOR SHIELD WEIGHTS

A. Shield Weight Calculations for Crew Tolerance of 1 r/hr and 1/4 r/hr.

1. Specifications

Before embarking upon detailed calculations of the size of the shield for the aircraft reactor, it will be well to recall the specifications for the aircraft reactor and ideal unit shield as set forth in ANP-53.[1]

a. Aircraft Reactor Specifications

Power	200 megawatts
Coolant	Sodium, primary and secondary systems
Reflector	Steel or BeO
Shape	Right cylinder, 3 ft. diameter*
Power Density	Radially uniform; longitudinally represented by a constant plus a cosine term
Composition:	Moderator 70% by volume
	Structure 5%
	Coolant 22%
	Fuel (UO_2) 100 lb

b. Unit Shield Specifications

Fe-Pb-H_2O shield such that at 50 ft separation between crew compartment and reactor the radiation dosage at crew will not exceed 1r/hr during flight. 1/4 r/hr is to be taken in neutron dosage and 3/4 r/hr in gamma dosage. Details of the shield are given in Table 1-1 of Chap. I.

* A 3.8-ft spherical reactor is regarded as its equivalent for the purpose of calculating shield thickness and weight (see Ref. 1).

There is a necessity for mentioning three reactors during the course of these calculations. To avoid confusion, they are defined as follows:

a. The Bulk Shielding Reactor (BSR)

This reactor is the experimental 10-kw reactor now in use at the Bulk Shielding Facility.

b. The Aircraft Reactor (AR)

This is the theoretical reactor specified by ANP-53, which will power the nuclear airplane and for which these present calculations are being made.

c. The Unit Shield Reactor (USR)

For purposes of these calculations the USR is the reactor that extends into the air void of the experimental shield mockup, as shown in Fig. 3-1. The one-inch thickness of iron to the left of the air void is imagined pressed close to the 2 in. of iron on the right to simulate a 3-in. pressure shell about the reactor. The reactor itself is assumed to be a sphere 13 in. in diameter with a power of 10 kw. The pressure shell is assumed to be part of the shield, so that measurements listed below in distances from the USR will mean measurements from the inside edge of the pressure shell.

SECRET

DWG. 13089

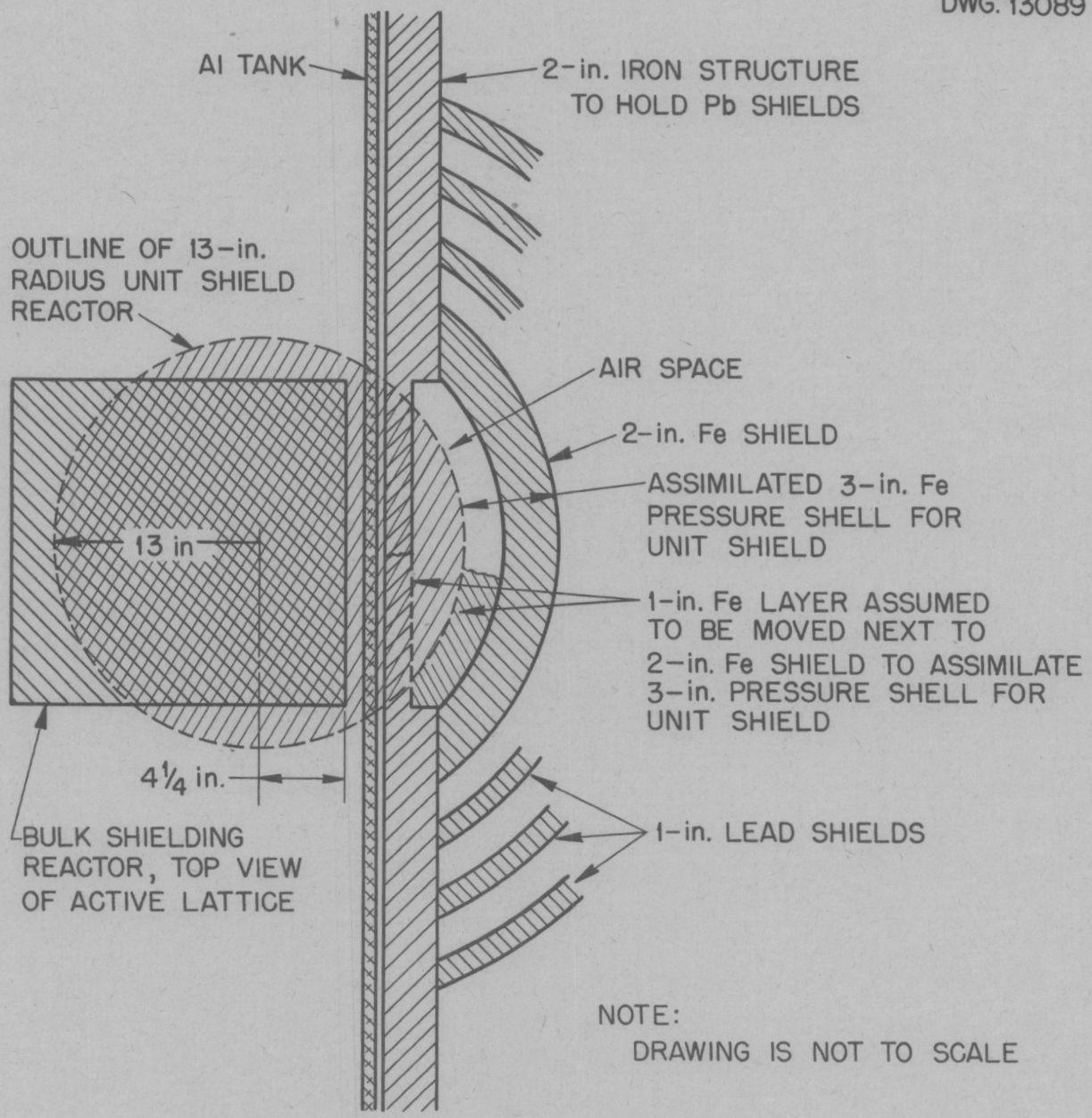

FIG. 3-1 THE UNIT SHIELD REACTOR

2. Leakage from the Aircraft Reactor

Leakage from the aircraft reactor may be estimated as follows. The probability that nuclear radiations produced from fission within a reactor will escape from its surface is assumed to be proportional to $e^{-Z/\lambda}$, where Z is the distance inward from the surface, and λ is the relaxation length within the reactor of the type of radiation under consideration. In the present case λ is chosen so as to represent those fast neutrons which leave the reactor with essentially all of their initial energy. The leakage from a given surface may be expressed as

$$L = F \int_0^{Z\ max} P_1(Z) e^{-Z/\lambda}\, dZ,$$

where F is a factor converting power to the appropriate type of radiation leaking out (this factor does not need to be evaluated since leakage ratios are to be used), and $P_1(Z)$ is the power density, which is proportional to the fission rate per unit volume.

For a right circular cylinder P_1 is assumed to be uniform radially and hence a constant. If λ is small compared to the integration distance, the upper limit of the above integral becomes of small consequence and for convenience may be set at infinity. Thus the leakage from the aircraft reactor is given closely by

$$L_a \Big/ F = P_1 \int_0^\infty e^{-Z/\lambda} = P_1 \lambda$$

$$= \frac{P \lambda}{V} ,$$

where $P_1 = P/V$, the total power of the reactor divided by its volume. Substituting numerical values, the leakage from the AR* is

$$L_a/F = \frac{(2 \times 10^8 \text{ watts})\ (9.2 \text{ cm})}{\pi (45.7 \text{ cm})^2\ (91.4 \text{ cm})}$$

$$= 3.07 \times 10^3 \text{ watts/cm}^2.$$

3. Leakage from the Unit Shield Reactor

It will be assumed that, except for a small attenuation correction, the leakage from the USR was the same as from the BSR. The attenuation correction was necessary because it was physically impossible to place the experimental reactor against the steel plate that held the shield when the aluminum tank which surrounded the shield was in place. Radiation from the reactor had to pass through a slight amount of water and aluminum to reach the air void which represented the USR. This separation turned out to be one inch and the corresponding attenuation of neutrons in water for that distance was 0.826. The leakage calculations described in Appendix D give the value of L/F escaping from the experimental face of the reactor as 7.35×10^{-5} watts/cm^2/watt power, where F is the same conversion factor mentioned above. Thus for the USR the leakage is

* λ is given as 9.2 cm for the AR in ANP-53.

$$L_a/F = (0.826)(7.35\times10^{-5} \text{ watts/cm}^2\text{/watt power})(10^4 \text{ watts power})$$
$$= 0.607 \text{ watts/cm}^2 \text{ at 10 kw power.}$$

4. The Dosage Unit, D

It is convenient for purposes of these calculations to define a dosage unit, D. The D-unit is the maximum dosage rate that may be taken by military personnel during a 25-hr flight of a nuclear-powered aircraft. In accordance with this definition, the D-unit is equivalent to the following dosages of nuclear radiations:

$$1 \text{ D} = 1 \text{ r/hr of gamma radiation}$$
$$1 \text{ D} = 0.1 \text{ rep/hr of fast neutrons}$$

The tolerance dose of 1 D is not to be exceeded for a combination of fast neutrons and gamma radiation. The following amounts of radiation are specified by the ANP Shielding Board as the proper tolerance combination:

$$D_n = 1/4 \text{ D} = 25 \text{ mrep/hr of fast neutrons}$$
$$D_\gamma = 3/4 \text{ D} = 0.75 \text{ r/hr of gamma radiation}$$
$$1 \text{ D} = D_n + D_\gamma$$

5. The Allowed Dose at the Surface of the Shield

The dose D_a allowed at the surface of the USR shield* is given by

$$D_a = 1\ D \times (S/R)^2 \times (L_u/L_a) \times (r_u/r_a) ,$$

where

S is the crew separation of 50 ft,

R is the outside radius of the shield required around the USR,

L_u and L_a are the leakages given above,

r_u = the radius of the USR = 33 cm, and

r_a = the radius of the AR = 58 cm.

The significance of each of the terms of the above expression is:

1 D is the dosage allowed at the crew compartment,

$(S/R)^2$ is the inverse-square correction due to reactor-crew separation,

(L_u/L_a) is leakage ratio of the two reactors, and

(r_u/r_a) is a factor correcting for geometrical attenuation in a shield with spherical surfaces.

Substitution of numerical values gives the following allowed doses as specified:

a. Total dose (neutrons or gamma rays)

$$D_a = 1\ D \times \left(\frac{50 \times 30.5}{R}\right)^2 \times \left(\frac{.607}{3070}\right) \times \left(\frac{33}{58}\right)$$

$$= \frac{260}{R^2} \text{ D-units}$$

---

* Formula by E. P. Blizard, private communication.

b. Apportioned neutron dose

$$D_n = \frac{1}{4} \cdot \frac{260}{R^2}$$

$$= \frac{65}{R^2} \text{ D-units}$$

c. Apportioned gamma dose

$$D_\gamma = \frac{3}{4} \cdot \frac{260}{R^2}$$

$$= \frac{195}{R^2} \text{ D-units}$$

Table 8 in Appendix A presents values of the doses D_a, D_n, and D_γ for various radii R of the USR shield. Table 9 in Appendix A presents a summary of the measured values of the neutron and gamma doses in D units for various thicknesses of shield. The total experimental dose is the sum of the experimental neutron and gamma doses.

6. The Proper Thickness t of the Unit Shield

Figure 3-2 shows curves of the allowed and measured dosage rates as a function of shield thickness. The intersection points of interest are encircled on the graph. For convenience the pertinent data are tabulated in Table 3-1.

TABLE 3-1

Intersection Points of Figure 3-2

Intersection Point	Type of Radiation	Thickness of Shield, t (cm)	Outer Radius of Aircraft Shield (cm)	Total Dose for Shield Weight Calculation
A	Fast neutrons	121.5	179.5	---
B	Gamma rays	122	180	---
C	Fast neutrons	136	194	1 D
D	Total dose	130	188	1 D
E	Total dose	159	217	1/4 D

The minimum shield thickness indicated by point A (121.5 cm) is that point at which the total dose is taken in neutrons. Point B is only of academic interest. Practical shield weights may be calculated for thicknesses t of shield indicated by intersection points C, D, and E.

7. Evaluation of Shield Weights

a. Weight for total thickness of shield of 130 cm (Point D)

For this shield the total tolerance is 1 D, but the neutron dose comprises 44 per cent of the total dose instead of 25 per cent as specified. The shield specifications given in Table 3-2 are calculated on this basis.

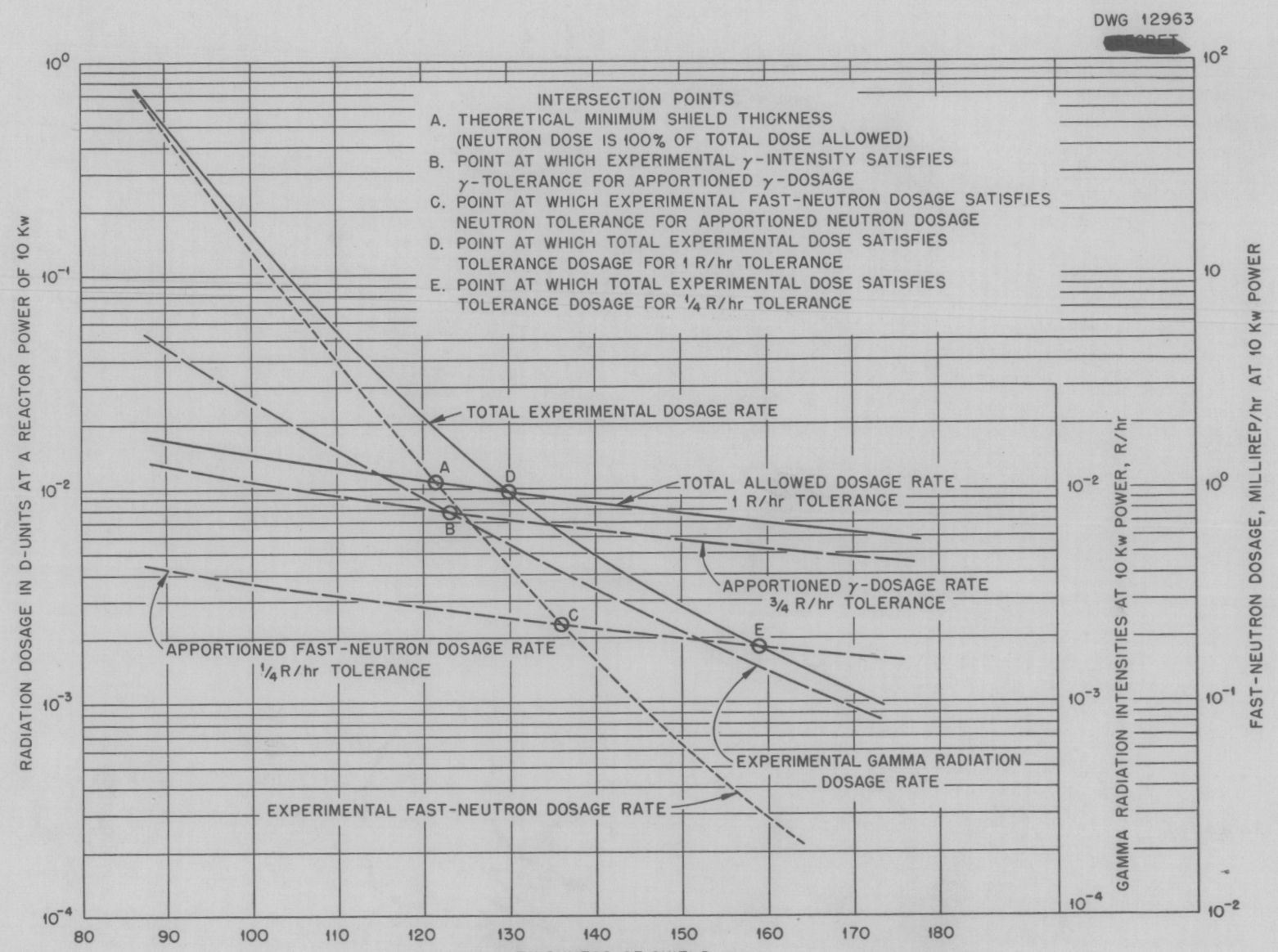

FIG. 3-2
BULK SHIELDING FACILITY

EXPERIMENTAL AND ALLOWED DOSAGE CURVES FOR THE UNIT SHIELD MOCK-UP, ILLUSTRATING THE METHOD OF OBTAINING THE REQUIRED SHIELD THICKNESSES.

TABLE 3-2

Specifications for Shield No. 1

Outer radius, 188 cm

Shield thickness, 130 cm

Total lead thickness, 22.9 cm

Layer	Material		Density (g/cm^3)	Inner Radius(cm)	Thickness (cm)	Weight, ($g \times 10^6$)
1	Fe		7.6	58.0	7.62	2.78
2		0.4%B-H_2O	1.0	65.6	2.6	0.146
3	Pb		11.3	68.2	2.54	1.74
4		0.4%B-H_2O	1.0	70.8	2.56	0.167
5	Pb		11.3	73.3	2.54	2.01
6		0.4%B-H_2O	1.0	75.9	3.18	0.240
7	Pb		11.3	79.0	2.54	2.33
8		0.4%B-H_2O	1.0	81.6	3.83	0.335
9	Pb		11.3	85.4	2.54	2.71
10		0.4%B-H_2O	1.0	87.95	6.10	0.635
11	Pb		11.3	94.05	2.54	3.28
12		0.4%B-H_2O	1.0	96.6	7.98	1.01
13	Pb		11.3	104.6	2.54	4.04
14		0.4%B-H_2O	1.0	107.1	4.46	0.670
15	Pb		11.3	111.6	2.54	4.59
16		0.4%B-H_2O	1.0	114.1	3.49	0.589
17	Pb		11.3	117.6	2.54	5.09
18		0.4%B-H_2O	1.0	120.1	11.8	2.36
19	Pb		11.3	131.9	2.54	6.40
20		0.4%B-H_2O	1.0	134.5	53.5	17.6
Total					130.0	58.7

The weight of Shield No. 1 is

58.7 metric tons

64.6 short tons

129,200 lb.

The importance of the foregoing calculations is that they were made directly from the specifications of the shield as mocked-up and measured, with merely the size determined from the data. No extrapolation of the data was needed, as was necessary for the next shield calculation.

b. Weight for total shield thickness of 136 cm (Point C)

This is a shield with the experimental neutron tolerance of 1/4 D as specified; however, the total experimental dose is below the total allowed dose, so that some lead may be removed to increase the gamma dose to its allowed proportioned dose of 3/4 D. To determine how much lead may be removed, the following doses are noted from Fig. 3-2:

allowed gamma dose, .0068 D-units

experimental gamma dose, .0041 D-units

It is desired to remove enough lead so that the measured gamma intensity is increased by the factor

$$\frac{.0068}{.0041} = 1.66.$$

When lead is replaced by water the apparent relaxation length ℓ of the radiation in the lead is given by

$$\frac{1}{\ell} = \frac{1}{\lambda(\mathrm{Pb})} - \frac{1}{\lambda(\mathrm{H_2O})} ,$$

where $\lambda(\mathrm{Pb})$ is the local relaxation length of gammas in lead and $\lambda(\mathrm{H_2O})$ is the local relaxation length of gammas in water.

Results of Lid Tank experiments[5] mentioned in Chap. I indicated an experimental value of about 3 cm for ℓ for shields of 136-cm thickness for the outer lead layer. Using this value of ℓ, the thickness Δt of lead to be removed is given by

$$e^{\Delta t/3} = 1.66$$

or

$$\Delta t = 1.52 \text{ cm} = 19/32 \text{ in.}$$

Thus, it is specified to remove 19/32 in. of lead from layer 19 to obtain Shield No. 2 (see Table 3-3).

TABLE 3-3

Specifications for Shield No. 2

Outer radius, 194 cm

Shield thickness, 136 cm

Total lead thickness, 21.3 cm

Layer	Material	Inner Radius(cm)	Thickness (cm)	Weight (g x 10^6)
1-18	Identical with Shield No. 1		73.9	34.7
19	Pb	131.9	1.02	2.54
20	0.4%B-H_2O	132.9	61.1	20.75
Total			136.0	58.0

The weight of Shield No. 2 is

58.0 metric tons

63.8 short tons

127,600 lb.

This shield has the same amount of lead as that predicted by the ANP Shielding Board from Lid Tank data but has 6 cm less water thickness and therefore weighs less. The predicted shield weighed 134,000 lb, only 5 per cent higher than Shield No. 2. This fact is the most significant result of this report.

c. Weight for shield with tolerance of 1/4 D at crew compartment

Reduction of the tolerance level at the crew compartment to 1/4 D requires a thickness of shield indicated by point E (t = 159 cm) of Fig. 3-2. At this point the gamma dose comprises about 80 per cent of the total dose, so that this shield (see Table 3-4) approximately satisfies the requirement that three-fourths of the total dose be taken as gammas.

TABLE 3-4

Specifications for Shield No. 3

Outer radius, 217 cm

Shield thickness, 159 cm

Total lead thickness, 21.3 cm

Layer	Material	Inner Radius(cm)	Thickness (cm)	Weight (g x 10^6)
1-19	Identical with Shield No. 1		76.5	41.1
20	0.4%B-H_2O	134.5	82.5	32.6
Total			159.0	73.7

The weight of Shield No. 3 is

73.7 metric tons

81.1 short tons

162,000 lb.

The weight of this shield may be reduced somewhat by allowing a greater proportionate amount of the dose in neutrons.

B. Variation of Shield Weight with Shield Thickness

Of prime consideration in the design of a reactor and shield for a nuclear-propelled aircraft are low weight and small size. It is important then to know what relationship exists between shield thickness and shield weight for given tolerance conditions. A fair understanding of this relationship is to be found from a study of Fig. 3-2. A shield designed for a thickness indicated by point A would be very heavy because of the considerable amount of lead required to reduce the gamma radiation to negligible proportions. Thicker shields would require less lead but more water and would weigh less. For very thick shields the excess amount of water necessary would make the shields heavier again. It is clear that at some point there is a minimum-weight shield.

A series of shield weight calculations was carried out for a tolerance of 1 D and for various thicknesses of shield, using the method outlined in connection with Shield No. 2 (see preceding section, 7(b).) These are summarized in Table 9 in Appendix A and presented graphically in Fig. 3-3.

It is of interest to note the points on the figure indicating the positions of Shield Nos. 1 and 2. Shield No. 1 is somewhat thinner than Shield No. 2, but because it contains more lead it weighs more. The fact that Shield No. 2 falls on the minimum point of the curve shows that it is optimized for a neutron-to-gamma ratio of 1/3. On the same graph there appears a dashed line showing what percentage of the total dose can be expected to be taken in neutrons. It is evident that the thinner the shield,

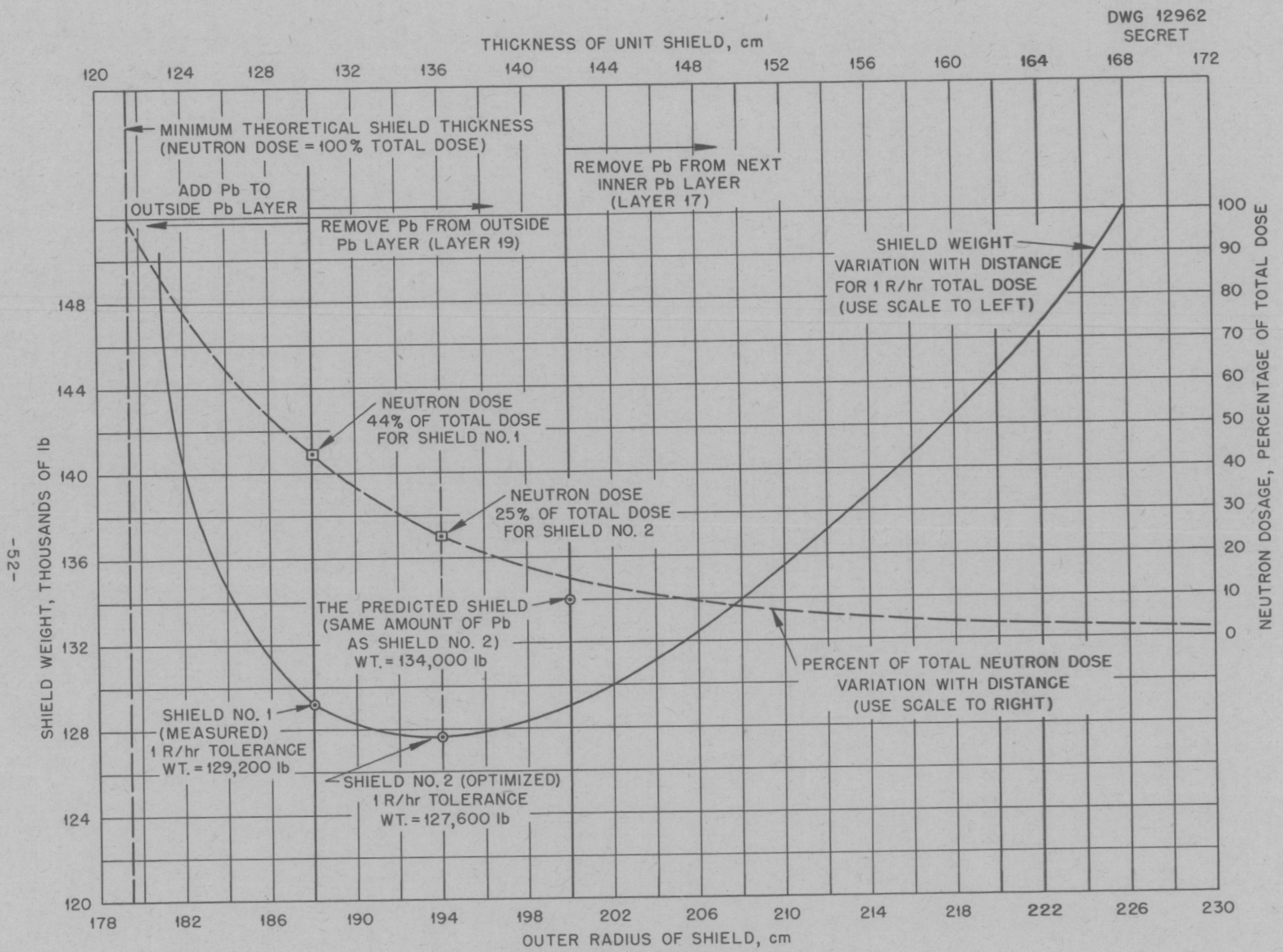

FIG. 3-3
BULK SHIELDING FACILITY
UNIT SHIELD EXPERIMENTS

ILLUSTRATING THE DEPENDENCE OF THE WEIGHT OF THE UNIT SHIELD
UPON ITS THICKNESS FOR TOLERANCE RADIATION DOSAGES

the greater is the percentage neutron dose. Thus, a thin shield can be designed only at the expense of increased neutron level and excess weight. There is an incentive other than weight for keeping the neutron dose as low as possible. The relative biological effect of fast neutrons is less well-known than that of gamma radiation, and the uncertainty is less important when the neutron level is kept low.

The point labeled "predicted shield" in Fig. 3-3 is also of interest. As mentioned above, this shield, based on Lid Tank studies, is only 5 per cent higher in weight than Shield No. 2 measured in the present experiments.

It should be noted that the most accurate point on the curve is the measured Shield No. 1. A possibility of error is introduced by the use of an average value of ℓ as chosen for the calculations. Actually ℓ varies directly with the amount of extra lead introduced, so that the error becomes greater at the extremes of the curve. At the point indicated by Shield No. 2, a change of 20 per cent in the value of ℓ gives only an error of about 1 per cent in the weight of the shield.

C. Effects of Boration of Water upon Shield Weights

The results of the unit shield experiments described in this report indicate that the boration of the water greatly reduced the gamma radiation intensities behind the shield but had no effect upon the fast-neutron dose. It was observed that as the boron concentration increased, the rate of reduction in gamma intensity with change in boron concentration decreased.

An analysis of the effectiveness of the boron in reducing gamma intensities has been given separately in Appendix B. This analysis established the fact that the 0.4% boron concentration used in the experiments was entirely adequate and predicted that further boration of the water would reduce the gamma intensities at the surface of the shield by small amounts.

It is of interest at this point to inquire what effect does varying the amount of boron in the shield have upon its weight, if the shield is designed in every case for tolerance conditions. The theoretical limit to which a shield weight could be lowered by increasing the boron concentration becomes an important consideration.

The boron content of the water may be increased only to its limit of solubility, 0.6%, using B_2O_3. However, it is possible to dissolve boric oxide and other boron compounds to a much greater extent in other solutions, such as potassium hydroxide.

Suppose, for example, that a 1% boron concentration could be achieved by dissolving boric acid in potassium hydroxide, or perhaps a concentration as high as 10% boron could be reached by some means. There arises the question as to whether the reduction in weight would be enough to justify study of such a system.

On the basis of the calculations which follow, an estimate of savings of shield weight will be made, and a tentative answer to the above question will be given. These calculations are based upon the optimized shield (Shield No. 2). They show what happens to the weight of this shield as the boron concentration is changed.

Table 2 of Appendix B lists the experimental gamma intensities in relative units at any point behind the unit shield for various concentrations of boron. From this table the ratio Γ_e / Γ_a is determined, where Γ_a is the value of the gamma intensity for the 0.4% boron solution, and Γ_e the value of the gamma radiation at other concentrations of boron. From the value of Γ_e / Γ_a the thickness of lead to be added or removed is calculated, from which the shield weight for the boron concentration being considered is obtained. Allowance is made for the increase in weight due to increased boron concentration.

Calculations of shield weights are made for B_2O_3 solution in water up to 1% B concentration and for B_2O_3 in KOH solution ($K_2B_2O_4$ solution) up to 5% B concentration. The borated water was assumed to extend only 1 ft beyond the last lead layer in order to minimize the weight increase. These calculations are summarized in Table 11 in Appendix A. The results are plotted in Fig. 3-4. The reductions in weight for Shield No. 2 are shown in Table 3-5.

TABLE 3-5

Variation of Shield Weight with Boron Concentration

Solution	Boron Concentration (%)	Weight of Shield (lb)	% Reduction in Weight over Shield No. 2
B_2O_3 in H_2O	0.6	126,100	1.2
	1.	122,500	4
B_2O_3 in KOH solution	0.6	126,800	1
	1	124,500	2.5
	1.25	124,300	2.7
	1.5	124,400	2.6
	2	124,800	2.2
	5	129,400	(1% increase)

It is evident from Fig. 3-4 that with the given layer configuration the greatest reduction in weight attainable over Shield No. 2 is 2.7% at a boron concentration of 1.25%. Attempts to further reduce the weight is offset by the higher density of solutions needed.

A further reduction in weight may be accomplished by reoptimizing the shield for higher boron concentrations. Such an experiment is now in progress at the Lid Tank.

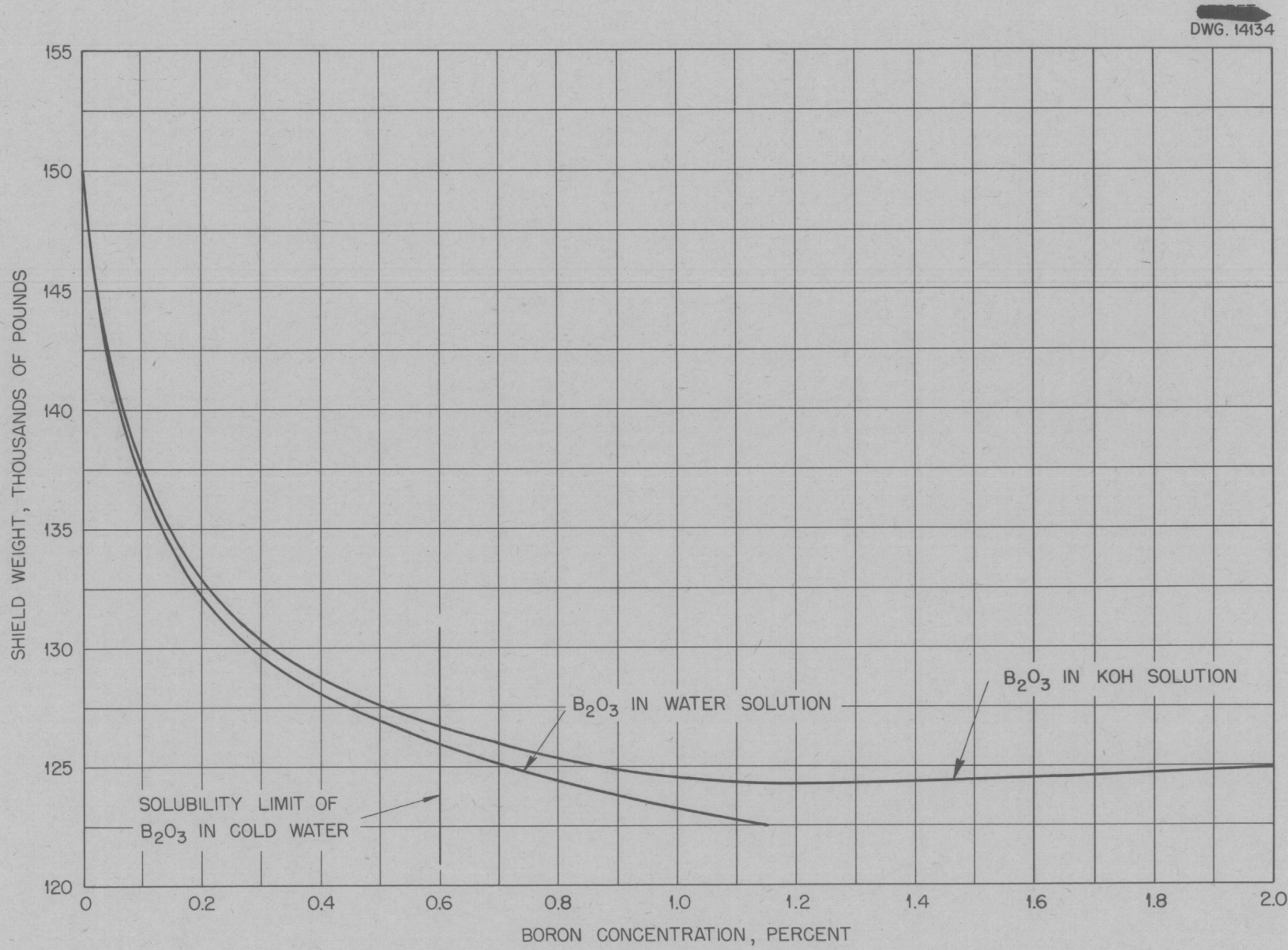

FIG. 3-4 VARIATION OF SHIELD WEIGHT WITH BORON CONCENTRATION (BASED UPON SHIELD NO.2)

D. Errors in the Estimation of Shield Weights

The nature of the calculations involved in determining shield weights is such that relatively large errors in the measurements and calculated constants may be tolerated without their producing important errors in the final results. For the aircraft reactor considered by the Shielding Board[1] the main uncertainties appear in the following factors:

1. Calibration of the detectors used for determining neutron and gamma dosage.
2. The power of the reactor (see reference 3).
3. The value of λ used in calculating the core leakage (see Appendix D) and in the value of ℓ used in calculating the lead removal (see pages 48 and 53).
4. The geometric transformations; these are
   a. The assumptions used in transforming from the BSR to the USR (see page 38), and
   b. The inverse square correction in determining the allowed dose at the crew (see page 43).

   The geometric transformations are conservative and the errors involved are small.

Table 3-6 lists the effects of the first three factors on the weight of Shield No. 2 (see Fig. 3-3). The largest uncertainty produces an error of no more than 3% in the shield weight, and the combined uncertainties produce a root mean square error of less than 4%.

TABLE 3-6

Errors in Shield Weight

Source of Uncertainty	Maximum Error (%)	Error in Shield Thickness (cm)	Change in Shield Weight (lb)	Error in Shield Weight (%)
Fast Neutron Dosimeter	30	2.7 (H_2O)	2800	2.2
Gamma Ion Chamber	5	0.15 (Pb)	800	0.6
Reactor Power Calibration	20	2.0 (H_2O) 0.24 (Pb)	3300	2.6
Leakage Constant, λ	10	1.0 (H_2O) 0.1 (Pb)	1500	1.2
Lead Removal Constant, ℓ	20	0.25 (Pb)	1400	1.1
Total R.M.S. Error - - - - -			4700	3.7

IV. CONCLUSIONS AND OBSERVATIONS

The most important result of these unit shield measurements has been the confirmation of the earlier Lid Tank tests by means of independent measurements. Further, the validation of the shielding principles involved in the design of the ideal unit shield has been accomplished. These principles include the use of simple theoretical relationships, the extrapolation of fast-neutron dosage measurements by means of thermal-neutron measurements, and the employment of the necessary geometric transformations.

Specifically, a minimum-weight shield was obtained for 1r/hr tolerance at the crew which had the same lead configuration as the shield predicted by the ANP Shielding Board and varied only in that the water thickness behind the lead proved to be 6 cm less than originally estimated. The minimum-weight shield was obtained by calculation from the shield as measured. The numerical results are tabulated in Table 4-1.

Other results to be noted are that for a tolerance of 1r/hr at crew no lead-water shield may be thinner than 121.5 cm for the given size and power of the aircraft reactor. Reduction of the radiation level at the crew compartment to 1/4 r/hr increases the shield weight to 162,000 lb. The weight of the shield in its present configuration may be reduced somewhat by increasing the boron concentration of the water in the shield.

TABLE 4-1

Shield Weights

Shield	Total Thickness (cm)	Lead Thickness (cm)	Weight (lb)
The shield as measured	130	22.9	129,200
The minimum weight shield	136	21.3	127,600
Shield predicted by Lid Tank tests	142	21.3	134,000

APPENDIX A

Tables for the Unit Shield Experiments

APPENDIX A

This appendix contains tables of the experimental data obtained during the unit shield experiments plus tables summarizing the various shield-weight calculations. These tables were removed from the main body of the report in order not to destroy its continuity.

For handy reference a list of the tables is given.

Table 1 Gamma Radiation Traverses behind the Unit Shield Mockup to Determine the Effect of Streaming

Experiment 3

Table 2 Gamma Radiation Measurements behind the Unit Shield

Table 3 Thermal-Neutron Measurements behind the Unit Shield

Table 4 Fast-Neutron Dose Measurements behind the Unit Shield

Experiment 4

Table 5 Gamma Radiation Measurements behind the Borated-Water Unit Shield with Various Concentrations of Boron

Table 6 Thermal-Neutron Measurements behind the Borated-Water Unit Shield

Table 7 Fast-Neutron Dose Measurements behind the Borated-Water Unit Shield

Shield Weight Calculations

Table 8 Tolerance Dosages of Radiation Allowed at the Surface of the USR Shield

Table 9 Experimental Dosage Rates in D-units at the Surface of the USR Shield for Various Shield Thicknesses

Table 10 Calculation of Shield Weights for Various Thicknesses of Shield for Radiation Tolerance of 1 r/hr at Crew

Table 11 Variation of Shield Weight with Boron Concentration, Based upon Shield No. 2.

TABLE 1

Gamma Radiation Traverses Behind the Unit Shield Mockup To Determine the Effect of Streaming

(Traverses made on a radius of 175 cm with 10^{12} standard 50-cc chamber)

Run No.	Description	x, Distance from Centerline (cm)	z, Distance from Reactor (cm)	Angle of Chamber with z-axis	Gamma Radiation Intensity (r/hr/watt)
3	Measurement of gamma streaming around the unit shield	0.0	171.0	0°	1.180×10^{-6}
		-45.3	165.0	-15°	1.172×10^{-6}
		-87.5	147.6	-30°	1.208×10^{-6}
		-123.7	119.8	-45°	3.076×10^{-6}
		-155.6	83.5	-60°	5.511×10^{-5}
		0.0	171.0	0°	1.179×10^{-6}
		+45.3	165.0	+15°	1.134×10^{-6}
		+87.5	147.6	+30°	1.103×10^{-6}
		+123.7	119.8	+45°	2.399×10^{-6}
		+155.6	83.5	+60°	4.044×10^{-5}
4	Measurement of gamma streaming around the unit shield with reactor walled in with concrete blocks	0.0	171.0	0°	1.129×10^{-6}
		-45.3	165.0	-15°	1.246×10^{-6}
		-87.5	147.6	-30°	1.246×10^{-6}
		-123.7	119.8	-45°	1.934×10^{-6}
		-155.6	83.5	-60°	8.578×10^{-6}
		0.0	171.0	0°	1.270×10^{-6}
		+45.3	165.0	+15°	1.188×10^{-6}
		+87.5	147.6	+30°	1.110×10^{-6}
		+123.7	119.8	+45°	1.425×10^{-6}
		+155.6	83.5	+60°	5.073×10^{-6}

Note Data plotted in Fig. 2-2

TABLE 2

Experiment 3

Gamma Radiation Measurements Behind Unit Shield Mockup
(Centerline Data)

Distance from Reactor (cm)	Distance from Shield (cm)	GAMMA RADIATION INTENSITY (r/hr/watt)				
		Run 14A, 50-cc Standard 10^{12} Chamber	Run 14B, 900-cc 10^{10} Chamber	Run 14C, 900-cc 10^{12} Chamber	Run 18, 50-cc Standard 10^{12} Chamber	Summary and Average
Plotting Symbols		⊙	△	⊡	●	
99.9	2.0	5.065×10^{-5}				5.065×10^{-5}
101.1	3.2		4.791×10^{-5}			4.791×10^{-5}
102.9	5.0				4.298×10^{-5}	4.298×10^{-5}
105.0	7.1	3.851×10^{-5}	3.752×10^{-5}			3.802×10^{-5}
110.0	12.1	2.877×10^{-5}	2.846×10^{-5}			2.862×10^{-5}
112.9	15.0				2.245×10^{-5}	2.245×10^{-5}
120.0	22.1	1.610×10^{-5}	1.608×10^{-5}			1.609×10^{-5}
122.9	25.0				1.330×10^{-5}	1.330×10^{-5}
130.0	32.1	9.37×10^{-6}	9.161×10^{-6}			9.265×10^{-6}
132.9	35.0				7.729×10^{-6}	7.729×10^{-6}
140.0	42.1		5.500×10^{-6}	5.413×10^{-6}		5.456×10^{-6}
150.0	52.1		3.277×10^{-6}	3.268×10^{-6}		3.273×10^{-6}
152.9	55.0				2.81×10^{-6}	2.81×10^{-6}
160.0	62.1		1.921×10^{-6}	1.993×10^{-6}		1.157×10^{-6}
170.0	72.1			1.245×10^{-6}		1.245×10^{-6}
172.9	75.0				1.09×10^{-6}	1.09×10^{-6}
180.0	82.1			7.889×10^{-7}		7.889×10^{-7}
190.0	92.1			5.145×10^{-7}		5.145×10^{-7}

Continued

TABLE 2 (Cont'd)

Distance from Reactor (cm)	Distance from Shield (cm)	GAMMA RADIATION INTENSITY (r/hr/watt)				
		Run 14A, 50-cc Standard 10^{12} Chamber	Run 14B, 900-cc 10^{10} Chamber	Run 14C, 900-cc 10^{12} Chamber	Run 18, 50-cc Standard 10^{12} Chamber	Summary and Average
Plotting Symbols		⊙	△	⊡	⊙	
200	102.1			3.348×10^{-7}		3.348×10^{-7}
210.0	112.1			2.233×10^{-7}		2.233×10^{-7}
220.0	122.1			1.513×10^{-7}		1.513×10^{-7}
230.0	132.1			1.040×10^{-7}		1.040×10^{-7}
240.0	142.1			7.267×10^{-8}		7.267×10^{-8}
250.0	152.1			4.905×10^{-8}		4.905×10^{-8}
260.0	162.1			3.470×10^{-8}		3.470×10^{-8}
270.0	172.1			2.526×10^{-8}		2.526×10^{-8}
280.0	182.1			1.894×10^{-8}		1.894×10^{-8}
290.0	192.1			1.318×10^{-8}		1.318×10^{-8}

NOTE: Data plotted in Fig. 2-3

TABLE 3

Experiment 3

Thermal Neutron Flux Measurements
Behind Unit Shield Mockup

(Centerline Data)

Distance from Reactor (cm)	Distance from Shield (cm)	THERMAL-NEUTRON FLUX (nv_{th}/watt)				
		Run 5 3-in. Fission Counter	Run 11 8-in. BF_3 Counter	Run 13 Indium Foils	Run 15 12-in. BF_3 Double Chamber Counter	Summary
Plotting Symbol		-⊙-	⊡	X	△	
97.9	0.0	3.120×10^{1}				3.120×10^{1}
99.1	1.2			2.436×10^{1}		2.436×10^{1}
107.9	10.0	5.272				5.272
117.3	20.0	1.178				1.178
117.9	20.0	1.178				1.178
119.2	21.3			1.017		1.017
122.3	24.4		6.618×10^{-1}			6.618×10^{-1}
127.3	29.4		3.464×10^{-1}			3.464×10^{-1}
127.9	30.0	3.183×10^{-1}				3.183×10^{-1}
129.2	31.3			2.538×10^{-1}		2.538×10^{-1}
132.3	34.4		1.872×10^{-1}			1.872×10^{-1}
137.9	40.0	9.400×10^{-2}				9.400×10^{-2}
138.3	40.4		8.965×10^{-2}			8.965×10^{-2}
142.3	44.4		5.603×10^{-2}			5.603×10^{-2}

Continued

Table 3 (Con't.)

Distance from Reactor (cm)	Distance from Shield (cm)	THERMAL-NEUTRON FLUX (nv_{th}/watt)				
		Run 5 3-in. Fission Counter	Run 11 8-in. BF_3 Counter	Run 13 Indium Foils	Run 15 12-in. BF_3 Double Chamber Counter	Summary
Plotting Symbol		-⊖-	⊡	X	⧋	
147.3	49.4		3.078×10^{-2}			3.078×10^{-2}
147.9	50.0	2.850×10^{-2}				2.850×10^{-2}
152.3	54.4		1.742×10^{-2}			1.742×10^{-2}
155.1	57.2				1.289×10^{-2}	1.289×10^{-2}
157.3	59.4		9.949×10^{-3}			9.949×10^{-3}
162.3	64.4		5.720×10^{-3}			5.720×10^{-3}
165.1	67.2				4.236×10^{-3}	4.236×10^{-3}
167.3	69.4		3.359×10^{-3}			3.359×10^{-3}
175.1	77.2				1.438×10^{-3}	1.438×10^{-3}
185.1	87.2				5.008×10^{-4}	5.008×10^{-4}
195.1	97.2				1.751×10^{-4}	1.751×10^{-4}
205.1	107.2				6.257×10^{-5}	6.257×10^{-5}
215.1	117.2				2.265×10^{-5}	2.265×10^{-5}
225.1	127.2				8.600×10^{-6}	8.600×10^{-6}
235.2	137.3				3.310×10^{-6}	3.310×10^{-6}
245.2	147.3				1.29×10^{-6}	1.29×10^{-6}
255.2	157.3				6.59×10^{-7}	6.59×10^{-7}

NOTE: Data plotted in Fig. 2-4.

TABLE 4

Experiment 3

Fast-Neutron Dosage Measurements
Behind Unit Shield Mockup

(Centerline Data)

Plotting Symbol, ⊙

Distance from Reactor (cm)	Distance from Shield (cm)	FAST NEUTRON DOSAGE (mrep/hr/watt)		
		Run 19	Run 21	Summary
104.6	7.7		1.245×10^{-2}	1.245×10^{-2}
112.8	13.4	4.01×10^{-3}		4.01×10^{-3}
114.6	17.7		3.41×10^{-3}	3.41×10^{-3}
122.8	23.4	1.17×10^{-3}		1.17×10^{-3}
124.6	27.7		1.015×10^{-3}	1.015×10^{-3}
132.8	33.4	3.67×10^{-4}		3.67×10^{-4}
134.6	37.7		3.12×10^{-4}	3.12×10^{-4}
142.8	43.4	1.25×10^{-4}		1.25×10^{-4}
152.8	53.4	4.12×10^{-5}		4.12×10^{-5}
164.6	67.7		1.45×10^{-5}	1.45×10^{-5}

NOTE: Data plotted in Fig. 2-5.

TABLE 5

Experiment 4

Gamma Radiation Intensity Measurements
Behind Borated-Water Unit Shield Mockup
with Various Concentrations of Boron

(Centerline Measurements)

A. 0.0% Boron Concentration
(Pure H_2O)

Distance from Reactor (cm)	Distance from Shield (cm)	GAMMA RADIATION INTENSITY (r/hr/watt)				
		Run 1A 50-cc 10^{12} Std. Chamber	Run 1B 900-cc 10^{12} Chamber	Run 2 900-cc 10^{12} Chamber	Run 3 900-cc 10^{12} Chamber	Summary and Average
Plotting Symbol		●	■	■	■	
159.9	62.0				1.786×10^{-6}	1.786×10^{-6}
160.0	62.1	1.774×10^{-6}	1.694×10^{-6}			1.734×10^{-6}
160.9	63.0			1.725×10^{-6}		1.725×10^{-6}
169.9	72.0				1.100×10^{-6}	1.100×10^{-6}
170.0	72.1		1.081×10^{-6}			1.081×10^{-6}
170.9	73.0			1.054×10^{-6}		1.054×10^{-6}
179.9	82.0				6.844×10^{-6}	6.844×10^{-6}
180.0	82.1		6.926×10^{-7}			6.926×10^{-7}
180.9	83.0			6.606×10^{-7}		6.606×10^{-7}
189.9	92.0				4.350×10^{-7}	4.350×10^{-7}
190.9	93.0			4.159×10^{-7}		4.159×10^{-7}
199.9	102.0				2.784×10^{-7}	2.784×10^{-7}
200.0	102.1		2.904×10^{-7}			2.904×10^{-7}
200.9	103.0			2.637×10^{-7}		2.637×10^{-7}
209.9	112.0				1.816×10^{-7}	1.816×10^{-7}

Continued

Table 5 (Con't.)

A. 0.0% Boron Concentration (Con't.)

Distance from Reactor (cm)	Distance from Shield (cm)	GAMMA RADIATION INTENSITY (r/hr/watt)				
		Run 1A 50-cc 10^{12} Std. Chamber	Run 1B 900-cc 10^{12} Chamber	Run 2 900-cc 10^{12} Chamber	Run 3 900-cc 10^{12} Chamber	Summary and Average
Plotting Symbol		●	■	■	■	
210.9	113.0			1.689×10^{-7}		1.689×10^{-7}
219.9	122.0				1.197×10^{-7}	1.197×10^{-7}
220.9	123.0			1.09×10^{-7}		1.09×10^{-7}
229.9	132.0				7.983×10^{-8}	7.983×10^{-8}
239.9	142.0				5.378×10^{-8}	5.378×10^{-8}
249.9	152.0				3.714×10^{-8}	3.714×10^{-8}
259.9	162.0				2.561×10^{-8}	2.561×10^{-8}
269.9	170.0				1.751×10^{-8}	1.751×10^{-8}

NOTE: Data plotted in Fig. 2-3.

Table 5 (Con't.)

B. 0.1% Boron Concentration

Run 4, 900-cc 10^{12} Chamber
Plotting Symbol, ■

Distance from Reactor (cm)	Distance from Shield (cm)	γ Intensity (r/hr/watt)
159.9	62.0	6.964×10^{-7}
169.9	72.0	4.414×10^{-7}
179.9	82.0	2.788×10^{-7}
189.9	92.0	1.779×10^{-7}
199.9	102.0	1.139×10^{-7}
204.9	107.0	9.606×10^{-8}
209.9	119.0	7.662×10^{-8}
219.9	122.0	5.197×10^{-8}
229.9	132.0	3.534×10^{-8}
239.9	142.0	2.398×10^{-8}
249.9	152.0	1.633×10^{-8}
245.9	162.0	1.366×10^{-8}

NOTE: Data plotted in Fig. 2-3.

Table 5 (Con't.)

C. 0.2% Boron Concentration

Run 5, 900-cc 10^{12} Chamber
Plotting Symbol, ■

Distance from Reactor (cm)	Distance from Shield (cm)	γ Intensity (r/hr/watt)
159.9	62.0	5.447×10^{-7}
169.9	72.0	3.396×10^{-7}
179.9	82.0	2.170×10^{-7}
189.9	92.0	1.395×10^{-7}
199.9	102.0	9.069×10^{-8}

D. 0.4% Boron Concentration

Run 5, 900-cc 10^{12} Chamber
Plotting Symbol, ■

Distance from Reactor (cm)	Distance from Shield (cm)	γ INTENSITY (r/hr/watt)		
		Run 6 G-M Counter	Run 7 900-cc 10^{12} Chamber	Summary
Plotting Symbol		◆	■	
159.9	62.0		3.817×10^{-7}	3.817×10^{-7}
169.9	72.0		2.360×10^{-7}	2.360×10^{-7}
173.2	75.3	2.000×10^{-7}		2.000×10^{-7}
179.9	82.0		1.472×10^{-7}	1.472×10^{-7}
183.2	85.3	1.278×10^{-7}		1.278×10^{-7}
189.9	92.0		9.481×10^{-8}	9.481×10^{-8}
193.2	95.3	8.164×10^{-8}		8.164×10^{-8}
199.9	102.0		6.220×10^{-8}	6.220×10^{-8}

Continued

Table 5 (Con't.)

D. 0.4% Boron Concentration (Con't.)

Distance from Reactor (cm)	Distance from Shield (cm)	γ INTENSITY (r/hr/watt)		
		Run 6 G-M Counter	Run 7 900-cc 10^{12} Chamber	Summary
Plotting Symbol		◆	■	
209.9	112.0		3.923×10^{-8}	3.923×10^{-8}
213.2	115.3	3.454×10^{-8}		3.454×10^{-8}
219.9	122.0		2.586×10^{-8}	2.586×10^{-8}
229.9	132.0		1.757×10^{-8}	1.757×10^{-8}
233.2	135.3	1.47×10^{-8}		1.47×10^{-8}
239.9	142.0		1.222×10^{-8}	1.222×10^{-8}
249.9	152.0		8.39×10^{-9}	8.39×10^{-9}

NOTE: Data plotted in Fig. 2-3.

TABLE 6

EXPERIMENT 4

Thermal-Neutron Flux Measurements Behind

0.4% Borated Water Unit Shield Mockup

(Centerline Data)

DISTANCE FROM REACTOR (cm)	DISTANCE FROM SHIELD (cm)	THERMAL-NEUTRON FLUX (nv_{th}/watt)										
		RUN 8, 3-in. FISSION COUNTER	RUN 9, 3-in. FISSION COUNTER	RUN 10, 12-in. BF_3 SINGLE CHAMBER COUNTER	RUN 12, 3-in. FISSION COUNTER	RUN 13, 3-in. FISSION COUNTER	RUN 14, 8-in. BF_3 COUNTER	RUN 15, 12-in. BF_3 SINGLE CHAMBER COUNTER	RUN 16, 12-in. BF_3 DOUBLE CHAMBER COUNTER	RUN 17, 12-in. BF_3 DOUBLE CHAMBER COUNTER	RUN 18-19, 12-in. BF_3 SINGLE CHAMBER COUNTER	SUMMARY AND AVERAGE
PLOTTING	SYMBOLS	●	●	▼	●	●	■	▼	▲	▲	▼	
146.5	48.6	1.749×10^{-2}										1.749×10^{-2}
149.0	51.1	2.029×10^{-2}										2.029×10^{-2}
151.5	53.6	1.779×10^{-2}			1.722×10^{-2}	1.782×10^{-2}						1.761×10^{-2}
156.5	58.5	1.15×10^{-2}	1.130×10^{-2}									1.140×10^{-2}
161.5	63.6	6.65×10^{-3}			6.98×10^{-3}	6.55×10^{-3}						6.73×10^{-3}
166.5	68.6	3.69×10^{-3}										3.69×10^{-3}
171.0	73.1						2.251×10^{-3}					2.251×10^{-3}
171.5	73.6	2.15×10^{-3}										2.15×10^{-3}
172.5	74.6			1.856×10^{-3}								1.856×10^{-3}
176.0	78.1						1.275×10^{-3}					1.275×10^{-3}
177.2	79.3								1.122×10^{-3}			1.122×10^{-3}
181.0	83.1						7.431×10^{-4}					7.431×10^{-4}
182.5	84.6			6.300×10^{-4}								6.300×10^{-4}
186.0	88.1						4.408×10^{-4}					4.408×10^{-4}
187.2	89.3								3.905×10^{-4}			3.905×10^{-4}
191.0	93.1						2.66×10^{-4}					2.66×10^{-4}
192.5	94.6			2.206×10^{-4}				2.200×10^{-4}			2.10×10^{-4}	2.169×10^{-4}
196.0	98.1						1.58×10^{-4}					1.58×10^{-4}
197.2	99.3								1.368×10^{-4}			1.350×10^{-4}
202.5	104.6			7.977×10^{-5}						1.331×10^{-4}		7.977×10^{-5}
212.5	114.6			3.030×10^{-5}								3.030×10^{-5}
217.2	119.3									1.774×10^{-5}		1.774×10^{-5}
222.5	124.6			1.08×10^{-5}								1.08×10^{-5}
232.5	134.6			4.31×10^{-6}				4.13×10^{-6}				4.22×10^{-6}
237.2	139.3									2.59×10^{-6}		2.59×10^{-6}
242.5	144.6							1.59×10^{-6}				1.59×10^{-6}
247.2	149.3									1.21×10^{-6}		1.21×10^{-6}
252.5	154.6							8.69×10^{-7}				8.69×10^{-7}
257.2	159.3									5.51×10^{-7}		5.51×10^{-7}

NOTE: Data plotted in Fig. 2-4.

TABLE 7

Experiment 4

Fast-Neutron Dosage Measurements
Behind 0.4% Borated-Water Unit Shield Mockup

(Centerline Data)

Plotting Symbol, •

Distance from Reactor (cm)	Distance from Shield (cm)	FAST-NEUTRON DOSAGE (mrep/hr/watt)		
		Run 20	Run 23	Summary
153.2	55.3		4.03×10^{-5}	4.03×10^{-5}
154.9	57.0	3.25×10^{-5}		3.25×10^{-5}
158.2	60.3		2.39×10^{-5}	2.39×10^{-5}
159.9	62.0	2.06×10^{-5}		2.06×10^{-5}
163.2	65.3		1.48×10^{-5}	1.48×10^{-5}
164.9	67.0	1.22×10^{-5}		1.22×10^{-5}
174.9	77.0	5.37×10^{-6}		5.37×10^{-6}
179.9	82.0	3.70×10^{-6}		3.70×10^{-6}

NOTE: Data plotted in Fig. 2-5.

TABLE 8

Tolerance Dosages of Radiation Allowed
at the Surface of the USR Shield

Outside Radius of USR Shield (cm)	Thickness of Shield (cm)	Maximum Allowed Radiation Dose (D-Units)	Apportioned Neutron Dose (D-Units)	Apportioned Gamma Dose (D-Units)
90	57	.0320	.00800	.0240
100	67	.0259	.00648	.0194
110	77	.0214	.00535	.0161
120	87	.0180	.00450	.0135
130	97	.0153	.00383	.0115
140	107	.0132	.00330	.00990
150	117	.0115	.00287	.00863
160	127	.0101	.00252	.00758
170	137	.00896	.00224	.00672
180	147	.00799	.00200	.00599
190	157	.00717	.00179	.00538
200	167	.00622	.00156	.00466

Apportioned doses:

Neutrons, 25% of total.

Gammas, 75% of total.

NOTE: Data plotted in Fig. 3-2.

TABLE 9

Experimental Dosage Rates in D-Units
at the Surface of the USR Shield
for Various Shield Thicknesses

Distance from BSR (cm)	Shield Thickness (cm)	Outside Radius of USR Shield (cm)	Fast Neutron Dose (D-Units)	Gamma Radiation Dose (D-Units)	Total Experimental Dose (D-Units)
100	77.8	110.8	2.32	.0990	2.42
110	87.8	120.8	.610	.0530	.663
120	97.8	130.8	.175	.0295	.205
130	107.0	140.8	.0532	.0171	.0703
140	117.8	150.8	.0160	.0102	.0262
150	127.8	160.8	.00545	.00613	.0116
160	137.8	170.8	.00192	.00375	.00567
170	147.8	180.8	.00077	.00235	.00312
180	157.8	190.8	.00034	.00157	.00191

NOTE: Data plotted in Fig. 3-2.

TABLE 10

Calculations of Shield Weights
for Various Thicknesses of Shield

(All weights are based on a total radiation tolerance of 1 r/hr.)

Shield Thickness (cm)	Total Allowed Dose, $D_{(a)}$ (D-Units)	Exp'l. Neutron Dose, $D_{n(e)}$ (D-Units)	Allowed γ Dose, $D_{\gamma(a)}$ (D-Units)	Exp'l. γ Dose, $D_{\gamma(e)}$ (D-Units)	Ratio: $\frac{D_{\gamma(e)}}{D_{\gamma(a)}}$	Change in Lead Thickness (cm)*	Shield Weight (lb)
121.5	.0107	.0107	0	.00830	∞		
123	.0106	.00910	.00150	.00768	5.12	+ 4.90	148,700
125	.0103	.00735	.00295	.00700	2.37	+ 2.59	137,100
127	.0101	.00590	.00420	.00640	1.52	+ 1.26	132,900
129	.00984	.00478	.00506	.00579	1.14	+ .39	130,200
130	.00968	.00423	.00545	.00545	1.00	0	129,200**
131	.00960	.00389	.00571	.00522	.914	- .27	128,700
133	.00937	.00317	.00620	.00474	.765	- .81	128,000
135	.00915	.00257	.00658	.00430	.653	- 1.28	127,700
136	.00903	.00223	.00680	.00410	.603	- 1.52	127,600***
137	.00896	.00209	.00687	.00390	.568	- 1.70	127,700
139	.00872	.00171	.00701	.00355	.506	- 2.04	128,200
141	.00852	.00143	.00709	.00323	.456	- 2.36	128,700
143	.00837	.00120	.00717	.00295	.411	- 2.67	129,600
145	.00818	.00099	.00719	.00268	.373	- 2.96	130,700
147	.00800	.00078	.00722	.00245	.339	- 3.25	131,800
152	.00760	.00054	.00706	.00198	.280	- 3.82	
157	.00720	.00036	.00684	.00162	.237	- 4.32	139,700
162	.00680	.00025	.00655	.00135	.206	- 4.74	
167	.00655	.00018	.00637	.00112	.176	- 5.21	150,500

* "+" indicates add, "-" indicates remove.

** Shield No. 1

*** Shield No. 2

NOTE: Data plotted in Fig. 3-3.

TABLE 11

Variation of Shield Weight
with Boron Concentration

(Based upon Configuration of Shield No. 2)

Boron Concentration (%)	γ Radiation Intensity Γ_e (Relative Units)	Ratio:* Γ_e/Γ_a	Change in Lead Thickness (cm)**	Wt. of Shield, Less Increase in Wt. due to Increased Density of Solution	Minimum Increase in Wt. by Addition of B_2O_3 (lb)	Minimum Increase in Wt. by Addition of $KOH+B_2O_3$ (lb)
0.0	1	4.51	+ 4.38	150,500		
0.1	.42	1.91	+ 1.94	137,500		
0.2	.30	1.36	+ 0.92	132,200	150	400
0.4	.22 = Γ_a	1.00	0	127,600	300	800
0.6	.193	.877	- 0.39	125,600	500	1,200
1.0	.155	.705	- 1.05	122,500	850	2,000
1.25				(121,700)***		2,600
1.5				(121,200)		3,100
2.0				(120,700)		4,100
5.0	.119	.541	- 1.84	119,200		10,300
10.0	.115	.523	- 1.94	118,800		20,500

* Γ_e is the γ intensity of a given boron concentration; Γ_a is the γ intensity at 0.4% boron concentration.

** "+" indicates add, "-" indicates remove.

*** Values enclosed in parentheses are interpolated.

NOTE 1: To find weight of borated-water shield add the proper value of either column 6 or column 7 to the weight given in column 5.

NOTE 2: Data plotted in Fig. 3-4.

APPENDIX B

Effectiveness of the Boron Solution

H. E. Hungerford

APPENDIX B

THE EFFECTIVENESS OF THE BORON SOLUTION

Boration of the water within the shield suppresses the production of secondary gammas by virtue of the relatively large cross-section boron has for the (n,γ) reaction. This process is accompanied by the emission of a single 0.49-Mev gamma ray which is readily absorbed by the shield; hence neutrons are removed which could otherwise generate hard gammas by other processes such as capture or inelastic scattering.

It has now to be determined what is the correct amount of boration for a lead-water unit shield. This can be done by extrapolation of the experimental data.

One may regard the gamma radiation emerging from the shield as composed of two parts: (1) radiation generated within the reactor, and (2) radiation generated within the shield.

Let Γ = the radiation emerging from shield

Γ_R = the radiation produced within the reactor (primary gammas)

Γ_S = the radiation produced within the shield (secondary gammas)

Then, if there is no boration,

$$\Gamma = \Gamma_R + \Gamma_S$$

If there is boration of the water, then Γ_S, the secondary gamma radiation will be reduced by the amount

$$\frac{\varepsilon_H}{\varepsilon_H + \varepsilon_B}$$

where: Σ_H is the macroscopic thermal neutron absorption cross-section for hydrogen, and

Σ_B is the macroscopic thermal neutron absorption cross-section for boron

Then

$$\Gamma = \Gamma_R + \Gamma_S \left(\frac{\Sigma_H}{\Sigma_H + \Sigma_B} \right)$$

$$= \Gamma_R + \Gamma_S \left(\frac{1}{1 + \Sigma_B / \Sigma_H} \right)$$

The ratio Σ_B / Σ_H may be evaluated as follows:

Let P = the percentage by weight of boron. Then, since the weight percent of oxygen in B_2O_3 is 2.2 times the weight percent of boron,

$\frac{100 - P - 2.2\,P}{100} = 1 - .032\,P$ = the percentage by weight of water.

Then

$$\Sigma_B = \frac{P}{100} \cdot \frac{No\, \sigma_B\, \rho}{M_B}, \text{ and}$$

$$\Sigma_H = (1 - .032\,P)\, \frac{No\, \sigma_H\, \rho}{M_H}$$

$$\frac{\Sigma_B}{\Sigma_H} = \frac{P}{100} \left(\frac{\sigma_B}{2\,\sigma_H} \right) \left(\frac{M_{H_2O}}{M_B} \right) \left(\frac{1}{1 - .032\,P} \right)$$

where

No = Avogadros' Number

P = density of the solution

M = molecular weight

σ = thermal neutron cross-sections

Substituting numerical values

$$\frac{\Sigma_B}{\Sigma_H} = \frac{P}{100}\left(\frac{715}{2\times 0.32}\right)\left(\frac{18}{10.82}\right)\left(\frac{1}{1 - .032\,P}\right)$$

$$= \frac{18.6\,P}{1 - .032\,P}$$

Therefore

$$\Gamma = \Gamma_R + \Gamma_S\left(\frac{1}{1 + 18.6\,P/1 - .032\,P}\right)$$

$$\approx \Gamma_R + \Gamma_S\left(\frac{1 - .032\,P}{1 + 18.6\,P}\right)$$

Using this formula, the BSF gamma radiation data at various concentrations was analyzed for several distances from the shield. Experimental values of Γ were plotted against the value of $\frac{1 - .032\,P}{1 + 18.6}$ for the concentrations 0, 0.1, 0.2, and 0.4 percent B. A straight line was drawn through the points to represent the function. The value of Γ_R was determined by extrapolation of the curve to 0. From this the value of Γ_S was determined by subtracting Γ_R from the value of Γ_o at P = 0. The curves representing these functions are shown in Fig. B-1.

The average ratio Γ_R/Γ_S, the ratio of gammas produced by the reactor to the gammas produced within the shield, turns out to be 0.13, which means that the gammas from the reactor are contributing only 11 per cent to the total emergent gamma flux from the shield.

To determine how effective the boron is in reducing the gamma radiation, it is necessary only to plot the ratio Γ_R/Γ for various boron concentrations. This ratio will be smallest at 0 per cent of boron and will increase to a

value of 1 when the concentration of boron is infinite. A plot of Γ_R/Γ against P is shown in Fig. B-2. On the same graph is shown a plot of the ratio Γ/Γ_o, where Γ_o is the gamma flux without boron.

The maximum concentration physically possible is 0.6 per cent. At this point the reduction of gammas over that accomplished by using a 0.4 per cent solution is only 12 per cent. If it were possible to achieve infinite concentrations, the reduction of gammas would only be by another factor of 2.

Thus it seems that the concentration 0.4 per cent B used in the experiment was entirely adequate. The reduction of gammas by this concentration is nearly a factor of 5. Increasing the concentration by 50 per cent would give only 12 per cent more reduction in gammas, as was already pointed out, which did not justify its use in the experiment.

Moreover, from the point of view of settling and sedimentation problems, the 0.4 per cent solution was best. Experiments made on this point indicated that 0.4 per cent solution was as high a concentration as could be used without excessive settling out of the boron and excess chemical reactions with structural elements, such as iron.

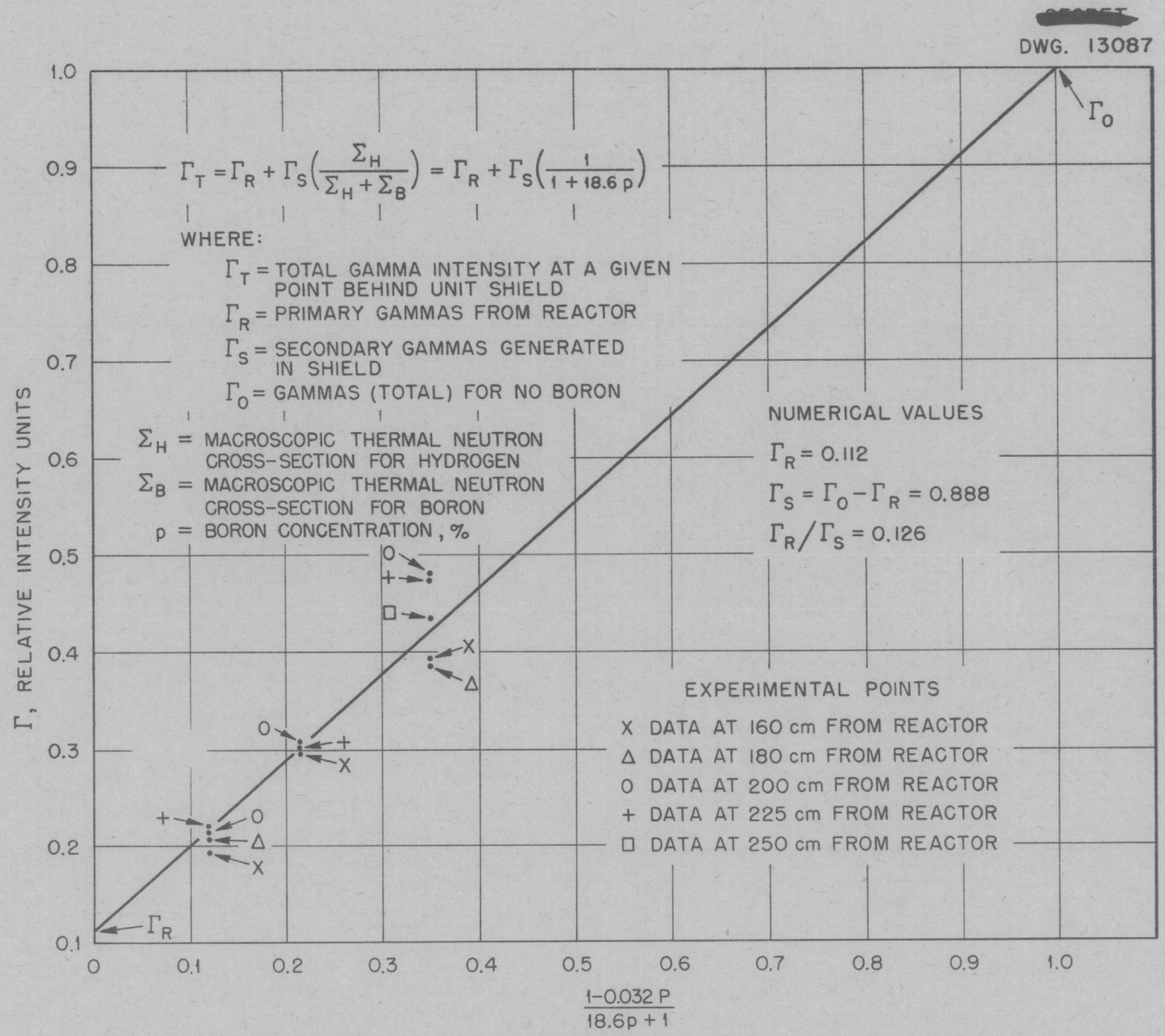

FIG. B-1 GAMMA-INTENSITIES AS A FUNCTION OF BORON CONCENTRATION, EXPERIMENTAL DATA

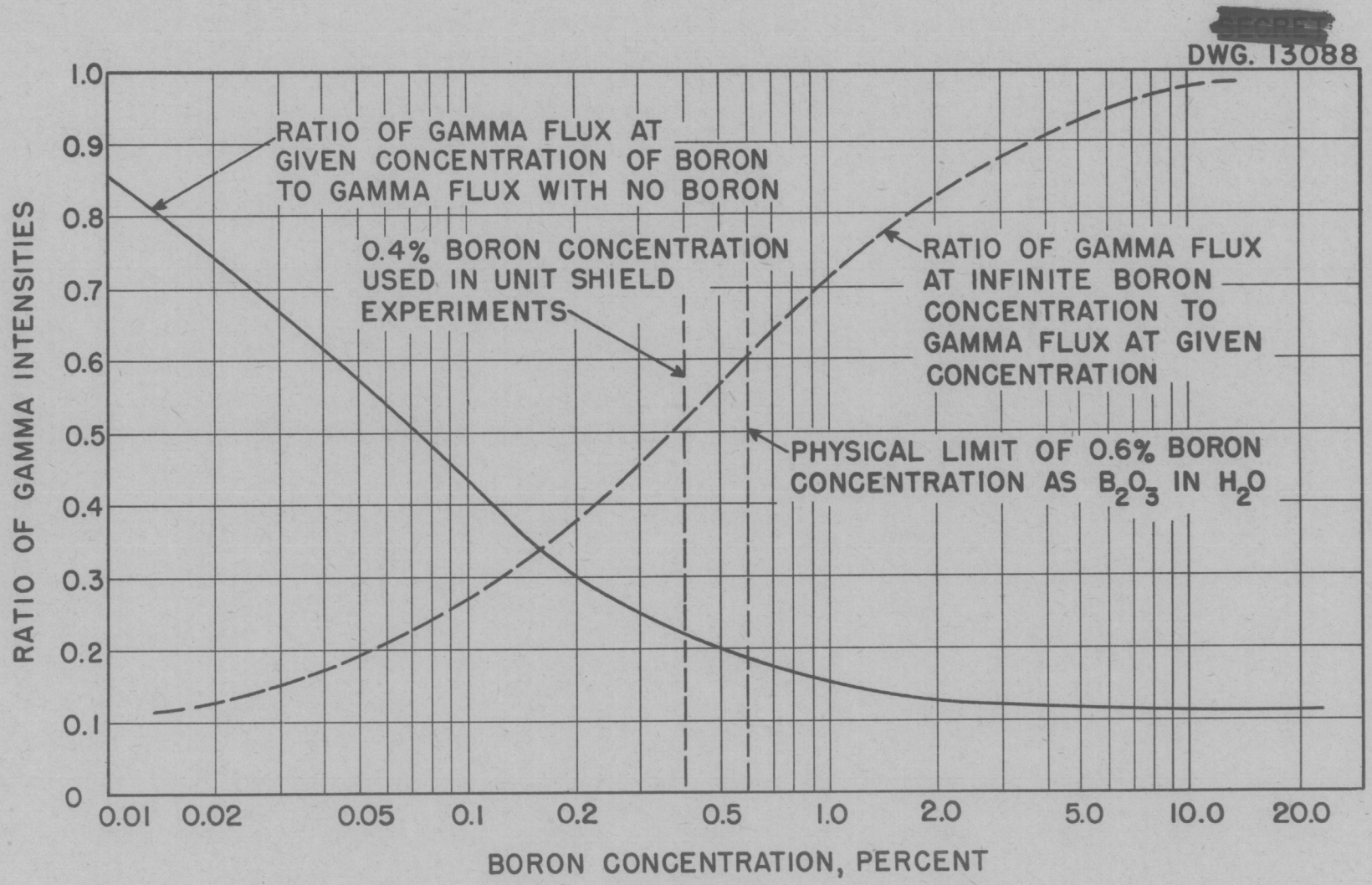

FIG. B-2 GAMMA FLUX RATIOS AS A FUNCTION OF BORON CONCENTRATION - EXTRAPOLATION OF EXPERIMENTAL DATA

APPENDIX C

Power Calculations of the Unit Shield Reactor

E. B. Johnson

(This memorandum has appeared as CF 51-9-112)

SECRET

Intra-Laboratory Correspondence

OAK RIDGE NATIONAL LABORATORY

To: J. L. Meem September 18, 1951

From: E. B. Johnson

Re: Power Calculations of the Unit Shield Reactor

Neutron flux measurements have been made in the water reflected reactor and the power distribution calculated*. In the process of taking measurements on the unit shield with the various instruments, it became obvious that another measurement of the flux and power distribution in the reactor at its position against the unit shield mock-up would be necessary. These measurements have been completed and the results are reported herein.

The reactor loading was the same as when the previous determination was made; a 5 x 5 lattice of fuel elements with water reflector on five sides and a permanent beryllium-oxide reflector on the back (south) side. However, when the reactor was in place against the unit shield, there was only about one inch of water between its north face and the borated water of the shield. As will be seen, this made a difference in the neutron flux patterns within the reactor, particularly along the north face.

Since the method of exposing the gold foils has been to fasten the foils on the outer surfaces of the fuel elements where flux measurements are desired, it was necessary to substitute "cold" elements of essentially the same U-235 content for those which had been in the reactor since the earlier calibrations. No such elements were available to replace those in positions 6 and 7 in the lattice, therefore it had to be determined experimentally whether the flux distribution was symmetrical around the n-s centerline of the reactor so that the measurements made in positions 3 and 4 could be used interchangeably with those in 6 and 7. Table 1 shows the results of this check in which bare gold foils were exposed on the fuel elements in positions 3, 4, and 5 and the saturated activities compared with those observed in previous exposures in positions 5, 6, and 7. The agreement was good.

Table 2 is a summary of all new experimental data taken on this lattice. It will be noted that cadmium difference measurements were made only along the north face of the reactor. The assumption was made that the cadmium ratio within the reactor would change too little (if at all) to make repetition of

---

* Meem, J. L. and E. B. Johnson, "Determination of the Power of the Shield-Testing Reactor - I. Neutron Flux Measurements in the Water-Reflected Reactor", ORNL-1027, August, 1951.

the cadmium difference measurements necessary. Consequently only total activities were measured inside the reactor. The method of calculation was the same as previously described. Symmetry around the north-south centerline and around midplane was assumed.

Table 3 shows the thermal neutron flux at the indicated positions within the reactor. To obtain most of these values (all values in parentheses), it was necessary to assume a cadmium ratio for each position. Values of the cadmium ratios not in parentheses were obtained experimentally either in the present or the previous calibration.

Table 4 shows the flux in the center of each quarter element as indicated and the "average" flux for the entire fuel element in each position.

In Table 5 are listed the amount of U-235 in each fuel element, the "average" thermal neutron flux, and the corresponding power per fuel element.

For purposes of comparison, Table 6 shows the corresponding data from the previous power calibration without the unit shield. This table is idential to Table 4 in ORNL-1027 except that the power generated in each row is also included. Fig. 1 shows a comparison of the power distribution by rows in the two reactors.

Since the leakage calculations require the average thermal flux for each plane perpendicular to the north-south centerline, these are given for both reactors in Table 7. In this table, nv_o for Row 00 refers to the average thermal neutron flux through the plane at the north face of the fuel elements in Row 00; while nv_m for Row 00 refers to the average flux through the plane at the center of the fuel in this row. Fig. 2 is a comparison of these values in the two reactors.

The total power of the reactor as calculated in this experiment is approximately 3% below the previous calibration, while the power generated in the north row of fuel elements is 16% below its value when the reactor was not against the unit shield.

TABLE I

Comparison of East and West Sides of Reactor - 100% H_2O

Assembly Face	Vertical Position on Assembly	West Side		East Side	
		Lattice Position	A_s Total	Lattice Position	A_s Total
North	CL	(3)	6.556×10^5	(7)	6.594×10^5
	6" above CL		5.036×10^5		5.346×10^5
	12" above CL		2.796×10^5		2.925×10^5
	6" below CL		5.363×10^5		5.420×10^5
	12" below CL		2.848×10^5		2.944×10^5
South	CL	(3)	7.297×10^5	(7)	7.334×10^5
South	CL	(4)	9.478×10^5	(6)	1.037×10^6
North	CL	(5)	9.831×10^5	(5)	1.007×10^6
	6" above CL		8.251×10^5		8.203×10^5
	12" above CL		4.499×10^5		4.371×10^5
	6" below CL		8.627×10^5		8.435×10^5
	12" below CL		4.556×10^5		4.551×10^5
South	CL	(5)	1.078×10^6	(5)	1.058×10^6

[redacted]

TABLE 2

Summary of Gold Foil Measurements in Lattice

Lattice Position	Assembly Face	Vertical Position on Assembly	A_s Total	A_s Epicadmium	A_s Thermal	Cadmium Ratio
(3)	North	CL	5.433×10^5	1.263×10^5	4.170×10^5	4.30
		6" above CL	4.263×10^5			
		6" below CL	4.495×10^5			
		12" above CL	2.384×10^5	3.816×10^4	2.002×10^5	6.25
		12" below CL	2.614×10^5	3.958×10^4	2.218×10^5	6.60
(3)	South	CL	7.127×10^5			
		6" above CL	5.630×10^5			
		6" below CL	5.919×10^5			
		12" above CL	3.731×10^5			
		12" below CL	3.381×10^5			
(4)	North	CL	7.519×10^5	1.853×10^5	5.666×10^5	4.06
		6" above CL	6.005×10^5			
		6" below CL	6.289×10^5	1.519×10^5	4.770×10^5	4.14
		12" above CL	3.534×10^5	5.603×10^4	2.974×10^5	6.31
		12" below CL	3.704×10^5	5.735×10^4	3.130×10^5	6.46
(4)	South	CL	9.393×10^5			
		6" above CL	7.595×10^5			
		6" below CL	7.692×10^5			
		12" above CL	5.210×10^5			
		12" below CL	5.069×10^5			
(5)	North	CL	7.486×10^5	2.067×10^5	5.419×10^5	3.62
		6" above CL	6.371×10^5			
		6" below CL	6.980×10^5	1.692×10^5	5.288×10^5	4.12
		12" above CL	3.653×10^5	6.353×10^4	3.018×10^5	5.75
		12" below CL	4.032×10^5	6.538×10^4	3.378×10^5	6.17
(5)	South	CL	1.006×10^6			
		6" above CL	7.926×10^5			
		6" below CL	8.643×10^5			
		12" above CL	5.479×10^5			
		12" below CL	5.744×10^5			
(25)	North	CL	1.341×10^6			
		6" above CL	1.048×10^6			
		6" below CL	1.099×10^6			
		12" above CL	6.823×10^5			
		12" below CL	6.964×10^5			

(Con't.)

Table 2 (Continued)

Lattice Position	Assembly Face	Vertical Position on Assembly	A_s Total
(25)	South	CL	1.704×10^6
		6" above CL	1.181×10^6
		6" below "	1.382×10^6
		12" above "	6.451×10^5
		12" below "	7.598×10^5
(27)	North	CL	9.183×10^5
		6" above CL	7.340×10^5
		6" below "	7.799×10^5
		12" above "	4.776×10^5
		12" below "	4.886×10^5
(27)	South	CL	9.712×10^5
		6" above CL	7.718×10^5
		6" below "	8.057×10^5
		12" above "	4.901×10^5
		12" below "	5.342×10^5
(45)	North	CL	1.551×10^6
		6" above CL	1.110×10^6
		6" below "	1.242×10^6
		12" above "	5.105×10^5
		12" below "	7.073×10^5
(45)	South	CL	1.158×10^6
		6" above CL	9.210×10^5
		6" below "	1.001×10^6
		12" above "	5.382×10^5
		12" below "	5.934×10^5
(46)	North	CL	1.173×10^6
		6" above CL	9.302×10^5
		6" below "	9.499×10^5
		12" above "	5.847×10^5
		12" below "	6.229×10^5
(46)	South	CL	1.102×10^6
		6" above CL	7.038×10^5
		6" below "	9.460×10^5
		12" above "	5.066×10^5
		12" below "	5.463×10^5

(Continued)

Table 2 (Continued)

Lattice Position	Assembly Face	Vertical Position on Assembly	A_s Total
(47)	North	CL	8.771×10^5
		6" above CL	6.919×10^5
		6" below "	7.110×10^5
		12" above "	4.458×10^5
		12" below "	4.550×10^5
(47)	South	CL	8.519×10^5
		6" above CL	6.634×10^5
		6" below "	7.449×10^5
		12" above "	3.956×10^5
		12" below "	4.112×10^5

TABLE 3

Neutron Traverses Through the Reactor

North Side of Lattice Position	A_s Total	A_s Epicadmium	A_s Thermal	nv_{th}	Cd Ratio
05-0	7.486×10^5	2.067×10^5	5.419×10^5	4.877×10^6	3.62
15-0	1.006×10^6	(3.31×10^5)	(6.75×10^5)	(6.07×10^6)	3.04*
25-0	1.341×10^6	(4.16×10^5)	(9.25×10^5)	(8.32×10^6)	3.22*
35-0	1.704×10^6	(4.38×10^5)	(1.27×10^6)	(1.14×10^7)	3.89*
45-0	1.551×10^6	(3.90×10^5)	(1.16×10^6)	(1.04×10^7)	3.98*
55-0	1.158×10^6	(3.21×10^5)	(8.37×10^5)	(7.53×10^6)	3.61*
05-6	6.675×10^5	1.675×10^5	5.000×10^5	4.500×10^6	3.98
15-6	8.284×10^5	(2.07×10^5)	(6.21×10^5)	(5.59×10^6)	(4.0)
25-6	1.073×10^6	(2.62×10^5)	(8.11×10^5)	(7.30×10^6)	(4.1)
35-6	1.281×10^6	(2.78×10^5)	(1.00×10^6)	(9.00×10^6)	(4.6)
45-6	1.176×10^6	(2.45×10^5)	(9.31×10^5)	(8.38×10^6)	(4.8)
55-6	9.610×10^5	(2.09×10^5)	(7.52×10^5)	(6.77×10^6)	(4.6)
05-12	3.842×10^5	6.445×10^4	3.197×10^5	2.877×10^6	5.96
15-12	5.611×10^5	(9.20×10^4)	(4.69×10^5)	(4.22×10^6)	(6.1)
25-12	6.893×10^5	(1.17×10^5)	(5.72×10^5)	(5.15×10^6)	(5.9)
35-12	7.024×10^5	(1.17×10^5)	(5.85×10^5)	(5.26×10^6)	(6.0)
45-12	6.089×10^5	(9.51×10^4)	(5.14×10^5)	(4.63×10^6)	(6.4)
55-12	5.658×10^5	(8.44×10^4)	(4.81×10^5)	(4.33×10^6)	(6.7)
06-0	7.519×10^5	1.853×10^5	5.666×10^5	5.099×10^6	4.06
16-0	9.393×10^5	(3.13×10^5)	(6.26×10^5)	(5.63×10^6)	(3.0)
26-0	(1.43×10^6)	(4.47×10^5)	(9.83×10^5)	(8.85×10^6)	(3.2)
36-0	(1.55×10^6)	(4.19×10^5)	(1.13×10^6)	(1.02×10^7)	(3.7)
46-0	1.173×10^6	(3.01×10^5)	(8.72×10^5)	(7.85×10^6)	(3.9)
56-0	1.102×10^6	(2.95×10^5)	(8.07×10^5)	(7.26×10^6)	3.73*
06-6	6.147×10^5	1.502×10^5	4.645×10^5	4.180×10^6	4.09
16-6	7.643×10^5	(1.91×10^5)	(5.73×10^5)	(5.16×10^6)	(4.0)
26-6	(1.23×10^6)	(3.00×10^5)	(9.30×10^5)	(8.37×10^6)	(4.1)
36-6	(1.24×10^6)	(2.76×10^5)	(9.64×10^5)	(8.68×10^6)	(4.5)
46-6	9.400×10^5	(1.96×10^5)	(7.44×10^5)	(6.70×10^6)	(4.8)
56-6	8.249×10^5	(1.75×10^5)	(6.50×10^5)	(5.85×10^6)	(4.7)

(Continued)

TABLE 3 (Con't.)

North Side of Lattice Position	A_s Total	A_s Epicadmium	A_s Thermal	nv_{th}	Cadmium Ratio
06-12	3.619×10^5	5.669×10^4	3.052×10^5	2.747×10^6	6.38
16-12	5.139×10^5	(8.42×10^4)	(4.30×10^5)	(3.87×10^6)	(6.1)
26-12	(6.6×10^5)	(1.12×10^5)	(5.48×10^5)	(4.93×10^6)	(5.9)
36-12	(6.8×10^5)	(1.13×10^5)	(5.67×10^5)	(5.10×10^6)	(6.0)
46-12	6.038×10^5	(9.43×10^4)	(5.09×10^5)	(4.58×10^6)	(6.4)
56-12	5.264×10^5	(7.86×10^4)	(4.48×10^5)	(4.03×10^6)	(6.7)
07-0	5.433×10^5	1.263×10^5	4.170×10^5	3.753×10^6	4.30
17-0	7.127×10^5	(2.37×10^5)	(4.76×10^5)	(4.28×10^6)	(3.0)
27-0	9.183×10^5	(2.87×10^5)	(6.31×10^5)	(5.68×10^6)	(3.2)
37-0	9.712×10^5	(2.73×10^5)	(6.98×10^5)	(6.28×10^6)	3.56*
47-0	8.771×10^5	(2.25×10^5)	(6.52×10^5)	(5.87×10^6)	(3.9)
57-0	8.519×10^5	(2.10×10^5)	(6.42×10^5)	(5.78×10^6)	4.05*
07-6	4.379×10^5	(1.09×10^5)	(3.29×10^5)	(2.96×10^6)	(4.0)
17-6	5.774×10^5	(1.44×10^5)	(4.33×10^5)	(3.90×10^6)	(4.0)
27-6	7.569×10^5	(1.85×10^5)	(5.72×10^5)	(5.15×10^6)	(4.1)
37-6	7.887×10^5	(1.79×10^5)	(6.10×10^5)	(5.49×10^6)	(4.4)
47-6	7.014×10^5	(1.46×10^5)	(5.55×10^5)	(4.99×10^6)	(4.8)
57-6	7.041×10^5	(1.44×10^5)	(5.60×10^5)	(5.04×10^6)	(4.9)
07-12	2.499×10^5	3.887×10^4	2.110×10^5	1.899×10^6	6.43
17-12	3.556×10^5	(5.83×10^4)	(2.97×10^5)	(2.67×10^6)	(6.1)
27-12	4.831×10^5	(8.19×10^4)	(4.01×10^5)	(3.61×10^6)	(5.9)
37-12	5.121×10^5	(8.53×10^4)	(4.27×10^5)	(3.84×10^6)	6.00*
47-12	4.504×10^5	(7.04×10^4)	(3.80×10^5)	(3.42×10^6)	(6.4)
57-12	4.034×10^5	(5.99×10^4)	(3.43×10^5)	(3.09×10^6)	6.73*

( ) Interpolated from curves.

* From 2nd lattice measurements.

TABLE 4

Thermal Neutron Flux

Center of Lattice Position	Quarter Elements Bounded by Midplane and 6 inch Plane	Quarter Elements Bounded by 6 inch Plane and 12 inch Plane	Average nv_{th} per Element
05	5.259×10^6	4.297×10^6	4.778×10^6
15	6.820×10^6	5.565×10^6	6.192×10^6
25	9.005×10^6	6.677×10^6	7.841×10^6
35	9.795×10^6	6.817×10^6	8.306×10^6
45	8.270×10^6	6.027×10^6	7.148×10^6
06	5.017×10^6	3.989×10^6	4.503×10^6
16	7.002×10^6	5.582×10^6	6.292×10^6
26	9.025×10^6	6.770×10^6	7.897×10^6
36	8.357×10^6	6.265×10^6	7.311×10^6
46	6.915×10^6	5.290×10^6	6.102×10^6
07	3.723×10^6	2.857×10^6	3.290×10^6
17	4.75×10^6	3.832×10^6	4.291×10^6
27	5.650×10^6	4.522×10^6	5.086×10^6
37	5.657×10^6	4.435×10^6	5.046×10^6
47	5.420×10^6	4.135×10^6	4.777×10^6

[redacted]

TABLE V

Lattice Position	G Grams of U^{235}	Average nv_{th} per Element	P Power in Watts per Fuel Element	Power in Watts by Rows
03	137.37	3.290×10^6	.01782	.1100
04	137.74	4.503×10^6	.02446	
05	138.00	4.778×10^6	.02601	
06	136.48	4.503×10^6	.02424	
07	135.04	3.290×10^6	.01752	
13	138.54	4.291×10^6	.02345	.1502
14	139.98	6.292×10^6	.03474	
15	138.54	6.192×10^6	.03383	
16	139.95	6.292×10^6	.03473	
17	138.41	4.291×10^6	.02342	
23	134.90	5.086×10^6	.02706	.1408
24	69.70	7.897×10^6	.02171	
25	139.48	7.841×10^6	.04313	
26	69.08	7.897×10^6	.02151	
27	136.39	5.086×10^6	.02736	
33	139.20	5.046×10^6	.02770	.1572
34	137.59	7.311×10^6	.03967	
35	69.14	8.306×10^6	.02265	
36	138.00	7.311×10^6	.03979	
37	137.55	5.046×10^6	.02737	
43	134.90	4.777×10^6	.02541	.1569
44	137.53	6.102×10^6	.03310	
45	138.28	7.148×10^6	.03898	
46	138.54	6.102×10^6	.03334	
47	138.22	4.777×10^6	.02604	
		Total	.7151	

[redacted]

TABLE 6

Lattice Position	G Grams of U^{235}	Average $n\nu_{th}$ per Element	P Power in Watts	Power Per Row
03	137.37	3.755×10^6	0.02034	
04	137.74	5.265×10^6	0.02860	
05	137.39	5.645×10^6	0.03059	
06	136.48	5.265×10^6	0.02834	0.1279
07	135.02	3.755×10^6	0.02000	
13	138.54	4.325×10^6	0.02363	
14	139.98	6.42×10^6	0.03544	
15	138.54	6.20×10^6	0.03388	
16	139.95	6.42×10^6	0.03544	0.1520
17	138.41	4.325×10^6	0.02361	
23	134.90	5.135×10^6	0.02732	
24	69.70	7.93×10^6	0.02180	
25	139.98	8.09×10^6	0.04466	
26	69.08	7.93×10^6	0.02160	0.1430
27	136.39	5.135×10^6	0.02762	
33	139.95	5.06×10^6	0.02792	
34	137.19	7.27×10^6	0.03934	
35	69.14	8.72×10^6	0.02378	
36	137.19	7.27×10^6	0.03934	0.1579
37	138.10	5.06×10^6	0.02756	
43	134.90	4.765×10^6	0.02535	
44	137.53	6.08×10^6	0.03298	
45	138.54	7.23×10^6	0.03950	
46	138.54	6.08×10^6	0.03322	0.1570
47	138.22	4.765×10^6	0.02598	
			0.7378	

TABLE 7

Row	Average nv_{th}			
	With Unit Shield		Without Unit Shield	
	nv_o	nv_m	nv_o	nv_m
00	3.616×10^6	4.074×10^6	4.802×10^6	4.738×10^6
10	4.531×10^6	5.473×10^6	4.674×10^6	5.537×10^6
20	6.415×10^6	6.762×10^6	6.399×10^6	6.844×10^6
30	7.109×10^6	6.605×10^6	7.289×10^6	6.678×10^6
40	6.100×10^6	5.782×10^6	6.067×10^6	5.787×10^6
50	5.464×10^6		5.506×10^6	

DWG 12510

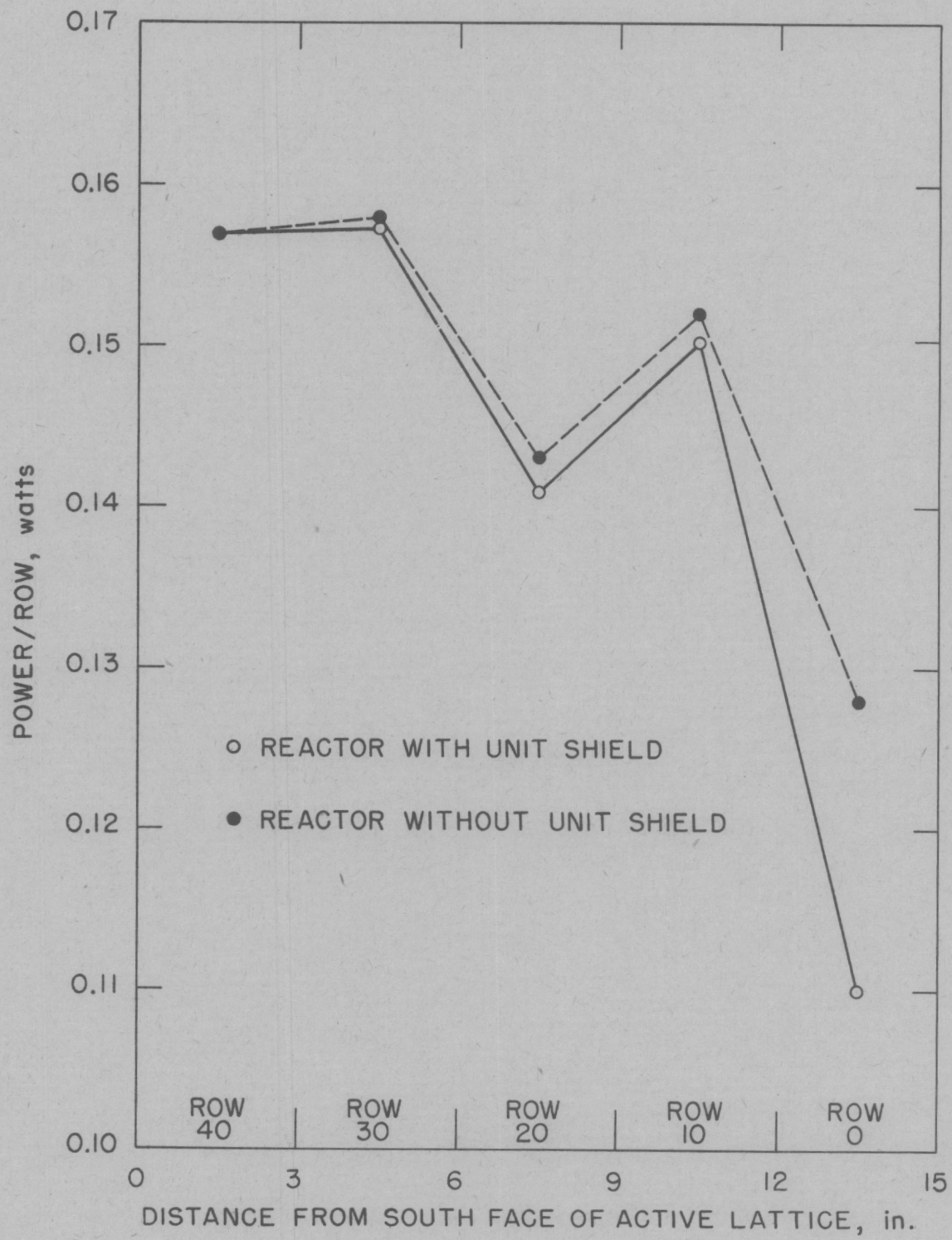

FIG. C-1 - POWER DISTRIBUTION THROUGH THE BULK SHIELDING REACTOR

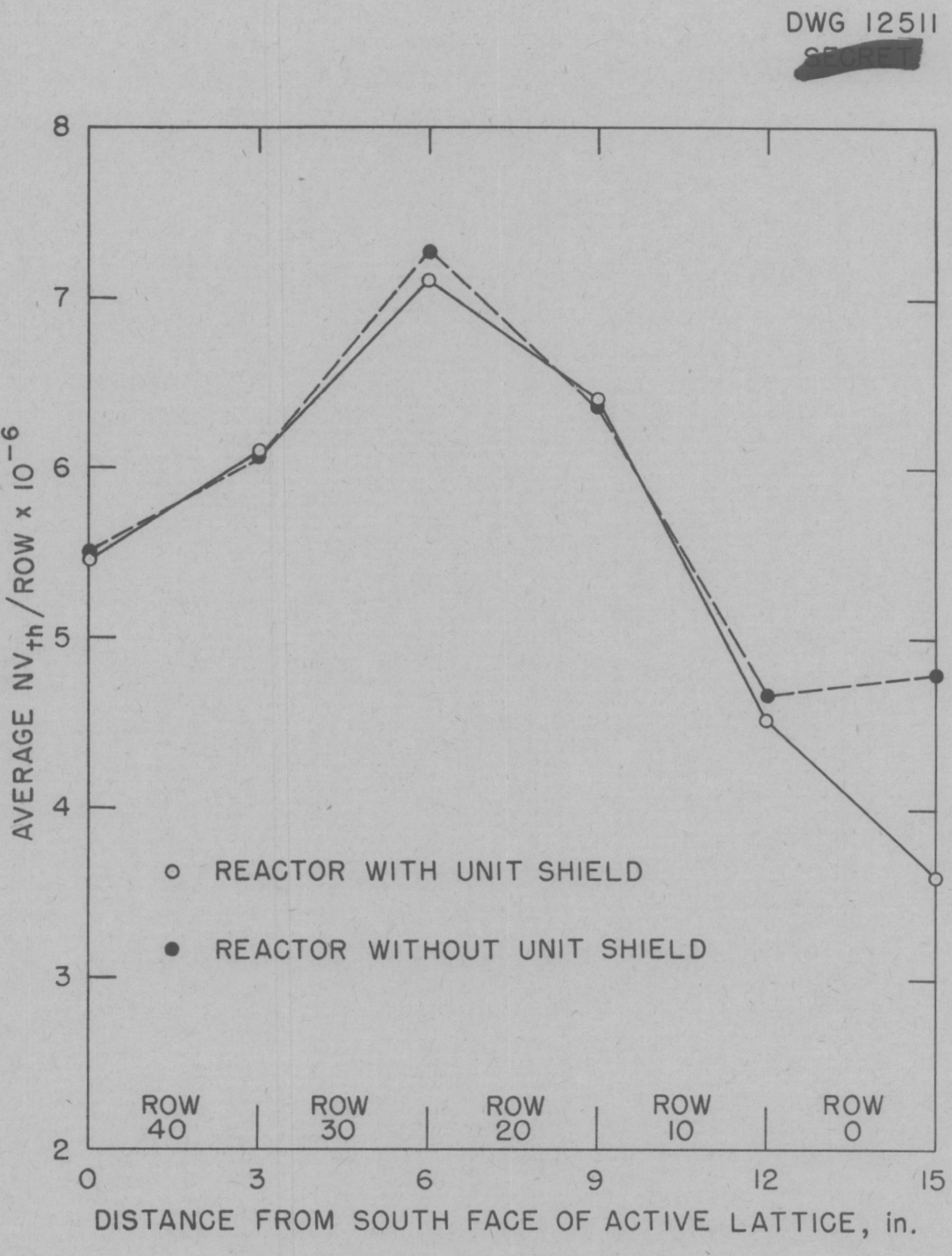

FIG. C-2 - THERMAL NEUTRON FLUX DISTRIBUTION THROUGH THE BULK SHIELDING REACTOR

APPENDIX D

Calculations of Leakage from the Bulk Shielding Reactor

H. E. Hungerford
J. L. Meem

(This memorandum has appeared as CF 51-10-94)

OAK RIDGE NATIONAL LABORATORY

To: E. P. Blizard

From: H. E. Hungerford and J. L. Meem

Re: CALCULATIONS OF LEAKAGE FROM THE BULK SHIELDING REACTOR

I. Outline of the Method

The thermal neutron flux patterns throughout the water reflected Bulk Shielding Reactor at the Bulk Shielding Facility have been determined by Meem and Johnson[1]. From these measurements one is able to calculate the leakage of nuclear radiations from any face of the reactor. Calculations below are for the north face since all measurements are made away from this face. Figure 1 is a schematic view of the north face of the Bulk Shielding Reactor showing the first 2 of the 5 rows of fuel elements.

The leakage from a reactor is given closely by[2]:

$$(1)\quad \mathcal{L} = F \int_{Z_o}^{Z_1} P(Z)\, e^{-Z/\lambda}\, dZ,$$

where F is a factor converting from power produced to the appropriate type of radiation dosage escaping,

Z is the distance inward from a given surface of the reactor,

$P(Z)$ is the power per unit distance produced along Z,

Z_o and Z_1 are appropriate limits of integration,

λ is the relaxation length of the escaping radiation.

---

(1) Meem, J. L. and Johnson, E. B., "Determination of the Power of the Shield Testing Reactor", ORNL-1027.

(2) Method due to E. P. Blizard in Shielding Board Report, ANP-53.

SECRET

DWG. 12604

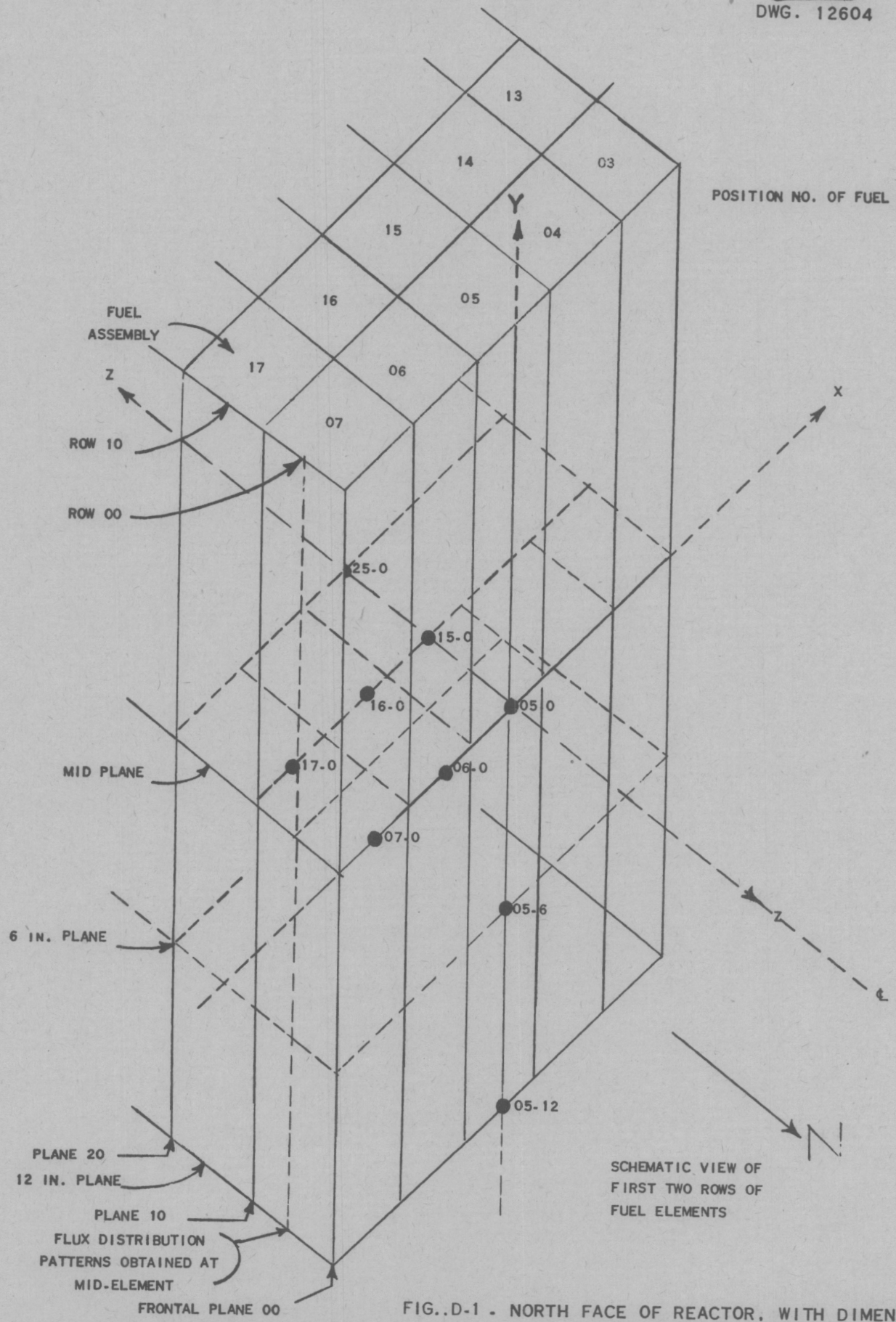

FIG. D-1 . NORTH FACE OF REACTOR, WITH DIMENSIONS AND POSITIONS MARKED

In the following calculations the function P(Z) is represented as a straight line function for each row of fuel elements. This function depends upon the thermal neutron flux and the amount of fissionable material within the row. P(Z) takes the form:

$$P(Z) = P_o + mZ, \tag{2}$$

where P_o is the power per unit distance at the north side of the row, and m is the slope of the power production within the row.

The leakage for each row is calculated and summed over all rows to obtain the total leakage.

II. The Effect of the Presence of the Borated Water Shield on the Reactor

During the experiments upon the borated water unit shield mock-up, it soon became apparent that the proximity of the borated water to the reactor was affecting the operation of the reactor and the measurements on the shield. The boron was absorbing many neutrons which normally would be reflected back in to the reactor, thus lowering the power production near the edge of the reactor. There arose the necessity of obtaining new measurements of the thermal neutron flux distribution within the reactor from which a new power calculation could be made. These measurements are reported by Johnson[3]. Figure 2 shows the effect of the borated water upon the flux pattern along the x-axis in the first row of fuel elements.

III. Evaluation of the Function P(Z)

The power produced in each row P_r, is known. The power/unit distance at the center of the row, P_M, is obtained by dividing P_r by the thickness of the row, 7.62 cm. Thus,

$$P_M = P_r/7.62 \tag{3}$$

The power produced within the reactor is given by

$$P = K \cdot nv(th) \cdot G \tag{4}$$

where K is a constant,

nv_{th} is the thermal neutron flux, and

G is the number of grams of fissionable material.

For any given row G is a constant, and the following relationship is true:

$$\frac{P_o}{(nv_{th})_o} = \frac{P_M}{(nv_{th})_M} \tag{5}$$

where the subscripts o and M refer to the north face and the center of the row respectively.

---

(3) Johnson, E. B. to Meem, J. L., "Power Calculations for the Unit Shield Reactor", C.F. #51-9-112

SECRET

DWG. 12605

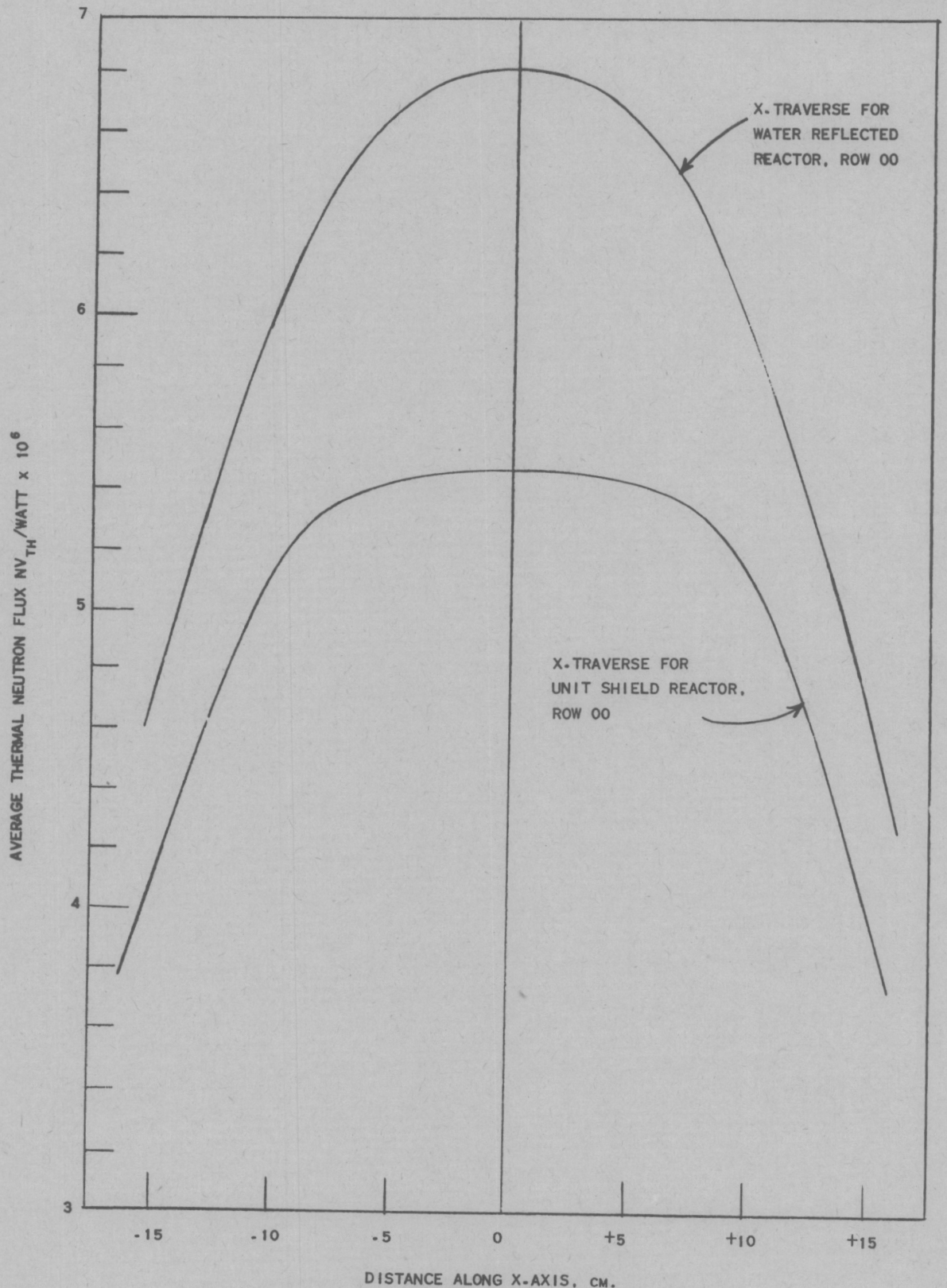

FIG. D-2 - COMPARISON OF THERMAL NEUTRON TRAVERSES ALONG X-AXIS IN MAGNITUDE AND SHAPE FOR THE WATER-REFLECTED AND UNIT-SHIELD REACTORS, FOR ROW 00

Table 1, which is reproduced from Reference 3 for convenience, shows the experimental values of $(nv_{th})_o$ and $(nv_{th})_M$. Since P_M is also known, P_o is found from relationship (5) above. The slope of the power production is found from

$$(6) \qquad m = \frac{P_M - P_o}{L/2} = \frac{P_M - P_o}{3.81}$$

Figure 3 illustrates the method of evaluating P(Z). Table 2 shows the calculations for P_o and m for each row of fuel elements. Figure 4 shows the power per unit distance by rows inward from north face of reactor.

IV. Evaluation of λ, the Relaxation Length of Escaping Radiation for Fast Neutrons

In order to evaluate λ it is necessary to calculate the percentage by volume of each component within the fuel assembly. Values for these calculations were taken from Table 3, which is reproduced in part from ORNL-951(4). Included as part of the fuel assemblies is a 1/32 inch layer of water around each assembly, as there is approximately 1/16 inch space between each element when the elements are in position in the reactor.

A list of the calculated values of the volumes of each component of a fuel assembly is given in Table 4. The total volume of a fuel element, obtained by adding the volumes of each part, is 3828 cm^3. This checks well with the value obtained by using the outside dimensions of a fuel element (adding 1/32 inch water thickness to each side):

$$V = (62.55)(7.70)(7.90) = 3805 \text{ cm}^3 \quad .$$

From the amount of uranium in the core of a fuel plate, the volume of uranium is found by the following calculation:

$$\text{Wt U/plate} = \frac{7.7 \text{ g } U^{235}}{.95} = 8.1 \text{ g}$$

$$\text{Volume of U in fuel element} = \frac{8.10 \text{ g/plate} \times 18 \text{ plates}}{18.9 \text{ g/cm}^3} = 7.7 \text{ cm}^3 \quad .$$

The total volume of 18 fuel plates is therefore composed of the following volumes:

Al	1232.3 cm^3
U	7.7 cm^3

(4) Smith, C. D., Drosten, F. W., and Kerze, F., "Production of Fuel Assemblies for the Materials Testing Reactor Mock-Up Critical Experiments", ORNL-951.

DWG. 12606

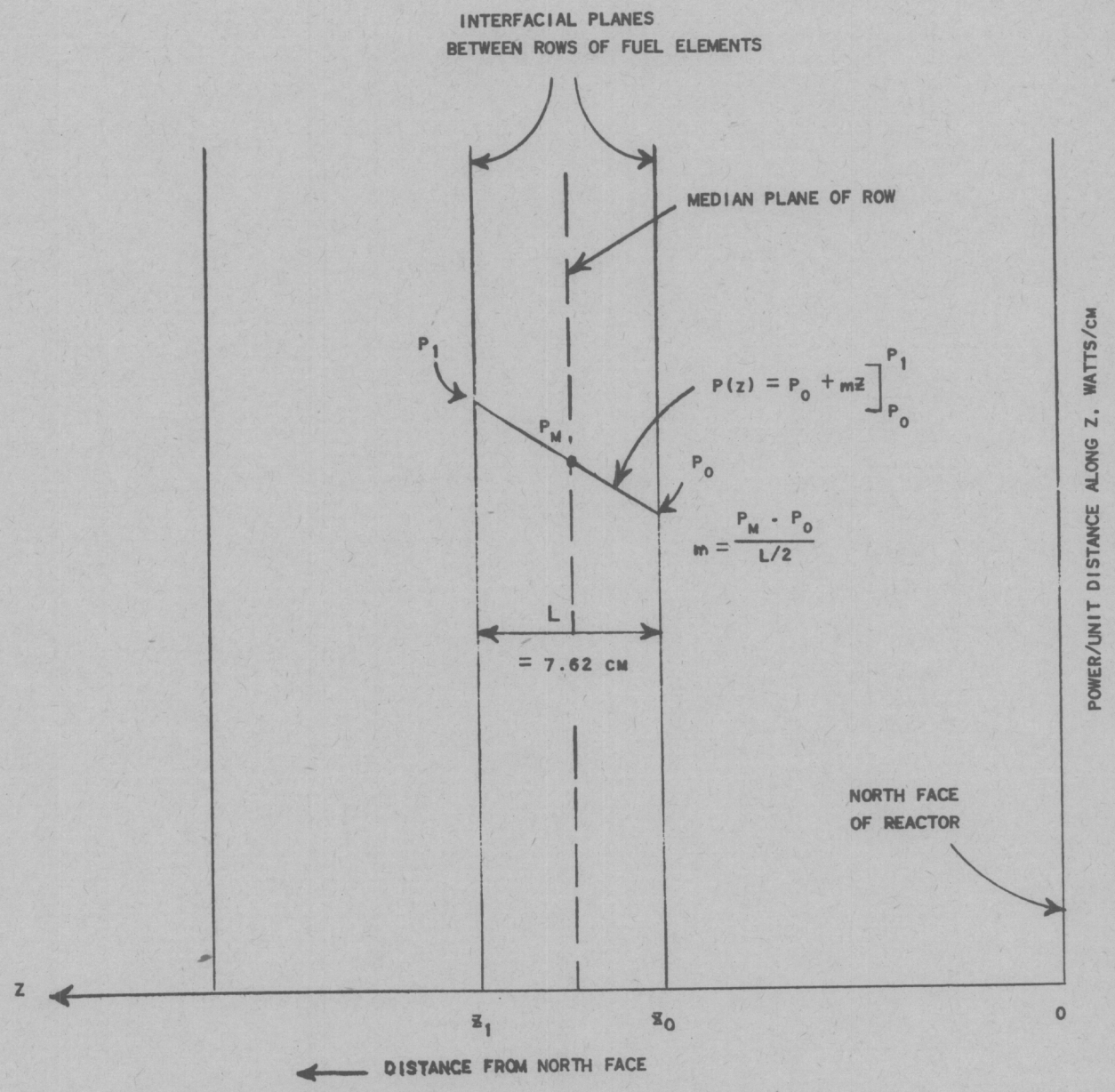

FIG. D-3 - ILLUSTRATING THE METHOD OF OBTAINING THE POWER FUNCTION P(Z) FOR EACH ROW OF FUEL ELEMENTS FOR THE LEAKAGE CALCULATIONS

SECRET

DWG. 12607

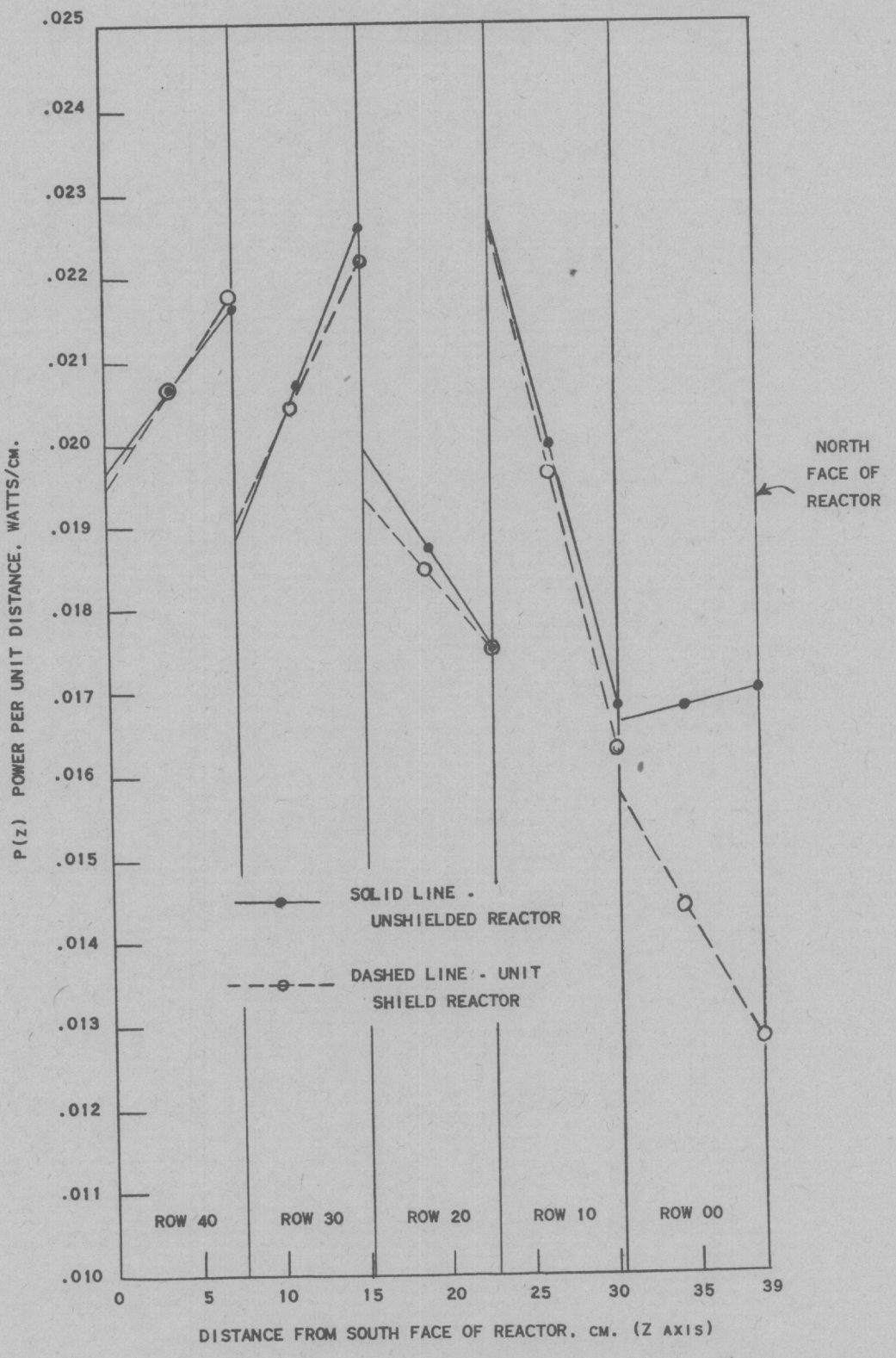

FIG. D-4 - POWER PER UNIT DISTANCE, P(z), IN REACTOR, WATTS/CM (DISTRIBUTION BY ROWS)

The total percentage by volume of each component of a fuel element is now determined from Table 4 and the above tabulations. From these, the macroscopic cross sections and the relaxation length λ for fast neutrons may be calculated. The calculations are presented in the following table(5).

Material	Volume/ Element	Percent by Volume	P, g/cm^3	Mol.Wt.	Mols/cm^3	σ,barns	Σ,cm^{-1}
Al	1588.3	41.5	2.7	27	.0415	1.4	.0350
H_2O	2232	58.3	1.0	18	.0324	3.44	.0671
U	7.7	0.2	18.9	235	.0002	4.2	.001
						ΣT =	.103

Therefore $\lambda = 1/.103 = 9.7$ cm.

Evaluation of the Leakage $\mathscr{L}$

For each row of fuel elements the leakage formula takes the form

$$\mathscr{L}_r/F = \int_{Z_o}^{Z_1} (P_o + mZ)\, e^{-Z/\lambda}\, dZ$$

where Z is the distance from the north face of reactor,

Z_o is the distance of north side of row from north face of reactor,

Z_1 is the distance of south side of row from north face of reactor.

Integration and substitution of the limits gives

$$(7)\quad \mathscr{L}_r/F = (P_o\lambda + m\lambda^2)(e^{-Z_o/\lambda} - e^{-Z_1/\lambda}) + m\lambda\,(Z_o e^{-Z_o/\lambda} - Z_1 e^{-Z_1/\lambda})$$

The numerical calculations of the leakage from each row of the water-reflected and unit shield reactors are listed in Table 5. The leakages per unit area for these reactors are (for each watt of power produced):

Water Reflected Reactor - 7.94×10^{-5} watts/cm^2

Borated Water Unit Shield Reactor - 7.35×10^{-5} watts/cm^2 .

The proximity of the shield lowers the leakage from the reactor by approximately 7.4%.

It is to be noted that the constant F does not need to be evaluated, since these calculations are to be used for comparison purposes only, in conjunction with calculations on the unit shield experiments at the BSF. A similar constant will be found in the leakage expression for the aircraft reactor.

(5) For values of σ, see ANP-53, Appendix F.

TABLE 1

Values of $(nv_{th})_o$ and $(nv_{th})_M$ for the Water Reflected and Unit Shield Reactors

	Water-Reflected Reactor		Borated Water Unit Shield Reactor	
Row	$(nv_{th})_o$	$(nv_{th})_M$	$(nv_{th})_o$	$(nv_{th})_M$
00	4.802×10^6	4.738×10^6	3.616×10^6	4.074×10^6
10	4.674×10^6	5.537×10^6	4.531×10^6	5.473×10^6
20	6.399×10^6	6.844×10^6	6.415×10^6	6.762×10^6
30	7.289×10^6	6.678×10^6	7.109×10^6	6.605×10^6
40	6.067×10^6	5.787×10^6	6.100×10^6	5.782×10^6

TABLE 2

Calculation of the Values of P_o and m for the Water-Reflected and Unit-Shield Reactors

Row	P_F Watts	P_M Watts/cm	$(nv_{th})_o$	$(nv_{th})_M$	P_o Watts/cm.	m
Water Reflected Reactor						
00	.1288	.01678	4.802×10^6	4.738×10^6	.01701	-0.6037×10^{-4}
10	.1520	.01995	4.674	5.537	.01684	+ 8.163
20	.1430	.01877	6.399	6.844	.01755	+ 3.202
30	.1579	.02073	7.289	6.678	.02263	- 4.987
40	.1570	.02061	6.067	5.787	.02161	- 2.625
Borated-Water Unit Shield Reactor						
00	.1100	.01443	3.616×10^6	4.074×10^6	.01281	$+ 4.252 \times 10^{-4}$
10	.1502	.01971	4.531	5.473	.01632	+ 8.898
20	.1408	.01848	6.415	6.762	.01753	+ 2.493
30	.1572	.02063	7.109	6.605	.02220	- 4.121
40	.1569	.02059	6.100	5.782	.02172	- 2.966

TABLE 3

Composition and Dimensions for Bulk Shielding Reactor Fuel Assemblies

Fuel Assembly: Parts	18 curved plates containing fissionable material			
	2 side plates of 2S aluminum			
	Spacing between fuel plates:	0.117 in.		
Fuel Plates: Core Dimensions:	Length	24-5/8 in.	=	62.55 cm.
	Width before curving	2.50 in.	=	6.350 cm.
	Thickness	0.021 in.	=	.05334 cm.
Over-all Dimensions:	Length	24-5/8 in.	=	62.55 cm.
	Width before curving	2.845 in.	=	7.226 cm.
	Thickness	.060 in.	=	.1524 cm.
Composition:	Total U in U-Al Alloy	13.3%		
	U-235 enrichment	95%		
	U-235 content/plate	7.70 gm.		
	Core Al	99.75% pure		
Side Plates: Dimensions:	Length (over active core)	24-5/8 in.	=	62.55 cm.
	Width	3.07 in.	=	7.80 cm.
	Thickness	3/16 in.	=	.4763 cm.
Groove Dimensions: (approximate)	Length	24-5/8 in.	=	62.55 cm.
	Width	3.07 in.	=	7.80 cm.
	Depth	1/8 in.	=	.3175 cm.
Slots Between Fuel Plates for Cooling Water:				
Dimensions:	Length	24-5/8 in.	=	62.55 cm.
	Width	2.595 in.	=	6.591 cm.
	Thickness	0.117 in.	=	0.297 cm.

TABLE 4

Calculation of the Volume of the Components of a Fuel Assembly

Part	Name of Part	Dimensions			No. of Parts	Volume, cm^3
		Length	Width	Thickness		
a	Fuel Plate, Core	62.55 cm.	7.226 cm.	.05334 cm.	18	434
b	Fuel Plate Exterior	62.55 cm.	7.226 cm.	.09906 cm.	18	806
c	Side Plate, including Grooves	62.55 cm.	7.80 cm.	.4763 cm.	2	465
d	Grooves	62.55 cm.	.3175 cm	.1524 cm.	36	109
e	Side Plate, less Grooves					356
f	H_2O Within Fuel Assembly	62.55 cm.	6.591 cm.	.297 cm.	17	2081
g.	H_2O Around Fuel Element	62.55 cm.	7.62 cm.	.0794 cm.	4	151
h	Total Volume	(Sum of Parts a, b, e, f, g)				3828 cm^3

TABLE 5

$\mathcal{L}_r/F$, The Leakage from the North Face of the Bulk Shielding Reactor,
(Watts per Watt of Power Produced)

Row	Water-Reflected Reactor	Borated Water Unit Shield Reactor
00	.08873	.07508
10	.06172	.06240
20	.02582	.02436
30	.00486	.00579
40	.00287	.00264
Totals	.1840 watts	.1703 watts
Leakage/unit area	7.94×10^{-5} watts/cm^2	7.35×10^{-5} watts/cm^2

Area of North Face: 2318 cm^2

APPENDIX E

Thermal Neutron Counter Measurements in Water at the Bulk Shielding Facility

H. E. Hungerford

(This memorandum has appeared as CF 51-5-62)

[redacted]

Intra-Laboratory Correspondence

OAK RIDGE NATIONAL LABORATORY

To: J. Lawrence Meem, Jr. May 4, 1951

From: H. E. Hungerford, Jr.

Re: Thermal Neutron Measurements in Water at the Bulk Shielding Facility

1. Description of Experiment

Experiment 1 in the Bulk Shielding Facility consisted of measurements of the radiation from the reactor in pure water along the centerline as shown in Figure 1. A rectangular coordinate system with its origin at the north face of the reactor was adopted for positioning. The positive directions from the origin are as follows:

X - Horizontal, to the west

Y - Vertical, upward

Z - Horizontal, to the north

Thus the centerline measurements described in this report are along the positive Z axis.

The thermal neutron detecting instruments used are similar to the instruments employed at the Lid Tank, which have been described previously[1]. They are as follows:

1. A 1/2 inch Fission Counter
2. A 3 inch Fission Counter
3. A 1 x 8 inch BF_3 Counter

---

1. ORNL-402, "The ORNL Shield Testing Facility", C. E. Clifford.

CF-50-1-153, "Measurements of Neutron and Gamma Distribution in 100% Water from a 28" Diameter Fission Source", C. E. Clifford.

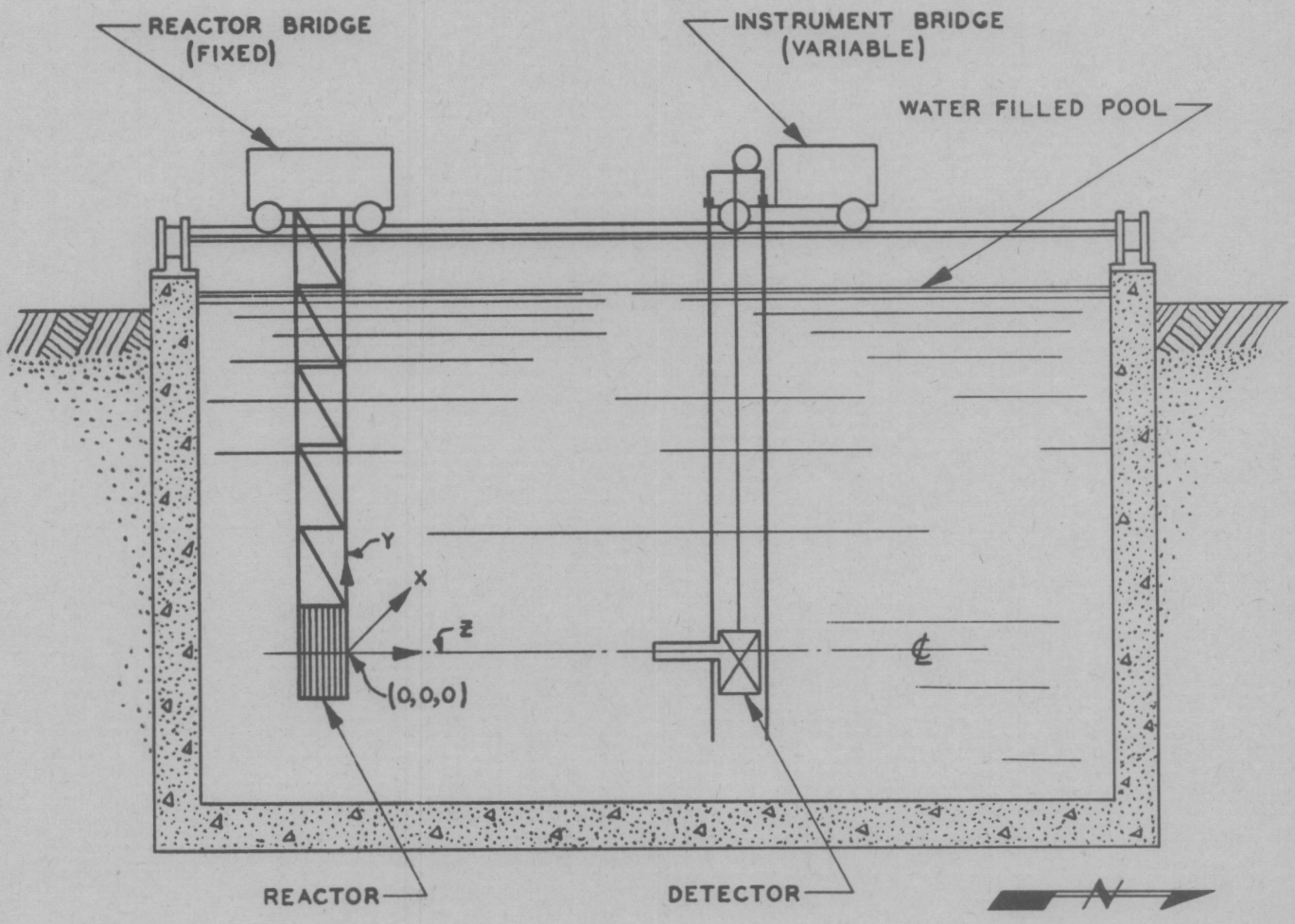

FIG. E-1

BULK SHIELDING FACILITY

METHOD OF OBTAINING

CENTERLINE MEASUREMENTS

DWG.# 11201

4. a 2 x 12 inch BF_3 Single Chamber Counter

5. a 2 x 12 inch BF_3 Double Chamber Counter

The main electronic apparatus for counting is located on the instrument bridge. Watertight cables connect the counters to the instruments on the bridge. Leakage of water into the counter during measurements is prevented by application of a pressure of 12 or more gauge lb/in^2 of dry air at the counter.

The counter-dolly and shaft arrangement for positioning the counters has been described in ORNL-991.[2] The centerline position of the dolly for each instrument was determined prior to the experiment.

For Experiment 1, the north face of the reactor was located in a convenient fixed position. Measurements were obtained by rolling the instrument bridge outward from the reactor, in the positive Z direction.

The Z-distances of the counters were obtained by telescopic means as follows. Mounted on the east and west sides of the pool are identical metric steel tapes. A transit mounted on the instrument bridge rides directly over the west-side tape. A plumb-bob dropped from the axis of the telescope to this tape gives its position. The telescope is then focused on the east-side tape, and the instrument adjusted to bring the cross-hairs to the same reading as the instruments' plumb-bob. A second plumb-bob is dropped from the counter dolly and its position adjusted by means of the telescope to exactly coincide with a known point on the counter. When the cross-hairs of the transit are coincident with the second plumb-bob string, a reading of either scale gives the position of the counter. It was our practice to read both

---

2 ORNL-991, "The New Bulk Shielding Facility at ORNL", W. M. Breazeale

scales simultaneously with the cross-hairs to insure accuracy of transit adjustment. By this method the counters could be positioned accurately to 0.05 cm. Figure 2 illustrates this method of finding Z positions.

The data was taken with the reactor operating at various powers between .7½ watt to 7.½ kilowatts to obtain convenient counting rates. For all points at least two five-minute counts were made, and at least a total of 8000 total counts were obtained. An effort was made to vary the power of the reactor as needed, to keep the counting rate above a few hundred counts per minute.

The raw data obtained from each instrument was corrected for center of sensitivity position[3], and normalized to the data from the 3" fission counter, in counts/min/watt. These results were then normalized in their entirety to indium foil measurements taken along the centerline of the BSF, and reported to J. L. Meem in a memorandum by E. B. Johnson[4].

2. Thermal Neutron Counter Measurements

The thermal neutron data obtained from the counters is presented in Tables 1 to 6 below in terms of flux values, nv_{th}/watt. A plot of the data of Table 6 appears in Figure 3, which is a summary of the data of this experiment.

Lid Tank pure water data[5], reduced by a factor of six, is reproduced here for comparison. (The power of the Lid Tank source plate is generally considered to be 6 watts).

---

3 Memorandum J. L. Meem from H. E. Hungerford, "Center of Detection Corrections for Neutron Counters and Ion Chambers", pending.

4 Memorandum J. L. Meem from E. B. Johnson, "Centerline Foil Measurements of Thermal Neutron Intensities for Experiment 1", C.F.51-4-15

5 CRML-629, "ANP Project Quarterly Progress Report for Period Ending February 28, 1950".

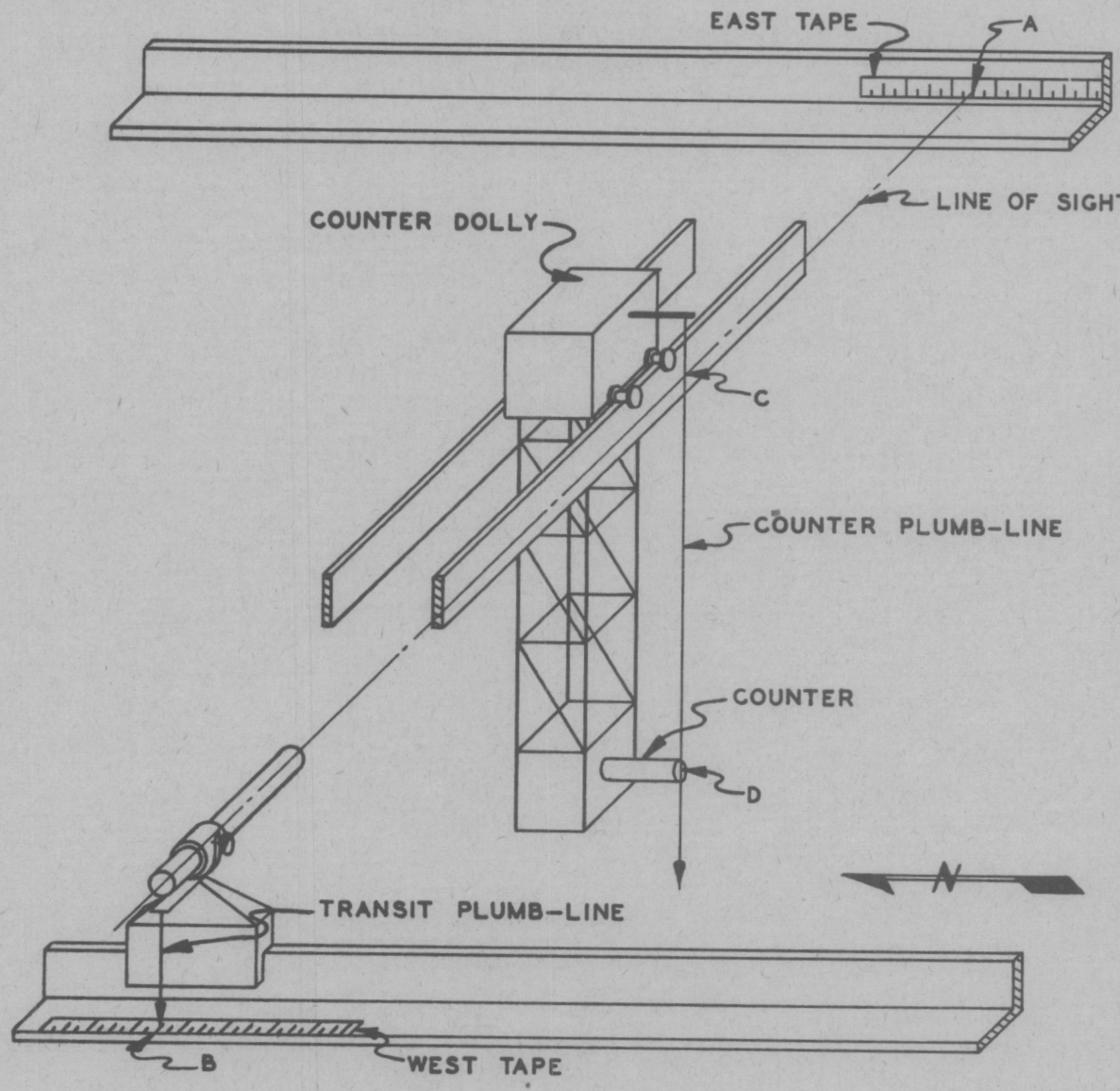

A & B - IDENTICAL READINGS OF TAPES
C —— TRANSIT CROSSHAIRS FOCUSED ON COUNTER PLUMB-LINE
D —— PLUMB-LINE IN COINCIDENCE WITH KNOWN POINT ON COUNTER

FIG. E-2

BULK SHIELDING FACILITY

METHOD OF FINDING

Z POSITION OF COUNTERS

DWG. # 11200

NOT CLASSIFIED

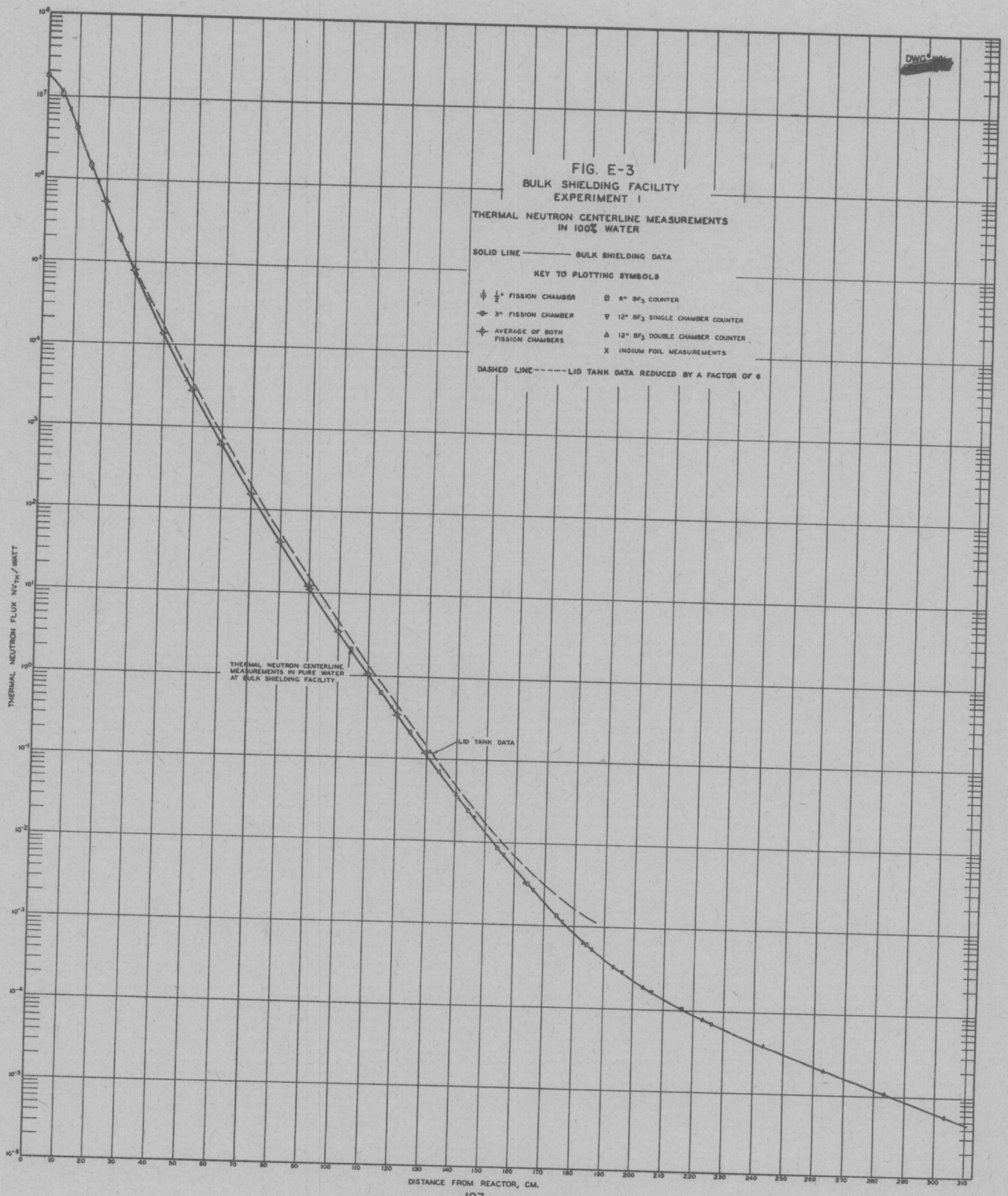
FIG. E-3
BULK SHIELDING FACILITY
EXPERIMENT I
THERMAL NEUTRON CENTERLINE MEASUREMENTS
IN 100% WATER
SOLID LINE ——— BULK SHIELDING DATA
KEY TO PLOTTING SYMBOLS
½" FISSION CHAMBER
3" FISSION CHAMBER
AVERAGE OF BOTH FISSION CHAMBERS
8" BF3 COUNTER
12" BF3 SINGLE CHAMBER COUNTER
12" BF3 DOUBLE CHAMBER COUNTER
X INDIUM FOIL MEASUREMENTS
DASHED LINE - - - - - LID TANK DATA REDUCED BY A FACTOR OF 6
THERMAL NEUTRON CENTERLINE MEASUREMENTS IN PURE WATER AT BULK SHIELDING FACILITY
LID TANK DATA
THERMAL NEUTRON FLUX NVTH/WATT
DISTANCE FROM REACTOR, CM.

TABLE 1

3" Fission Chamber Measurements - Experiment 1

Distance from Reactor	Thermal Neutron Flux, nv_{th}/watt						Average and Summary
	Run 20	Run 23	Run 24	Run 25	Run 26	Run 44	
20.0 cm	5.306×10^{5}	5.313×10^{5}	-	-	5.266×10^{5}	-	5.295×10^{5}
30.0 cm	-	7.893×10^{4}	-	-			7.893×10^{4}
40.0 cm	1.386×10^{4}	1.372×10^{4}	1.355×10^{4}	1.304×10^{4}	-	-	1.354×10^{4}
50.0 cm	-	-	2.789×10^{3}	2.736×10^{3}	-	-	2.763×10^{3}
60.0 cm	-	-	6.083×10^{2}	6.073×10^{2}	-	-	6.078×10^{2}
70.0 cm	-	-	1.528×10^{2}	1.515×10^{2}	-	-	1.522×10^{2}
80.0 cm	-	-	-	4.060×10^{1}	-	-	4.060×10^{1}
89.9 cm	-	-	-	-	-	1.192×10^{1}	1.192×10^{1}
90.0 cm	-	-	-	1.157×10^{1}	-	-	1.157×10^{1}
100.0 cm	-	-	-	3.315×10^{0}	-	3.499×10^{0}	3.407×10^{0}
110.0 cm	-	-	-	-	-	1.080×10^{0}	1.080×10^{0}
120.0 cm	-	-	-	-	-	3.483×10^{-1}	3.483×10^{-1}
130.2 cm	-	-	-	-	-	1.188×10^{-1}	1.188×10^{-1}

TABLE 2

1/2" Fission Chamber Measurements - Experiment 1

Distance from Reactor	Thermal Neutron Flux, nv_{th}/watt		Average and Summary
	Run 27	Run 29	
0.0 cm	1.814×10^7	1.773×10^7	1.794×10^7
5.0 cm	-	1.079×10^7	1.079×10^7
10.0 cm	-	4.139×10^6	4.139×10^6
15.0 cm	1.445×10^6	1.460×10^6	1.453×10^6
20.0 cm	5.266×10^5	5.266×10^5	5.266×10^5
25.0 cm	-	1.948×10^5	1.948×10^5
30.0 cm	-	7.919×10^4	7.919×10^4
35.0 cm	-	3.332×10^4	3.332×10^4

TABLE 3

8" BF_3 Counter Measurements - Experiment 1

Distance from Reactor	Thermal Neutron Flux, nv_{th}/watt Run 42
104.4 cm.	2.125×10^{0}
114.5 cm.	6.409×10^{-1}
124.5 cm.	2.110×10^{-1}
134.5 cm.	6.981×10^{-2}
144.4 cm.	2.377×10^{-2}
154.3 cm.	8.521×10^{-3}
164.3 cm.	3.218×10^{-3}
174.3 cm.	1.316×10^{-3}
184.3 cm.	6.051×10^{-4}

TABLE 4

12" BF_3 Single Chamber Measurements - Experiment 1

Distance from Reactor	Thermal Neutron Flux, nv_{th}/watt Run 52
146.1 cm.	1.957×10^{-2}
156.1 cm.	7.187×10^{-3}
166.2 cm.	2.716×10^{-3}
176.1 cm.	1.163×10^{-3}
186.1 cm.	5.389×10^{-4}
196.2 cm.	2.867×10^{-4}
206.3 cm.	1.665×10^{-4}
216.3 cm.	1.030×10^{-4}
226.3 cm.	6.889×10^{-5}

TABLE 5

12" BF_3 Double Chamber Centerline Measurements - Experiment 1

Distance from Reactor	Average Distance	Thermal Neutron Flux, nv_{th}/watt			Average and Summary
		Run 53	Run 54	Run 55	
163.6 cm	163.65 cm	-	3.283×10^{-3}	-	3.284×10^{-3}
163.7 cm		3.285×10^{-3}	-	-	
183.6 cm	183.65 cm	-	6.372×10^{-4}	5.942×10^{-4}	6.238×10^{-4}
183.7 cm		6.401×10^{-4}	-	-	
193.6 cm	193.65 cm	-	-	-	3.237×10^{-4}
193.7 cm		3.237×10^{-4}	-	-	
203.6 cm	203.65 cm	-	1.868×10^{-4}	-	1.868×10^{-4}
203.7 cm		1.867×10^{-4}	-	-	
223.6 cm	223.65 cm	-	7.787×10^{-5}	-	7.712×10^{-5}
223.7 cm		7.637×10^{-5}	-	-	
243.6 cm	243.65 cm	-	3.862×10^{-5}	-	3.847×10^{-5}
243.7 cm		3.832×10^{-5}	-	-	
263.6 cm		-	1.976×10^{-5}	-	1.976×10^{-5}
283.6 cm		-	-	1.072×10^{-5}	1.072×10^{-5}
303.6 cm		-	-	5.709×10^{-6}	5.709×10^{-6}

[redacted]

TABLE 6

A Summary of Thermal Neutron Counter Measurements - Experiment 1

Distance from Reactor	Plotting Symbol	nv_{th}/watt	Distance from Reactor	Plotting Symbol	nv_{th}/watt	Key to Plotting Symbols
0.0 cm	⊙	1.794×10^{7}	144.4 cm	⊡	2.377×10^{-2}	⊙ 1/2" Fission Chamber
5.0 cm	⊙	1.079×10^{7}	146.1 cm	▽	1.957×10^{-2}	
10.0 cm	⊙	4.139×10^{6}	154.3 cm	⊡	8.521×10^{-3}	⊙ 3" Fission Chamber
15.0 cm	⊙	1.453×10^{6}	156.1 cm	▽	7.187×10^{-3}	
20.0 cm	⊙	5.280×10^{5}	163.65 cm	△	3.284×10^{-3}	⊙ Average of Both Fission Chambers
25.0 cm	⊙	1.948×10^{5}	164.3 cm	⊡	3.218×10^{-3}	
30.0 cm	⊙	7.906×10^{4}	166.2 cm	▽	2.716×10^{-3}	
35.0 cm	⊙	3.332×10^{4}	174.3 cm	⊡	1.316×10^{-3}	⊡ 8" BF_3 Chamber
40.0 cm	⊙	1.354×10^{4}	176.1 cm	▽	1.163×10^{-3}	
50.0 cm	⊙	2.763×10^{3}	183.65 cm	△	6.238×10^{-4}	▽ 12" BF_3 Single Chamber
60.0 cm	⊙	6.078×10^{2}	184.3 cm	⊡	6.051×10^{-4}	
70.0 cm	⊙	1.522×10^{2}	186.1 cm	▽	5.389×10^{-4}	
80.0 cm	⊙	4.060×10^{1}	193.7 cm	△	3.237×10^{-4}	△ 12" BF_3 Double Chamber
89.9 cm	⊙	1.192×10^{1}	196.2 cm	▽	2.867×10^{-4}	
90.0 cm	⊙	1.157×10^{1}	203.65 cm	△	1.868×10^{-4}	
100.0 cm	⊙	3.407×10^{0}	206.3 cm	▽	1.665×10^{-4}	
104.4 cm	⊡	2.125×10^{0}	216.3 cm	▽	1.030×10^{-4}	
110.0 cm	⊙	1.080×10^{0}	223.65 cm	△	7.712×10^{-5}	
114.5 cm	⊡	6.409×10^{-1}	226.3 cm	▽	6.889×10^{-5}	
120.0 cm	⊙	3.483×10^{-1}	243.65 cm	△	3.847×10^{-5}	
124.5 cm	⊡	2.110×10^{-1}	263.6 cm	△	1.976×10^{-5}	
130.2 cm	⊙	1.188×10^{-1}	283.6 cm	△	1.072×10^{-5}	
134.4 cm	⊡	6.981×10^{-2}	303.6 cm	△	5.709×10^{-6}	

[redacted]

3. Results and Observations

It will be seen that in shape the BSF data repeats quite closely the Lid Tank data from 40 to 150 cm. Observed differences nearer than this probably results from differences in the sources and geometries. At distances greater than 150 cm. the Lid Tank data diverges due to the low counting rates at that distance.

An interesting phenomenon starts showing up in the BSF data at 180 cm. From this point to 200 cm. a radical change in the curve is noticed. The relaxation length changes from around 10 at 180 to around 28 at 210 cm. The curve flattens out slowly from this point to 300 cm. from the reactor, giving a relaxation length of 31 cm. near this point. This is just the relaxation length of the gamma ray measurements[6] in the BSF at the same position.

It is believed that in this region photo-neutrons are being detected from some type of (γ,n) process. An investigation is underway to determine the exact nature of the process and the origin of the gammas involved.

H. E. Hungerford, Jr.

HEH/reb

---

6 Ballweg to Meem, "Gamma-Ray Measurements in 100% Water at the Bulk Shielding Facility - Experiment 1", C.F. 51-4-110.

APPENDIX F

Foil Measurements of Thermal Neutron Intensities in Water at the Bulk Shielding Facility

E. B. Johnson
G. McCammon
M. P. Haydon

(This memorandum has appeared as CF-51-4-156.)

OAK RIDGE NATIONAL LABORATORY

To: J. L. Meem April 18, 1951

From: E. B. Johnson, G. McCammon, M. P. Haydon

Re: Foil Measurements of Thermal Neutron Intensities in Water at the Bulk Shielding Facility

The attentuation of thermal neutrons from the BSF reactor, described in ORNL-991, has been measured in water along the north-south centerline. The reactor was loaded as in fuel assembly arrangement #2, described in the ANP Quarterly Report, February 1951. Indium foils were exposed at various distances from the north face of the reactor. The resulting data has been normalized to a power level of 1 watt.

Indium foils 25 cm^2 in area and 5 mil thick were exposed in both aluminum and 30 mil cadmium covers. The maximum weight variation was 4.6%. The resulting activities were measured on two counters, one a thin-walled glass G.M. tube, the other a mica window tube whose counting rate had been normalized to the G.M. tube. In order to eliminate the current component of the flux both sides of every foil were counted and the saturated activities averaged.

Since a maximum of 5 foils could be exposed in one run, it was necessary to do a series of runs to obtain the entire curve. Each of these runs was corrected for "startup" by the equation derived by E. C. Campbell of the ORNL Physics Division,

$$\frac{A_o}{A_1 + A_o} = \frac{\frac{1}{\lambda + \mathcal{N}}\left(e^{\mathcal{N}t_o} - e^{-\lambda t_o}\right)e^{-\lambda(t_1 - t_o)}}{\frac{e^{-\mathcal{N}t_o}}{\lambda}\left[1 - e^{-\lambda(t_1 - t_o)}\right] + \frac{1}{\lambda + \mathcal{N}}\left(e^{\mathcal{N}t_o} - e^{-\mathcal{N}t_o}\right)e^{-\lambda(t_1 - t_o)}}$$

where A_o = activity induced during startup

A_1 = activity induced during level time

λ = decay constant of the detector

$\mathcal{N}$ = 1/pile period

t_o = startup time (time of changing flux)

$t_1 - t_o$ = exposure time (level time)

All runs were normalized together by means of 1 cm^2 gold foils placed on the fuel assembly in position 5 for runs at 0.74 watts and 74 watts, and by means of duplicate positions of the indium foils in the water at the higher power levels. The activity of the foils exposed in 30 mil cadmium covers was corrected by 14% for resonance absorption in the cadmium.

Since cadmium-covered measurements were not made at every position at which a bare foil was exposed, the following procedure was used to obtain flux values. The saturated activities of the bare and cadmium-covered foils and, where possible, the thermal saturated activities, were plotted as a function of distance from the reactor (Fig. 1). From the resulting $A_{s_{th}}$ curve, values were taken at 10 cm. intervals (Table I) and nv_{th} computed on the basis of calibration of these foils in the standard graphite pile. (See CP-2804 for flux values used for the standard pile). Because the calibration of the foils was done in a graphite pile and the exposures in water, it was necessary to increase the flux values by 22%. The basis of this correction is given in a memorandum (C.F. 51-4-103) from Ritchie to Meem.

[redacted]

The shape of the curve in Figure 2 was obtained from nv_{th} values calculated by the above method. The points shown on the curve represent thermal flux values for which A_{gth} was obtained by actual exposures of both bare and cadmium-covered at the indicated positions.

E. B. Johnson
E. B. Johnson

G. McCammon
G. McCammon

M. P. Haydon
M. P. Haydon

EBJ/reb

[redacted]

SI[redacted]

TABLE I

Centerline Foil Data - Experiment 1

z	A_s Total	A_s Epicadmium	A_s Thermal	nv_{th}	$\frac{nv_{th}}{watt}$	Cd Ratio
0	1.007×10^6	1.958×10^5	8.112×10^5	7.301×10^6	9.866×10^6	5.14
7.62	3.286×10^7	2.666×10^6	3.019×10^7	4.227×10^6	6.979×10^6	12.3
8.454		2.100×10^6				
10.00*			1.85×10^7	2.59×10^6	4.275×10^6	
17.70	4.265×10^6	2.758×10^5	3.989×10^6	5.585×10^5	9.221×10^5	15.5
20.00*			2.45×10^6	3.43×10^5	5.66×10^5	
27.74	5.786×10^5	3.835×10^4	5.402×10^5	7.563×10^4	1.248×10^5	15.1
28.57	5.329×10^5					
30.0*			3.48×10^5	4.87×10^4	8.04×10^4	
37.74	9.609×10^4					
38.57	8.799×10^4					
40.0*			5.60×10^4	7.84×10^3	1.29×10^4	
47.74	1.784×10^4	1.795×10^3	1.604×10^3	2.246×10^3	3.709×10^3	9.93
48.57	1.684×10^4					
50.0*			1.15×10^4	1.61×10^3	2.65×10^3	
57.82	4.101×10^3					
60.0*			2.72×10^3	3.81×10^2	6.28×10^2	
67.86	1.058×10^3					
67.90	9.910×10^2					
70.0*			6.80×10^2	9.52×10^1	1.57×10^2	
77.94	2.554×10^2					
80.0*			1.77×10^2	2.48×10^1	4.09×10^1	
87.94	7.123×10^1					

(Continued)

SE[redacted]

TABLE I (Con't.)

Centerline Foil Data - Experiment 1

Z	A_s Total	A_s Epicadmium	A_s Thermal	nv_{th}	$\frac{nv_{th}}{watt}$	Cd Ratio
90.0*			4.90×10^{1}	6.86	1.13×10^{1}	
97.94	1.943×10^{1}					
98.02	2.086×10^{1}	1.467	1.939×10^{1}	2.715	4.482	14.0
100.0*			1.45×10^{1}	2.03	3.35	
108.06	6.17					
108.10	6.273					
110.0*			4.58	6.41×10^{-1}	1.06	
118.06	2.13					
118.14	2.026	1.603×10^{-1}	1.866	2.61×10^{-1}	4.31×10^{-1}	12.6
120.0*			1.50	2.10×10^{-1}	3.47×10^{-1}	
128.06	6.35×10^{-1}					
128.14	6.49×10^{-1}					
128.22	6.61×10^{-1}					
130.0*			4.80×10^{-1}	6.72×10^{-2}	1.11×10^{-1}	
138.14	2.26×10^{-1}					
138.26	2.23×10^{-1}					
140.0*			1.64×10^{-1}	2.30×10^{-2}	3.80×10^{-2}	
148.26	7.70×10^{-2}					
150.0*			6.4×10^{-2}	8.96×10^{-3}	1.47×10^{-2}	
158.26	3.56×10^{-2}					
160.0*			3.1×10^{-2}	4.34×10^{-3}	7.16×10^{-3}	

* $A_{s_{th}}$ obtained from curve in Figure 1.

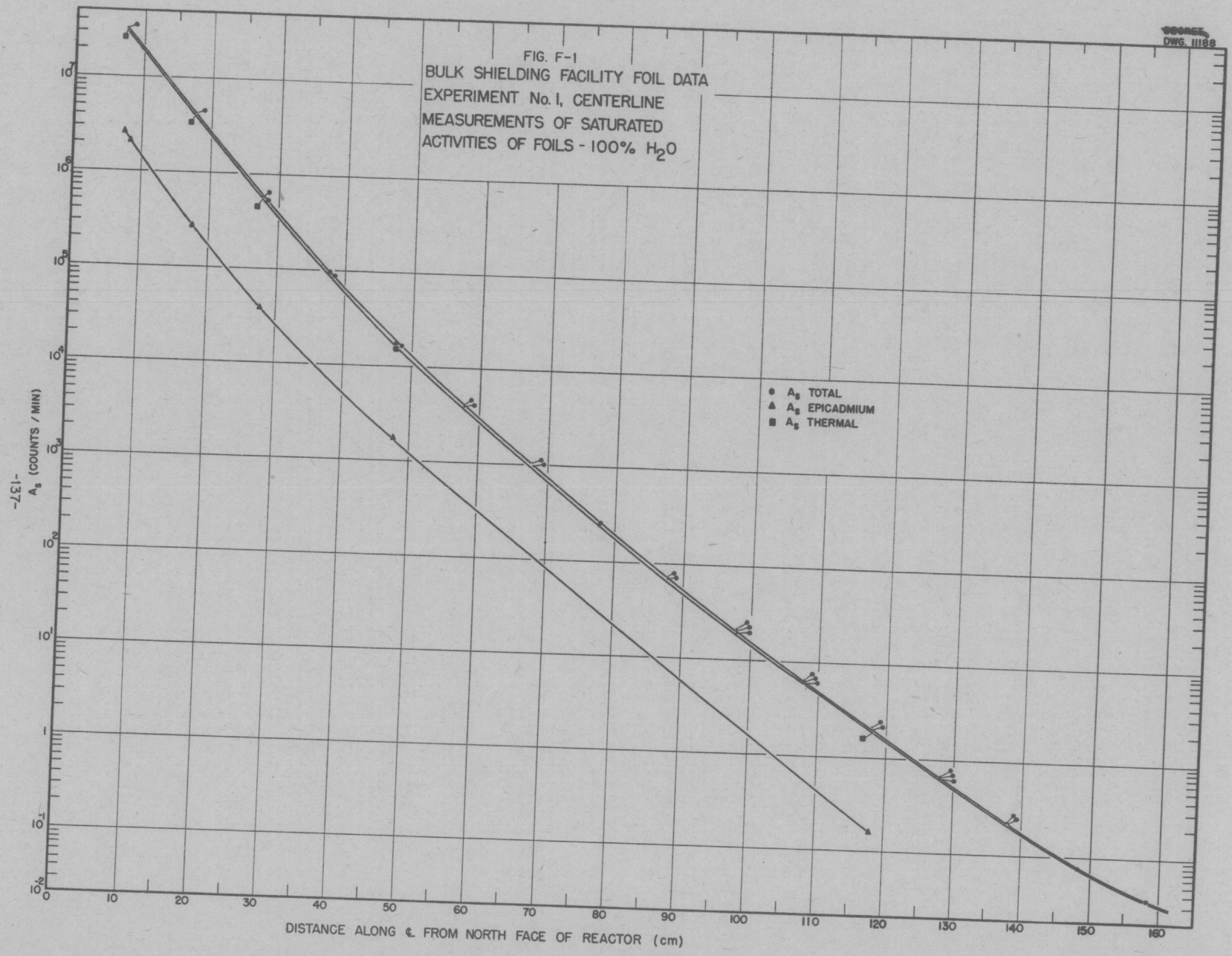
SECRET
DWG. 11188
FIG. F-1
BULK SHIELDING FACILITY FOIL DATA
EXPERIMENT No. 1, CENTERLINE
MEASUREMENTS OF SATURATED
ACTIVITIES OF FOILS - 100% H_2O
A_s TOTAL
A_s EPICADMIUM
A_s THERMAL
A_s (COUNTS / MIN)
DISTANCE ALONG ℄ FROM NORTH FACE OF REACTOR (cm)
0
10
20
30
40
50
60
70
80
90
100
110
120
130
140
150
160

SECRET

DWG. 11189

FIG. F-2

BULK SHIELDING FACILITY FOIL DATA, EXPERIMENT No. 1, NEUTRON ℄ MEASUREMENTS - 100% H_2O

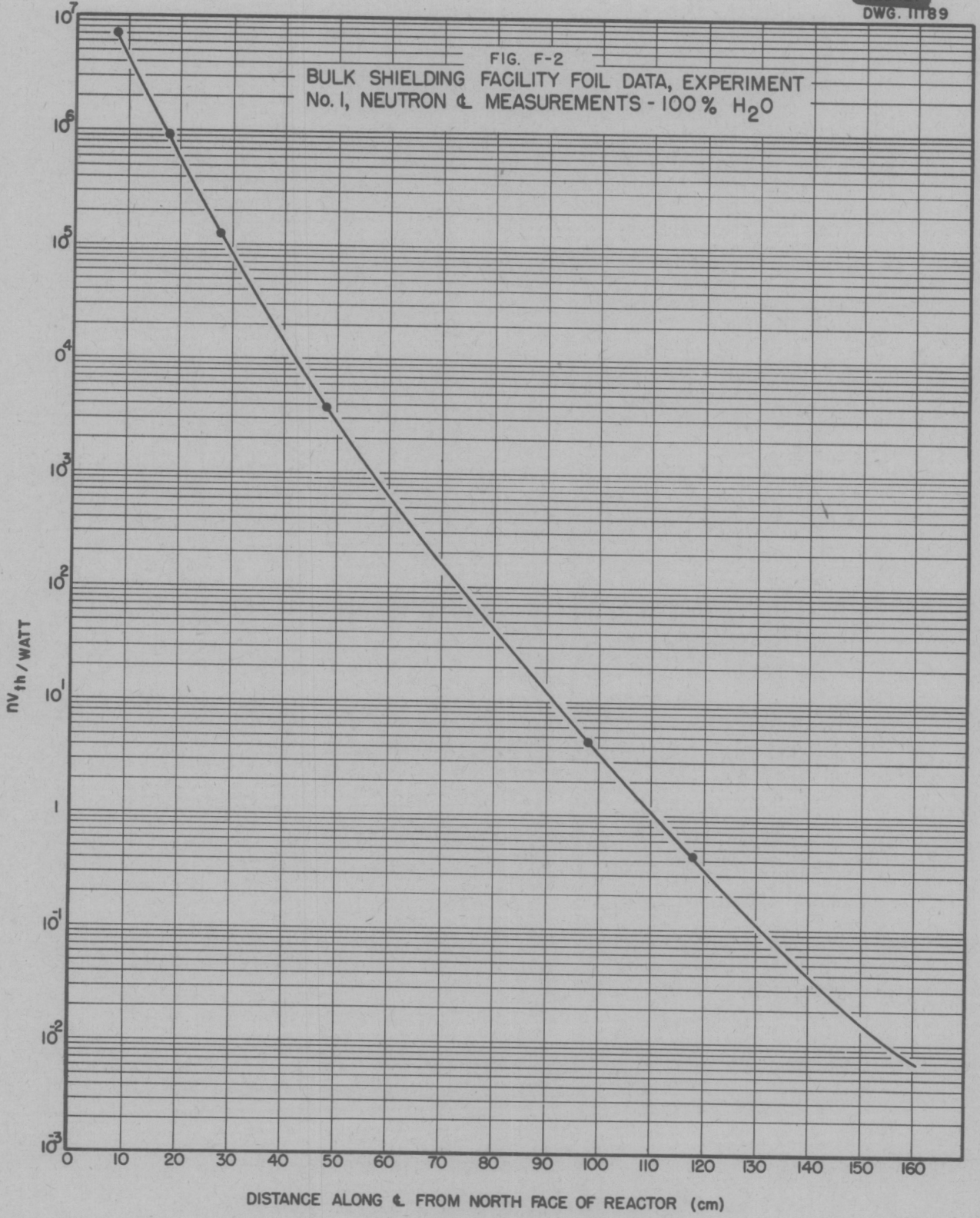

APPENDIX G

Fast Neutron Dosimeter Measurements in Water at the Bulk Shielding Facility

R. G. Cochran
H. E. Hungerford

(This memorandum has appeared as CF-51-5-61.)

Intra-Laboratory Correspondence

OAK RIDGE NATIONAL LABORATORY

To: J. L. Meem May 7, 1951

From: R. G. Cochran and H. E. Hungerford

Re: Fast Neutron Dosimeter Measurements in Water at the Bulk Shielding Facility

Fast neutron dosage measurements were taken in water to nearly 170 cm. with the bulk shielding facility dosimeter.

Several experimental difficulties were encountered during the experiment. It was realized that γ-ray pile-up in the intense γ-ray fields around the reactor would cause considerable trouble, thus an experiment was performed to determine the upper limit of γ-radiation that could be tolerated. The experiment was conducted in the following way. A Po-Be source was placed at a distance of 20 cm. from the proportional counter and readings taken of the neutron source. Then a Co^{60} γ-ray source was brought up to various distances from the counter and any change in counting rate noted. By this scheme it was found that the dosimeter would function in γ-radiation fields up to 10 r/hr.

Since the neutron to gamma ratio decreases rapidly with distance from the reactor, it was found necessary to adjust the reactor power so that the γ-ray intensity was below the 10 r/hr limit for each point taken. The γ-radiation was constantly monitored in this

experiment by mounting an ionization chamber 18 in. directly above the dosimeter proportional counter. Thus, the measurements in pure water were confined within a limited wedge of high gamma field verses low counting rates, so that about 70 cm. from the reactor was the limit of satisfactory measurement without doing something to reduce the γ-radiation.

By interposing a 3 in. lead plate between the reactor and the dosimeter a reduction factor of about 40 was obtained for the γ-rays. The measurements were then pushed to nearly 170 cm. keeping the distance between the dosimeter and the lead shield fixed at 32 cm. By checking a few points below 65 cm. using the lead slab, a small change in fast neutron flux was found and a 5% change in slope was observed.

The dosimeter was calibrated by comparing it to a Po-Be source before each run as discussed in reference 1.

The data are presented in Tables 1 and 2 in terms of millirep/hr/watt vs. distance in centimeters to center of detection. A plot of this data is given in Figure 1. A center of detection is calculated for the dosimeter as described in reference 2, to conform with the usual method of plotting data at this facility. At the present time,

---

1 Memorandum, R. G. Cochran to J. L. Meem, "Description and Calibration of a Fast Neutron Dosimeter"

2 Memorandum, H. E. Hungerford to J. L. Meem, "Center of Detection Calculations for Neutron Counters and Ion Chambers"

[redacted]

however, we have no basis for the choice of collimated and scattered radiation assumed. An experiment is contemplated to determine this ratio.

For purposes of comparison a plot of Lid Tank dosimeter measurements[3] in 0.5% borated water is shown in Figure 1 as a dashed line. The borated water data was chosen rather than the earlier 100% water data because it is generally considered to be more accurate. The data appears here reduced by a factor of 6, since the Lid Tank source is taken to be 6 watts.

Robert G. Cochran
R. G. Cochran

R. E. Hungerford, Jr.
R. E. Hungerford, Jr.

RGG/reb

---

3 ORNL-919, "ANP Project Quarterly Progress Report for Period Ending December 10, 1950", pages 131-132.

SEC[redacted]

TABLE 1

Dosimeter Measurements for Experiment 1

No Pb Shield

Distance from Reactor	Fast Neutron Dosage, mrep/hr/watt							Summary and Average
	Run 17	Run 31	Run 32	Run 36	Run 60	Run 61	Run 62	
3.4 cm	-	1.34×10^{4}	-	-	-	-	-	1.34×10^{4}
8.4 cm	-	6.66×10^{3}	-	-	-	-	-	6.66×10^{3}
13.4 cm	-	2.65×10^{3}	-	-	-	-	-	2.65×10^{3}
18.4 cm	-	1.08×10^{3}	-	-	-	-	-	1.08×10^{3}
22.7 cm	-	-	5.22×10^{2}	-	-	-	-	5.22×10^{2}
23.5 cm	-	4.57×10^{2}	-	-	-	-	-	4.57×10^{2}
29.7 cm	1.60×10^{2}	-	-	-	-	-	-	1.60×10^{2}
32.7 cm	-	-	9.69×10^{1}	9.59×10^{1}	-	-	-	9.64×10^{1}
33.5 cm	-	8.91×10^{1}	-	-	-	-	-	8.91×10^{1}
39.7 cm	3.18×10^{1}	-	-	-	-	-	-	3.18×10^{1}
42.7 cm	-	-	2.18×10^{1}	2.08×10^{1}	-	-	-	2.13×10^{1}
43.5 cm	-	1.82×10^{1}	-	-	-	-	-	1.82×10^{1}
46.2 cm	-	-	-	-	-	1.25×10^{1}	-	1.25×10^{1}
47.7 cm	-	-	-	9.98×10^{0}	-	-	-	9.98×10^{0}
49.7 cm	7.64×10^{0}	-	-	-	-	-	-	7.64×10^{0}
51.2 cm	-	-	-	-	-	5.64×10^{0}	-	5.64×10^{0}
56.2 cm	-	-	-	-	2.97×10^{0}	-	-	2.97×10^{0}
61.2 cm	-	-	-	-	1.57×10^{0}	1.53×10^{0}	-	1.55×10^{0}
66.2 cm	-	-	-	-	8.09×10^{-1}	-	-	8.09×10^{-1}
71.2 cm	-	-	-	-	4.43×10^{-1}	4.48×10^{-1}	4.53×10^{-1}	4.48×10^{-1}

[redacted]

TABLE 2

Dosimeter Measurements for Experiment 1

3" Pb Shield Located 32 cm. from Dosimeter

Distance from Reactor	Fast Neutron Dosage, mrep/hr/watt			Summary and Average
	Run 61	Run 62	Run 65	
46.2 cm	1.41×10^{1}	-	-	1.41×10^{1}
51.2 cm	7.68×10^{0}	-	-	7.68×10^{0}
61.2 cm	1.82×10^{0}	-	-	1.82×10^{0}
71.2 cm	4.92×10^{-1}	4.45×10^{-1}	-	4.68×10^{-1}
81.2 cm	-	1.27×10^{-1}	-	1.27×10^{-1}
91.2 cm	-	3.44×10^{-2}	-	3.44×10^{-2}
101.2 cm	-	1.09×10^{-2}	-	1.09×10^{-2}
111.2 cm	-	3.44×10^{-3}	-	3.44×10^{-3}
121.2 cm	-	1.23×10^{-3}	1.16×10^{-3}	1.20×10^{-3}
126.2 cm	-	-	6.87×10^{-4}	6.87×10^{-4}
131.2 cm	-	-	3.92×10^{-4}	3.92×10^{-4}
136.2 cm	-	-	2.35×10^{-4}	2.35×10^{-4}
141.2 cm	-	-	1.38×10^{-4}	1.38×10^{-4}
146.2 cm	-	-	7.96×10^{-5}	7.96×10^{-5}
151.2 cm	-	-	4.80×10^{-5}	4.80×10^{-5}
156.2 cm	-	-	2.87×10^{-5}	2.87×10^{-5}
161.2 cm	-	-	1.82×10^{-5}	1.82×10^{-5}
166.2 cm	-	-	1.18×10^{-5}	1.18×10^{-5}

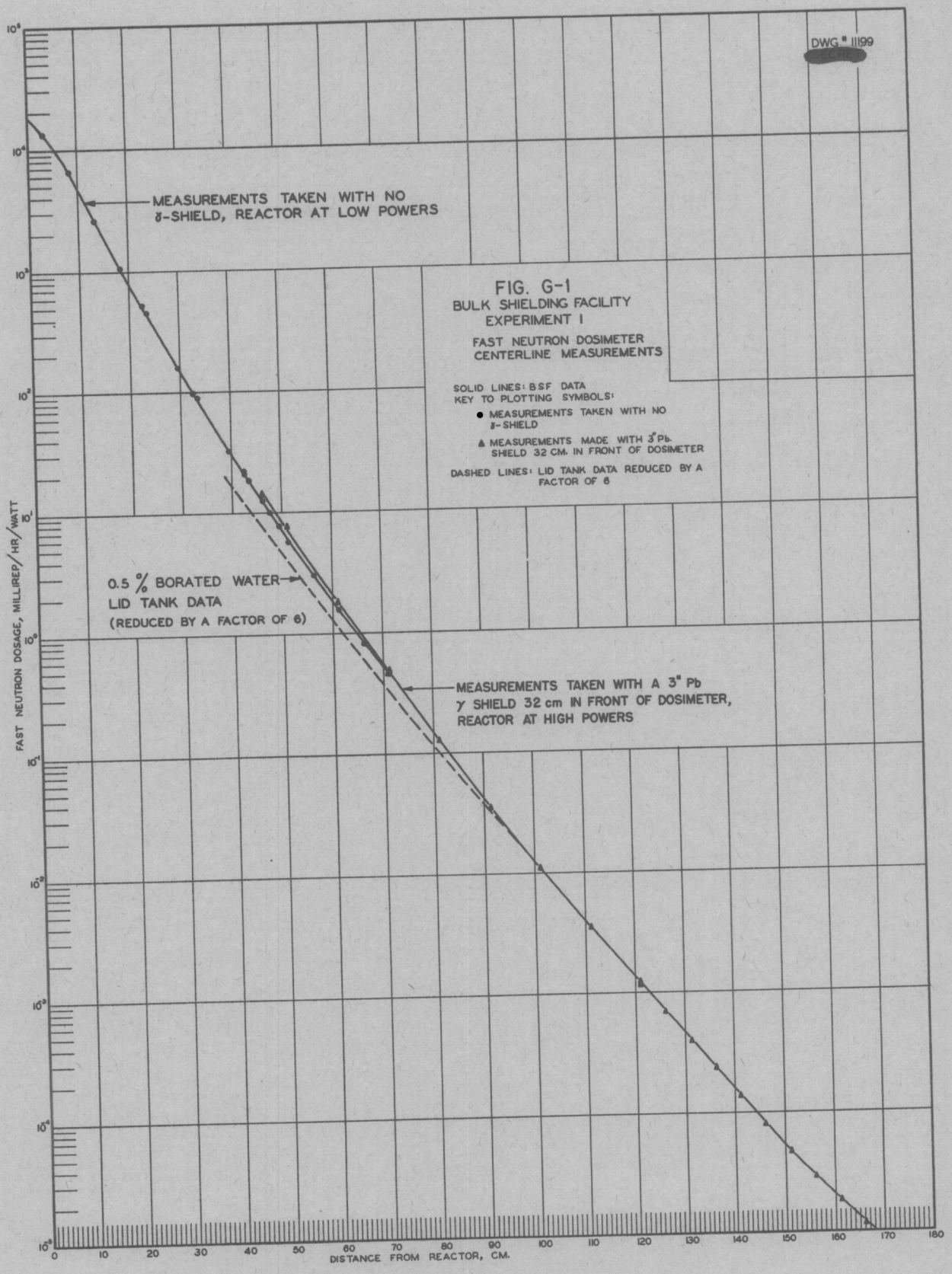
DWG. # 11199
MEASUREMENTS TAKEN WITH NO γ-SHIELD, REACTOR AT LOW POWERS
FIG. G-1
BULK SHIELDING FACILITY
EXPERIMENT I
FAST NEUTRON DOSIMETER
CENTERLINE MEASUREMENTS
SOLID LINES: BSF DATA
KEY TO PLOTTING SYMBOLS:
● MEASUREMENTS TAKEN WITH NO γ-SHIELD
▲ MEASUREMENTS MADE WITH 3" Pb. SHIELD 32 CM. IN FRONT OF DOSIMETER
DASHED LINES: LID TANK DATA REDUCED BY A FACTOR OF 6
0.5 % BORATED WATER
LID TANK DATA
(REDUCED BY A FACTOR OF 6)
MEASUREMENTS TAKEN WITH A 3" Pb γ SHIELD 32 cm IN FRONT OF DOSIMETER, REACTOR AT HIGH POWERS
FAST NEUTRON DOSAGE, MILLIREP/HR/WATT
DISTANCE FROM REACTOR, CM.
0
10
20
30
40
50
60
70
80
90
100
110
120
130
140
150
160
170
180

APPENDIX H

Gamma Radiation Measurements in Water at the Bulk Shielding Facility

L. H. Ballweg

(This memorandum has appeared as CF-51-4-110.)

Intra-Laboratory Correspondence

OAK RIDGE NATIONAL LABORATORY

To: J. L. Meem April 27, 1951

From: L. H. Ballweg

Re: Gamma Radiation Measurements in Water at the Bulk Shielding Facility

Centerline measurements were made of the gamma radiation of the bulk shielding reactor in 100% water (Experiment 1) at 100 watts and at 10 kilowatts.

The reactor had water as a reflector on all sides but the rear as described under Reactor Configuration No. 2 in the February ANP Report. The ionization chambers used to measure the gamma rays are described in a pending report, "A Standard Gamma Ray Ionization Chamber for Shielding Measurements", L. H. Ballweg and J. L. Meem.

The measurements were all converted to r/hr/watt. The following tables are a summary of the data. The results are plotted in Figure 1.

Experiment 1-I Run #8 Reactor at 100 watts power

Z Distance (cm)	r/hour/watt
2.4	61.643
7.4	39.080
17.4	16.505
27.4	7.441
37.4	3.542
47.4	1.756
57.4	9.05×10^{-1}
67.4	4.92×10^{-1}
77.4	2.75×10^{-1}
87.4	1.56×10^{-1}
97.4	9.08×10^{-2}
107.4	5.59×10^{-2}
117.4	3.41×10^{-2}
127.4	2.11×10^{-2}
137.4	1.32×10^{-2}
147.4	8.35×10^{-3}
157.4	5.27×10^{-3}
167.4	3.35×10^{-3}
177.4	2.14×10^{-3}

Experiment 1-I Run #38 Reactor at 100 w and 10 kw

100 watts

Z Distance (cm)	r/hour/watt
101.85	6.94×10^{-2}
152.1	6.6×10^{-3}
162.1	4.3×10^{-3}
172.1	2.8×10^{-3}

10 kw

172	2.808×10^{-3}
182	1.859×10^{-3}
192	1.266×10^{-3}
202	8.620×10^{-4}
212	5.951×10^{-4}
222	4.045×10^{-4}
232	2.795×10^{-4}
242	1.960×10^{-4}
252	1.394×10^{-4}
262	9.85×10^{-5}
272	6.98×10^{-5}
282	5.06×10^{-5}
292	3.69×10^{-5}
302	2.63×10^{-5}
309	2.06×10^{-5}

[redacted]

Experiment 1-I Run #39 Reactor at 10 kw

Z Distance (cm)	r/hour/watt
262	1.01×10^{-4}
272	7.25×10^{-5}
282	5.21×10^{-5}
292	3.78×10^{-5}
302	2.72×10^{-5}
312	2.03×10^{-5}
322	1.44×10^{-5}
332	1.03×10^{-5}
342	7.5×10^{-6}
352	5.6×10^{-6}
362	4.2×10^{-6}
372	3.0×10^{-6}
382	2.3×10^{-6}
388.3	1.9×10^{-6}

The dashed curve in Figure 1 is the lid tank data in 100% water. It was obtained by averaging Experiment 5 (CF-50-12-47), Experiments 6, 7 (ORNL-858), and Experiment 13 (to be published). The data was normalized to 1 watt because the lid tank source is 6 watts in power.

L. H. Ballweg

LHB:reb

DWG. 11006

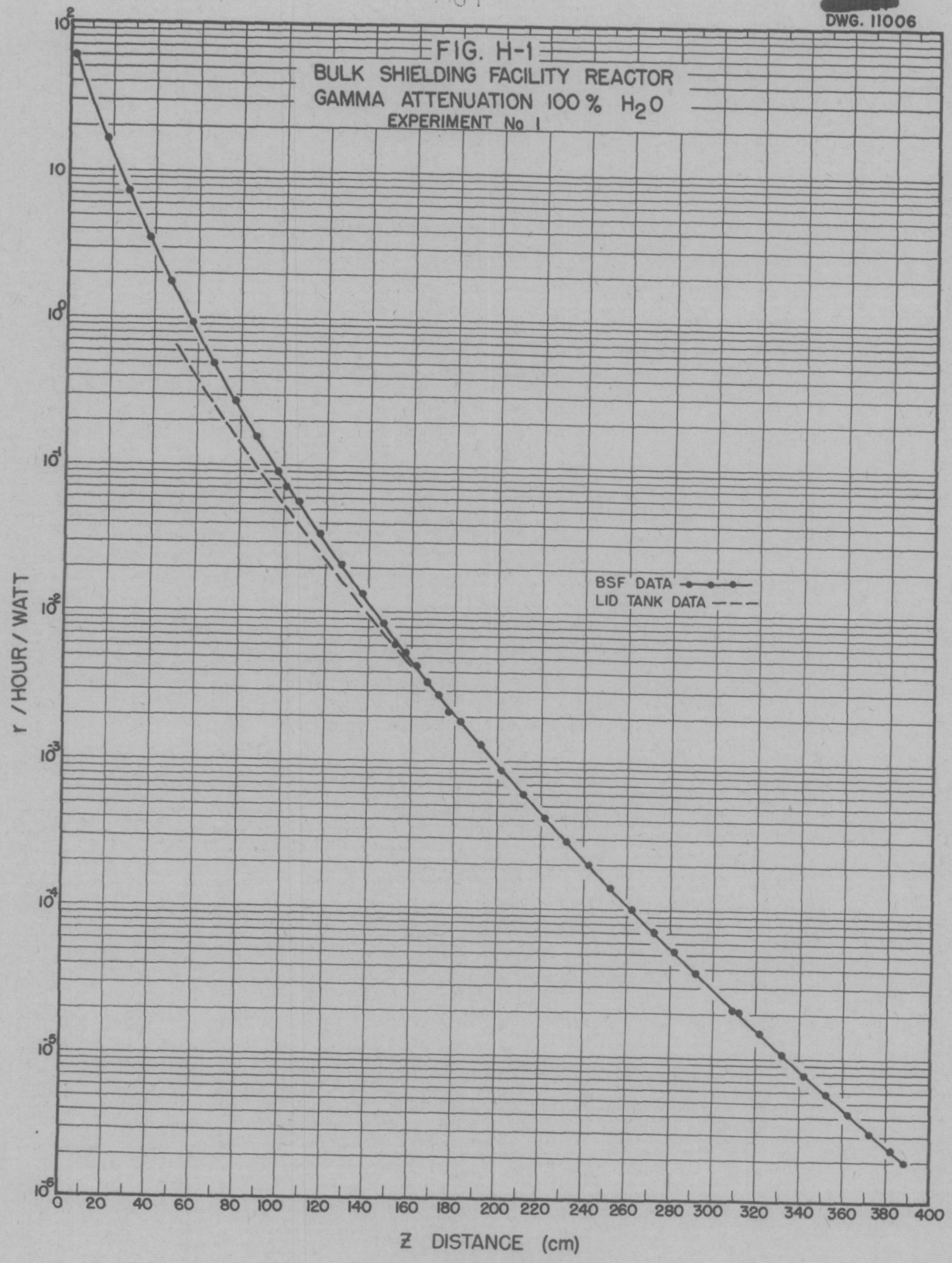
FIG. H-1
BULK SHIELDING FACILITY REACTOR
GAMMA ATTENUATION 100 % H_2O
EXPERIMENT No 1
BSF DATA
LID TANK DATA
r / HOUR / WATT
Z DISTANCE (cm)
0 20 40 60 80 100 120 140 160 180 200 220 240 260 280 300 320 340 360 380 400

APPENDIX I

Thermal Neutron Measurements Behind an Iron-Water Shield at the Bulk Shielding Facility

H. E. Hungerford
E. B. Johnson

(This memorandum has appeared as CF 51-5-72)

[redacted]

Intra-Laboratory Correspondence

OAK RIDGE NATIONAL LABORATORY

May 11, 1951

To: J. Lawrence Meem, Jr.

From: H. E. Hungerford, Jr. and E. B. Johnson

Subject: Thermal Neutron Measurements Behind an Iron-Water Shield at the Bulk Shielding Facility

Experiment 2 consisted of measurements of nuclear radiations along the centerline behind an iron shield approximately 17 in thick. The shield was made up of 18 iron slabs borrowed from the Lid Tank. They were placed adjacent to each other to form a continuous shield 43.75 cm thick. Since warpage of the slabs prevented a tight fit, there was a slight amount of water within the shield. The reactor was located 10.0 cm in front of the shield. Thus the shield extended to a point 53.75 cm from the reactor. Measurements were taken from this point outward along the centerline. A sketch of the experimental setup is shown in Fig. 1.

In order to measure the neutron attenuation through this shield, five bare indium foils were exposed along the centerline behind the iron. Calculations were done by the method described for Experiment 1.(1)

Since only bare foils were exposed to the flux coming through the iron, it was necessary to assume a cadmium ratio in order to calculate the thermal flux. Because the cadmium ratio in 100% water did not change appreciably between 10 cm and 120 cm from the reactor, the assumption was made that the presence of the iron and its resulting shift in the

(1) E. B. Johnson to J. L. Meem, Centerline Foil Measurements of Thermal Neutron Intensities for Experiment 1, CF #51-4-156.

neutron spectrum would not affect the cadmium ratio.

Thermal neutron measurements were taken also with the following counters: (1) 1/2" Fission Chamber, (2) 3" Fission Chamber, and (3) 12" BF_3 Double Chamber Counter.

The counter data were normalized[2] to the foil measurements to obtain values of the thermal neutron flux.

The data of this experiment are presented in Tables 1 through 5 in terms of nv_{th}/watt against distance from reactor, and distance from the shield. The foil data and calculations are shown in Table 1. The neutron counter data are given in Tables 2 through 4. Table 5 gives a summary of these measurements.

A curve showing the results is plotted in Fig. 2. The 100% water data of Experiment 1 is shown as a dashed curve.

H. E. Hungerford, Jr.

E. B. Johnson

HEH/reb

(2) H. E. Hungerford to J. L. Meem, Thermal Neutron Measurements for Experiment 1 in the Bulk Shielding Facility, CF #51-5-62.

[redacted]

TABLE 1

Foil Measurements for Experiment 2 - Bulk Shielding Facility

Distance from Reactor (cm.)	Distance from Iron (cm.)	A_s Bare	$A_{s_{th}}$*	nv_{th}	$\frac{nv_{th}}{watt}$
55.02	1.22	8.263×10^{4}	7.627×10^{4}	1.068×10^{4}	1.763×10^{4}
65.10	11.30	1.493×10^{4}	1.378×10^{4}	1.929×10^{3}	3.185×10^{3}
75.14	21.34	6.819×10^{2}	6.294×10^{2}	8.812×10^{1}	1.455×10^{2}
85.14	31.34	3.743×10^{1}	3.455×10^{1}	4.837	7.986
95.14	41.34	5.192	4.793	6.710×10^{-1}	1.108

Plotting Symbol: X

* Assume a Cd. ratio of 13

TABLE 2

Experiment 2, Bulk Shielding Facility

Thermal Neutron Centerline Data

1/2" Fission Counter Measurements

Run 6

Distance from Reactor	Distance from Shield	Nv_{Th}/Watt
53.75 cm.	0.0 cm.	2.657×10^{4}
54.75 cm.	1.0 cm.	2.767×10^{4}
55.75 cm.	2.0 cm.	2.614×10^{4}
56.75 cm.	3.0 cm.	2.328×10^{4}
57.75 cm.	4.0 cm.	2.011×10^{4}
58.75 cm.	5.0 cm.	1.614×10^{4}
59.75 cm.	6.0 cm.	1.286×10^{4}
61.75 cm.	8.0 cm.	7.809×10^{3}
63.75 cm.	10.0 cm.	4.573×10^{3}
66.25 cm.	12.5 cm.	2.140×10^{3}
68.75 cm.	15.0 cm.	9.748×10^{2}
71.25 cm.	17.5 cm.	4.610×10^{2}
73.75 cm.	20.0 cm.	2.140×10^{2}
76.25 cm.	22.5 cm.	9.785×10^{1}
78.75 cm.	25.0 cm.	4.714×10^{1}
83.75 cm.	30.0 cm.	1.175×10^{1}
88.75 cm.	35.0 cm.	3.590×10^{0}
93.75 cm.	40.0 cm.	1.361×10^{0}

Plotting Symbol: ⊕

TABLE 3

Experiment 2 , Bulk Shielding Facility

3" Fission Counter Measurements

Run 7

Distance from Reactor	Distance from Shield	Nv_{Th}/Watt
83.75 cm.	30.0 cm.	1.245×10^{1}
88.75 cm.	35.0 cm.	3.562×10^{0}
93.75 cm.	40.0 cm.	1.253×10^{0}
103.75 cm.	50.0 cm.	2.393×10^{-1}
113.75 cm.	60.0 cm.	6.184×10^{-2}
123.80 cm.	70.05 cm.	1.973×10^{-2}

Plotting Symbol: ⊙

TABLE 4

Experiment 2 - Run 8

Thermal Neutron Data

12" BF_3 Double Chamber Counter

Distance from Reactor	Distance from Shield	Nv_{Th}/Watt
109.45 cm.	55.7 cm.	1.124×10^{-1}
119.45 cm.	65.7 cm.	3.115×10^{-2}
129.45 cm.	75.7 cm.	9.474×10^{-3}
139.45 cm.	85.7 cm.	3.130×10^{-3}
149.45 cm.	95.7 cm.	1.072×10^{-3}
159.45 cm.	105.7 cm.	4.528×10^{-4}
169.45 cm.	115.7 cm.	1.489×10^{-4}
179.45 cm.	125.7 cm.	6.408×10^{-5}
189.45 cm.	135.7 cm.	2.939×10^{-5}

Plotting Symbol: △

TABLE 5

A Summary of the Thermal Neutron Data for Experiment 2

Distance from Reactor cm.	Distance from Shield cm.	Plotting Symbol	nv_{th}/ watt	Distance from Reactor cm.	Distance from Shield cm.	Plotting Symbol	nv_{th}/ watt
53.75	0.0	⊙	2.657×10^{4}	93.75	40.0	⊙	1.361×10^{0}
54.75	1.0	⊙	2.767×10^{4}	93.75	40.0	⊙	1.253×10^{0}
55.02	1.22	X	1.763×10^{4}	95.14	41.34	X	1.108×10^{0}
55.75	2.0	⊙	2.614×10^{4}	103.75	50.0	⊙	2.393×10^{-1}
56.75	3.0	⊙	2.328×10^{4}	109.45	55.7	△	1.124×10^{-1}
57.75	4.0	⊙	2.011×10^{4}	113.75	60.0	⊙	6.184×10^{-2}
58.75	5.0	⊙	1.614×10^{4}	119.45	65.7	△	3.115×10^{-2}
59.75	6.0	⊙	1.286×10^{4}	123.80	70.05	⊙	1.973×10^{-2}
61.75	8.0	⊙	7.809×10^{3}	129.45	75.7	△	9.474×10^{-3}
63.75	10.0	⊙	4.573×10^{3}	139.45	85.7	△	3.130×10^{-3}
65.10	11.3	X	3.185×10^{3}	149.45	95.7	△	1.072×10^{-4}
66.25	12.5	⊙	2.140×10^{3}	159.45	105.7	△	4.528×10^{-4}
68.75	15.0	⊙	9.748×10^{2}	169.45	115.7	△	1.489×10^{-4}
71.25	17.5	⊙	4.610×10^{2}	179.45	125.7	△	6.408×10^{-5}
73.75	20.0	⊙	2.140×10^{2}	189.45	135.7	△	2.939×10^{-5}
75.14	21.34	X	1.455×10^{2}				
76.25	22.5	⊙	9.785×10^{1}				
78.75	25.0	⊙	4.714×10^{1}				
83.75	30.0	⊙	1.245×10^{1}				
83.75	30.0	⊙	1.175×10^{1}				
85.14	31.34	X	7.986×10^{0}				
88.75	35.0	⊙	3.590×10^{0}				
88.75	35.0	⊙	3.562×10^{0}				

DWG. NO. 11220

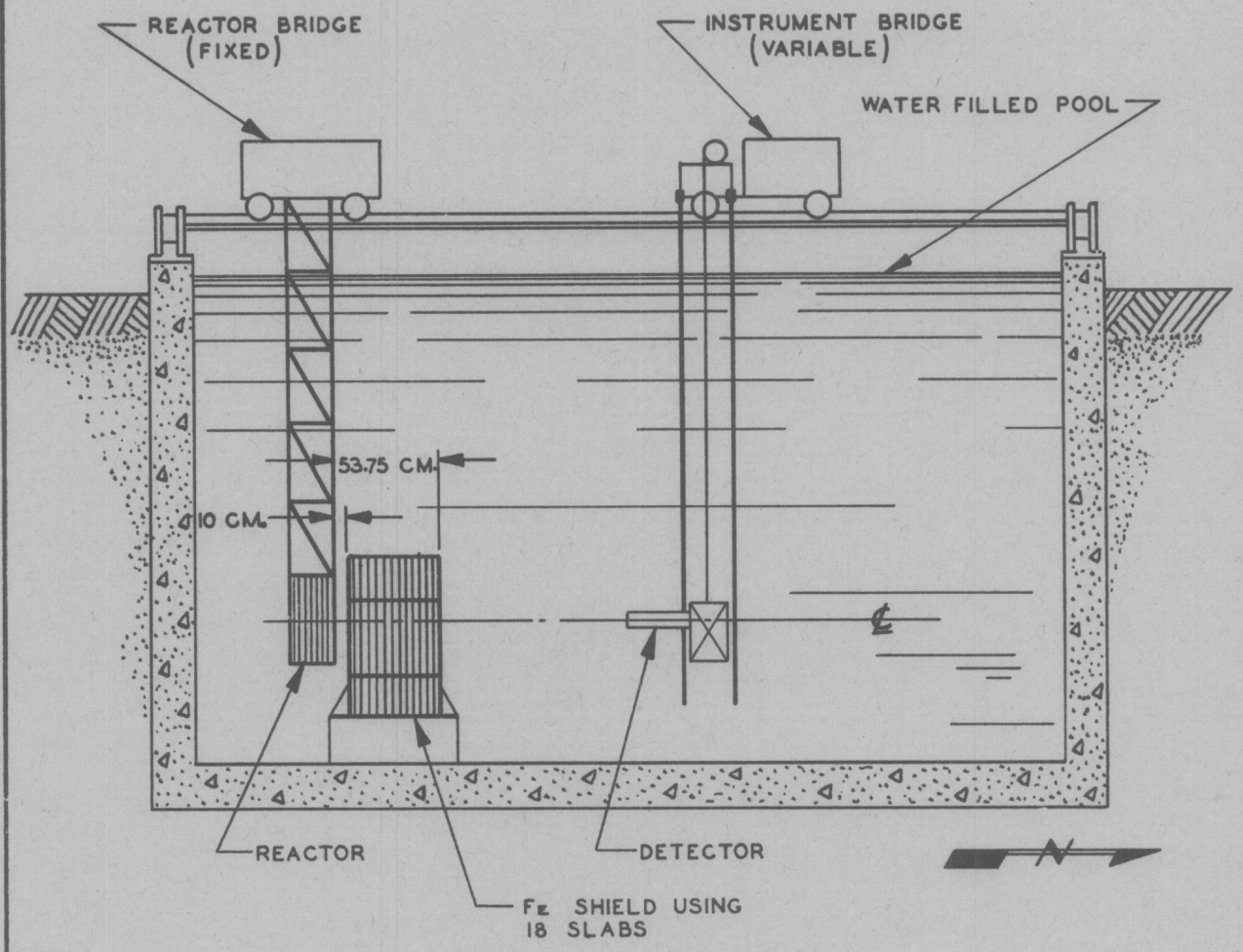

FIG. I-1

BULK SHIELDING FACILITY

IRON SHIELD ARRANGMENT

FOR EXPERIMENT 2

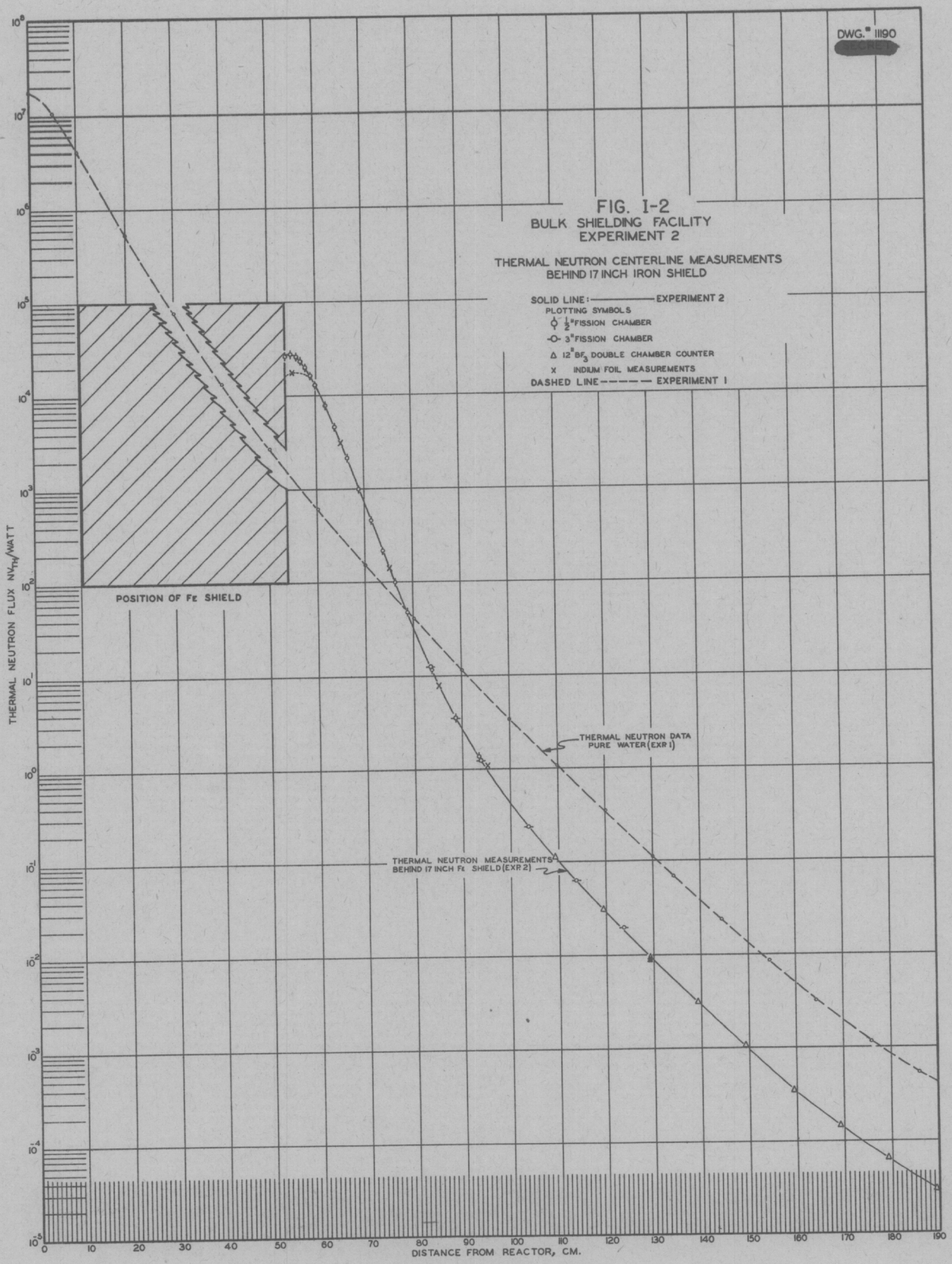
DWG. # 1190
FIG. I-2
BULK SHIELDING FACILITY
EXPERIMENT 2
THERMAL NEUTRON CENTERLINE MEASUREMENTS
BEHIND 17 INCH IRON SHIELD
SOLID LINE: ——— EXPERIMENT 2
PLOTTING SYMBOLS
½" FISSION CHAMBER
3" FISSION CHAMBER
12" BF3 DOUBLE CHAMBER COUNTER
X INDIUM FOIL MEASUREMENTS
DASHED LINE - - - - - EXPERIMENT 1
POSITION OF Fe SHIELD
THERMAL NEUTRON DATA PURE WATER (EXP 1)
THERMAL NEUTRON MEASUREMENTS BEHIND 17 INCH Fe SHIELD (EXP 2)
THERMAL NEUTRON FLUX NV$_{TH}$/WATT
DISTANCE FROM REACTOR, CM.

APPENDIX J

Fast Neutron Dosimeter Measurements Behind an Iron-Water Shield at the Bulk Shielding Facility

R. G. Cochran
H. E. Hungerford

(This memorandum has appeared as CF 51-5-73)

Intra-Laboratory Correspondence

OAK RIDGE NATIONAL LABORATORY

May 11, 1951

To: J. Lawrence Meem, Jr.

From: R. G. Cochran and H. E. Hungerford

Subject: Fast Neutron Dosimeter Measurements behind an Iron-Water Shield at the Bulk Shielding Facility

Measurements of fast neutron dosage have been made behind a 17 in iron shield at the Bulk Shielding Facility. Data was obtained with the Facility's dosimeter outward along the centerline to more than 130 cm from the reactor and 75 cm from the shield. The experimental setup and position of shield has been described in CF #51-5-72.(1)

The procedure followed for taking the data during this experiment was the same as that for Experiment 1. During runs an ion chamber was used to constantly monitor the γ-ray fields to prevent use of the dosimeter in excessive γ-radiation. The experimental points obtained were converted to dosage rates by means of calibrations before and after each run with a Po-Be source.(2) Since iron is a fairly effective γ-shield, it was not found necessary to further shield the counter with Pb, as was done in Experiment 1.

---

(1) H. E. Hungerford to J. L. Meem, Thermal Neutron Measurements for Experiment 2 in the Bulk Shielding Facility.

(2) R. G. Cochran to J. L. Meem, Calibration of the Fast Neutron Dosimeter, pending.

[redacted]

The results of the two runs is given in Table 1 in terms of millirep/hr/watt vs. distance from the reactor and shield. A plot of this data is shown in Figure 1. For comparison, the water data is shown on a dashed curve.

Robert G. Cochran
R. G. Cochran

H. E. Hungerford
H. E. Hungerford, Jr.

RGC/reb

TABLE 1

Fast Neutron Dosimeter Measurements - Experiment 2

Distance from Reactor	Distance from Shield	Fast Neutron Dosage, mrep/hr/watt		Summary and Average
		Run 3	Run 4	
56.45 cm	2.7 cm	7.79×10^{0} 7.63×10^{0}	--	7.71×10^{0}
61.25 cm	7.5 cm	1.49×10^{0} 1.50×10^{0} 1.43×10^{0}	-- --	1.47×10^{0}
66.25 cm	12.5 cm	3.42×10^{-1}	--	3.42×10^{-1}
76.25 cm	22.5 cm	3.50×10^{-2} 3.32×10^{-2}	--	3.41×10^{-2}
86.25 cm	32.5 cm	7.63×10^{-3} 6.35×10^{-3}	--	7.63×10^{-3} 6.35×10^{-3}
96.25 cm	42.5 cm	2.00×10^{-3}	1.92×10^{-3} 1.87×10^{-3}	1.93×10^{-3}
106.25 cm	53.5 cm	5.47×10^{-4}	--	5.47×10^{-4}
116.25 cm	63.5 cm	1.65×10^{-4}	1.53×10^{-4}	1.59×10^{-4}
121.25 cm	68.5 cm	8.74×10^{-3}	8.51×10^{-5}	8.62×10^{-5}
126.25 cm	73.5 cm	--	4.86×10^{-5}	4.86×10^{-5}
131.25 cm	78.5 cm	--	2.87×10^{-5} 2.80×10^{-5}	2.84×10^{-5}

DWG. NO. 11219

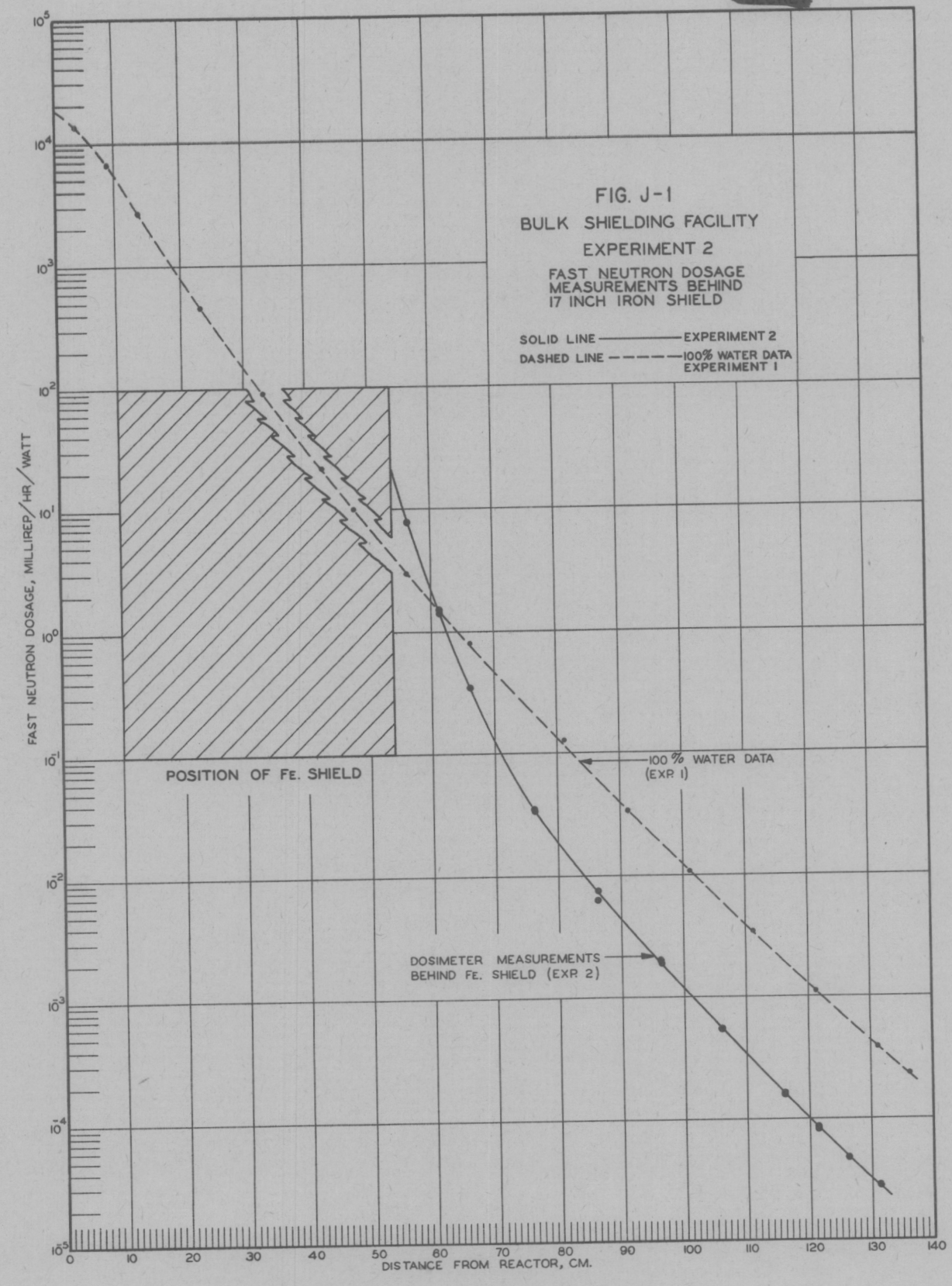
FIG. J-1
BULK SHIELDING FACILITY
EXPERIMENT 2
FAST NEUTRON DOSAGE
MEASUREMENTS BEHIND
17 INCH IRON SHIELD
SOLID LINE ——— EXPERIMENT 2
DASHED LINE - - - - - 100% WATER DATA EXPERIMENT 1
FAST NEUTRON DOSAGE, MILLIREP/HR/WATT
POSITION OF Fe. SHIELD
100 % WATER DATA (EXP. 1)
DOSIMETER MEASUREMENTS BEHIND Fe. SHIELD (EXP. 2)
DISTANCE FROM REACTOR, CM.

APPENDIX K

Gamma Radiation Measurements Behind an Iron-Water Shield at the Bulk Shielding Facility

L. H. Ballweg

(This memorandum has appeared as CF 51-5-16)

Intra-Laboratory Correspondence

OAK RIDGE NATIONAL LABORATORY

May 3, 1951

To: J. Lawrence Meem, Jr.

From: L. H. Ballweg

Subject: Gamma Ray Measurements Behind an Iron-Water Shield at the Bulk Shielding Facility

Centerline measurements were made of the gamma radiation for the Bulk Shielding Reactor in an iron-water mixture (Experiment 2). The reactor had water as a reflector on all sides but the rear as described under Reactor Configuration No. 2 in the February, 1951 ANP report.

The rear face of the iron was 10 cm from the face of the reactor and was 43.85 cm thick.

The measurements were all converted to r/hr/watt. The following table is a summary of the data. The results are plotted in Fig. 1. The dashed curve is the 100% water data (CF 51-4-110).

Z distance (cm) Reactor to Chamber	r/hour/watt
55.89	2.308×10^{-2}
60.	1.816×10^{-2}
62.5	1.511×10^{-2}
65.	1.247×10^{-2}
70.	8.500×10^{-3}
75.	6.113×10^{-3}
80.	4.346×10^{-3}
90.	2.400×10^{-3}
100.	1.388×10^{-3}
110.	8.383×10^{-4}
120.	5.109×10^{-4}
130.	3.253×10^{-4}
140.	2.098×10^{-4}
150.	1.380×10^{-4}
160.	9.218×10^{-5}
170.	6.236×10^{-5}
180.	4.229×10^{-5}
190.	2.928×10^{-5}
200.	1.979×10^{-5}
210.	1.396×10^{-5}
220.	9.896×10^{-6}
230.	7.036×10^{-6}
240.	4.948×10^{-6}
250.	3.525×10^{-6}
260.	2.481×10^{-6}
270.	1.735×10^{-6}

DWG. 11005

FIG. K-1

BULK SHIELDING FACILITY

EXPERIMENT NO. 2 IRON–WATER TEST

CENTER LINE GAMMA RADIATION MEASUREMENTS

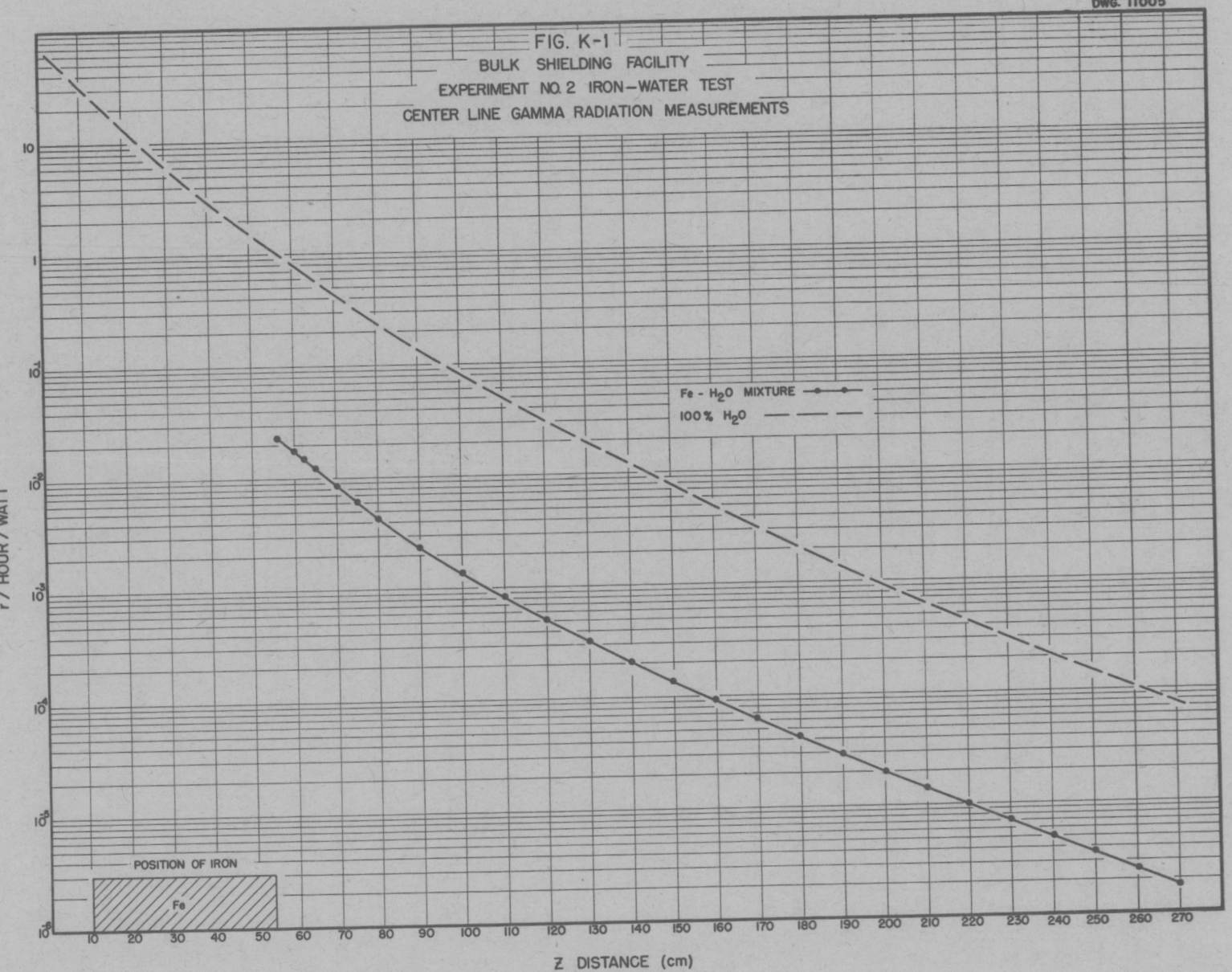

APPENDIX L

Preliminary Results on the Determination of Thermal Neutron Flux in Water

E. D. Klema
R. H. Ritchie

(This memorandum has appeared as CF 51-4-103)

[redacted]

Intra-Laboratory Correspondence

OAK RIDGE NATIONAL LABORATORY

To: J. L. Meem Date: 24 April 1951

From: E. D. Klema and R. H. Ritchie

Subject: Preliminary Results on the Determination of Thermal Neutron Flux in Water.

The determination of thermal neutron flux in water by the foil method requires that the flux be accurately known at various positions in the standard graphite pile in order that foils may be calibrated. It requires in addition that the difference in flux perturbation by a foil in graphite and in water be known.

The present standard pile calibration (CP-2804) seems to give a figure for the thermal flux which is approximately 20% too low (ORNL-409, p 12). Work is now being done on an independent method of determining the flux,(AECU-526) The absolute disintegration rate of a gold foil which has been exposed in the standard pile will be determined with an NaI scintillation counter of known efficiency for the main gamma ray from activated gold. The corrected figures for the flux in the sigma pile will be released later and at that time corrections to the present data may be made.

To take account of the difference in flux perturbation, a series of indium foils of various thickness was exposed in the graphite pile at 115 cm from a 1 gm Ra-Be source and in the water pile at the Bulk Shielding Facility at 20 cm from a 1/2 gm Ra-Be source. The foils were counted on both sides and the average activity was used. The saturated activity per unit thickness of the foil is given in the following table:

t (mils)	$A^s/t]_{water}$	$A^s/t]_{graphite}$
1.2	10,770	5,129
1.9	8,710	4,282
3.7	5,390	2,800
3.8	5,390	2,898
5.5	3,770	2,160

The cadmium ratio at the point of measurement was large in both cases. It is assumed that the shape of these two curves relative to one another is not influenced greatly by the source to foil spacings. This assumption is being checked experimentally at the present time.

By extending the curves drawn through the experimental points to 1 mil, one finds that a 5 mil foil activity in water should be corrected upward 16% to 1 mil in graphite.

[redacted]

[redacted]

Preliminary Results on the Determination of
Thermal Neutron Flux in Water

To obtain the correction at 1 mil we may employ the approximate theory of Skyrme (MS-91). Using $\sigma_{a\ In}$ = 197 barns and an equivalent radius of 2.83 cm for the foil, the activity per unit neutron flux for a 1 mil foil in graphite was found to be 1.05 times the activity per unit neutron flux for a 1 mil foil in water.

Combining these corrections, the activity of a 25 cm^2 area 5 mil thick Indium foil in water should be increased by a factor of 1.22 over its measured activity to account for the difference in effect upon the flux. Or,

$$(Nv)_{water} = CA_{water} \quad \frac{(Nv)_{graphite}}{A_{graphite}}$$

where A is the measured activity (counts per unit time) of the foil and C takes on the following values:

t(mils)	C
0	1.00
1.0	1.05
2	1.11
3	1.14
4	1.20
5	1.22

To obtain C, a smooth curve was drawn through the experimental points and values were read from the graph.

It is possible to go to thinner indium foils by employing an indium-aluminum alloy, for example. Since this alloy was not available when the experiment was performed the thinnest foil used was about 1 mil. It may be thought necessary later to re-perform this experiment using thinner foils to remove some of the uncertainty in employing the approximate correction at 1 mil. However, this error is probably small. The overall error in the value of C is thought to be ± 5%.

The foil measurements in water were made by Grace McCammon and in graphite by Thelma Arnette.

E. D. Klema
E. D. Klema

R. H. Ritchie
R. H. Ritchie

RHR:em

[redacted]

APPENDIX M

A Proportional Counter Method of Measuring The Fast Neutron Dose

G. S. Hurst

(This memorandum has appeared as CF 51-4-122)

A PROPORTIONAL COUNTER METHOD BY MEASURING THE FAST NEUTRON DOSE

by G. S. Hurst

Introduction

The problem under consideration is that of measuring the amount of energy absorbed per gram of animal tissue from a given beam of fast neutrons. If the neutron energy is above about 100 Kev, most of the energy transferred to tissue is transferred as a result of elastic collisions of the neutrons with the hydrogen, oxygen, nitrogen, and carbon components of tissue. These recoiling atoms then lose their energy by ionization and excitation. The amount of energy lost by a particle in producing an ion pair is very nearly independent of the particle energy, so that a measure of the number of ions produced in a tissue equivalent gas gives the amount of energy absorbed from the beam. The energy absorbed per gram of tissue has been adopted as a basis for dose measurements and the roentgen equivalent physical (rep) has been defined as that amount of radiation of any type that produces 95 ergs per gram of tissue.

For health physics and experimental biological work it is desirable to measure the dose in units of reps for each type of radiation separately, for it is known that the effectiveness of radiation in producing damage to cells depends on the density of ionization as well as the total amount of energy absorbed. For example, one rep of gamma or x-ray exposure produces only ten or twenty per cent as much damage as one rep of protons.

The following discussion will show how an ionization chamber method developed by L. H. Gray[1] can be applied to a proportional counter that enables one to measure the dose due to fast neutrons in the presence of high intensities of gamma or x-radiation.

(1) Gray, L. H., Proceedings of the Cambridge Philosophical Society, 40, 72 (1944).

Imagine a beam of fast neutrons to strike a metal chamber filled with a hydrogenous gas. Recoil protons are formed throughout the gas volume, and if the pressure is not made exceedingly large many of the protons escape into the metal surface and can produce no ionization current in the chamber. Therefore the current produced by the remaining ions would not represent the amount of energy that the neutron beam loses in the gas, and furthermore this discrepancy would be greater as the energy of the neutrons increase. If this gas cavity is surrounded by a solid hydrogenous material this loss of ionization from the gas will be exactly compensated for by the amount of ionization that the solid material contributes to the gas, provided the atomic composition of the solid is the same as the gas and provided the thickness of the solid is greater than the maximum proton ranges.

The tissue dose per neutron varies with energy as the quantity $E \Sigma_i \sigma_i f_i Q_i$, where E is the neutron energy, σ_i is the scattering cross section of the i'th kind of atom, f_i is the average loss of energy per collision with the i'th atom and Q_i is the number of the i'th kind of atom. The energy absorbed per unit mass of methane (CH_4) varies as $E \Sigma_i \sigma_i f_i Q_i$. The ratio $\frac{E \Sigma_i \sigma_i f_i Q_i}{E \Sigma_i \sigma_i f_i Q_i}$ is very nearly constant for energies between 100 Kev and 10 Mev, since the term $\sigma_h f_h Q_h$ for hydrogen is much greater than the sum of the other terms in both tissue and methane. Thus a methane filled chamber lined with a methane equivalent wall material serves as a satisfactory dosimeter for fast neutrons. Paraffin is an approximate methane equivalent wall material.

In order to make an instrument that is gamma insensitive, one can apply the Gray ionization method to a proportional counter. In this case, the counter can be so designed that the pulses produced by gamma rays are smaller than most

of the proton pulses. The associated electronic circuit must then bias out the gamma pulses and integrate the remaining proton pulses according to the pulse height. If one desires to make absolute energy measurements with a proportional counter it is necessary to insure that the gas amplification is uniform throughout the counter and is known. However, relative energy measurements can be made by calibration with a neutron source of known spectrum and known emission rate. In this case non-uniformities in the gas amplification affect the results only insofar as the spatial distribution of protons changes with neutron energy.

Experimental

Proportional counters were designed as shown in Figure 1 for the purpose of checking the response with monoergic beams of fast neutrons. (Construction details are given by ORNL Instrument Department Dwg. #Q-963-1). The purpose

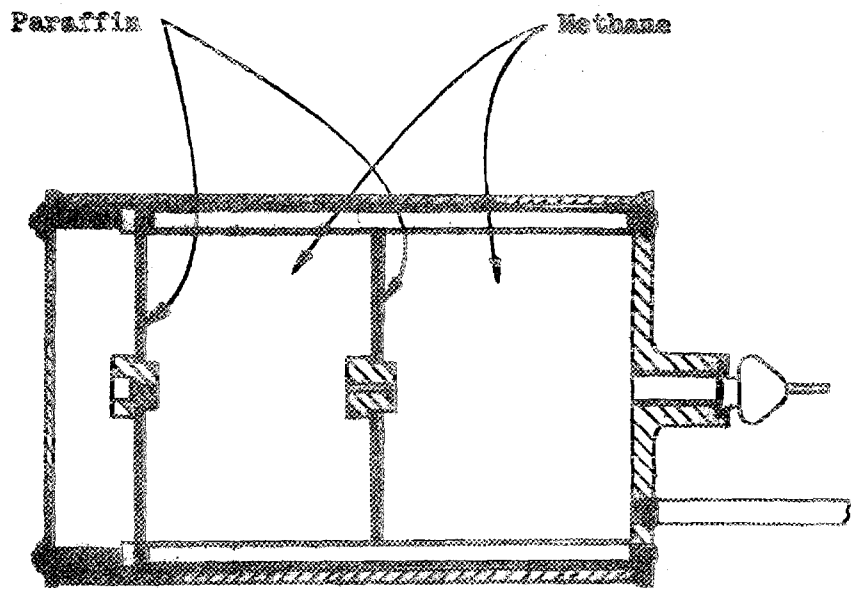

Figure 1.

of two sections is to raise the sensitivity, while keeping the maximum electron pulses small. Notice that the paraffin is only deposited on the two end plate sections. This satisfies the Gray principle fairly accurately for the case of well collimated beams. In cases where there is much scattered radiation, the entire counter must be lined with paraffin.

The experimental apparatus is shown in the block diagram of Figure 2. The bandwidth of the linear amplifier was set at 2 mc. The gain was set well above noise background and the high voltage was adjusted so that pulses from

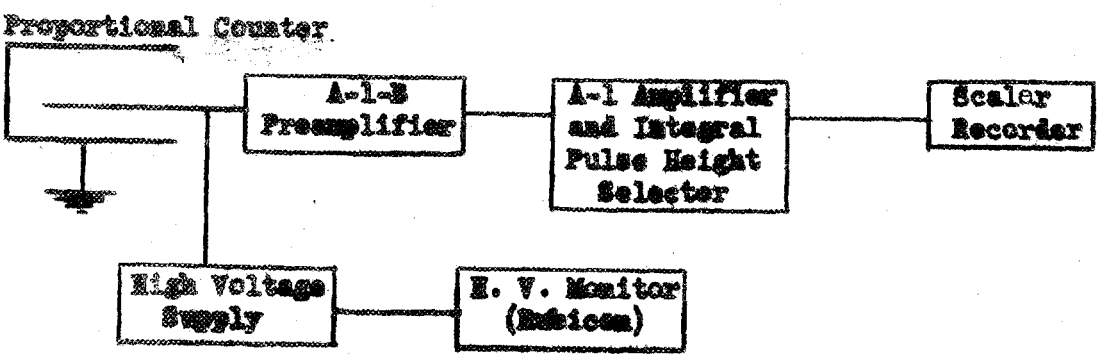

Figure 2.

Ra gamma were not more than about 15 volts, as measured by the integral pulse height selector. The complete spectrum of pulses above 15 volts was then determined with the PHS for neutrons of various energies.(2) The area under the number of pulses vs PHS curve is proportional to the total energy. Figure 3a shows the results obtained and a comparison is made with the variation of the dose per neutron as a function of the neutron energy, Figure 3b. In the case of Po-Be neutrons the spectrum obtained by Perlman, Richards, and Speck(3) was used as a basis for determining the dose per neutron.

A pulse integrator that measures the energy of the spectrum in one operation has been designed by F. M. Glass, Instrument Department. This circuit together with a counter of the non-directional type (ORNL-HP-Inst. Dev. Dwg. #C-207) is now being used by the "Lid Tank" group. That the counter is non directional may be seen from Table I, which shows the response of the counter as a function of laboratory angle. The pulse integrator provides an easy measurement of the average decrease in gas amplification for protons due to a high intensity gamma field. It was found the effect is about three per cent when the counter is subjected to a field of two roentgens per hour Ra gamma.

Angle of Source with Counter Axis	Relative Dose Reading (Source - Po - Be at 56 cm)
0°	1.00
45°	.98
90°	.99
120°	.95

Table I.

(2) The Monoergic Neutrons were produced by the reactions $H^3 + H^1 \rightarrow N + H^3 -$ 735 Kev, and $H^2 + H^2 \rightarrow N + He^3 + 3.3$ Mev at the Los Alamos Laboratory.
(3) MDDC-39

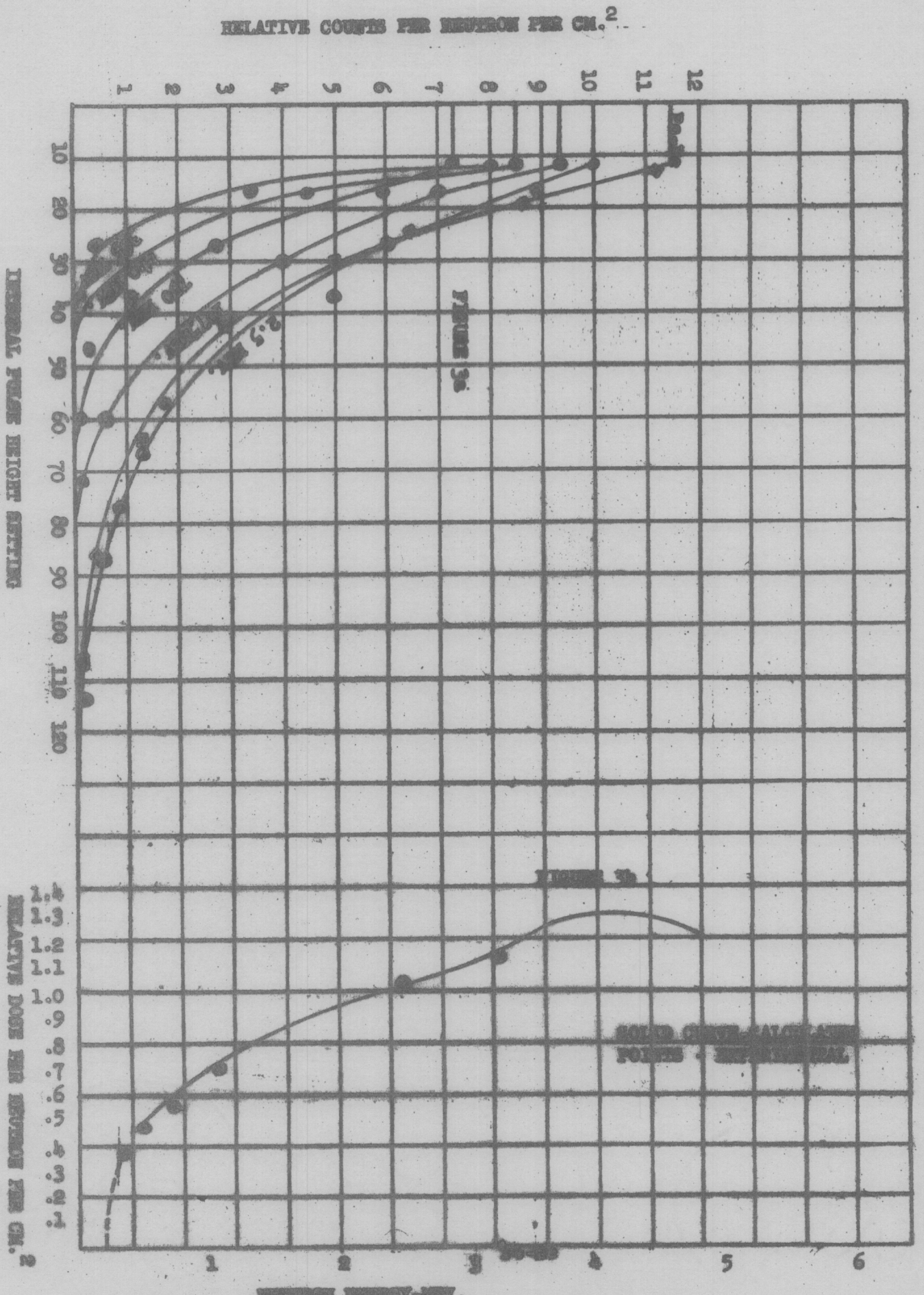
RELATIVE COUNTS PER NEUTRON PER CM.²
1 2 3 4 5 6 7 8 9 10 11 12
10 20 30 40 50 60 70 80 90 100 110 120
INTEGRAL PULSE HEIGHT SETTING
RELATIVE DOSE PER NEUTRON PER CM.²
1.4 1.3 1.2 1.1 1.0 .9 .8 .7 .6 .5 .4 .3 .2 .1
1 2 3 4 5 6
NEUTRON ENERGY-MEV.

Acknowledgements

The writer wishes to express his thanks to H. H. Wilson and W. B. McDonald for their work in designing and constructing counters; also to R. F. Taschek and his co-workers, at the Los Alamos Laboratory, for their help in obtaining data with monoergic neutrons.

GSH:em

G. S. Hurst
Health Physics Division

APPENDIX N

Calibration of the Fast Neutron Dosimeter Used at the Bulk Shielding Facility

R. G. Cochran

(This memorandum has appeared as CF 51-5-74)

[redacted]

Intra-Laboratory Correspondence

OAK RIDGE NATIONAL LABORATORY

May 11, 1951

To: J. Lawrence Meem, Jr.

From: Robert G. Cochran

Subject: Calibration of the Fast Neutron Dosimeter used at The Bulk Shielding Facilit

One of the most important measurements being made on shielding mockups at the bulk shielding facility is the fast neutron dosage. These measurements will be described in subsequent reports. This report is a brief description of the instrument used, method of calibration, and estimate of errors.

The fast neutron dosimeter consists of the following components; a proportional counter designed by G. S. Hurst[1], an integrator designed by F. Glass, an A-1 amplifier, power supplies, and scalers. The integrator is the most critical part of the equipment. It is equipped with a suitable metering circuit so that drift of the instrument can be detected and compensated for by suitable adjustment.

Therefore, the first problem was to determine the linearity of the integrator after it was properly adjusted. In this experiment, this was done by using a pulse generator as a source, which puts out a constant amplitude pulse, whose frequency can be varied. This source of pulses was monitored by use of a scaler to determine the frequency, and an oscilloscope to maintain

---

[1] "A Proportional Counter Method of Measuring Fast Neutron Dose", C.F. #51-4-122

a constant amplitude. The attached graph (Fig. 1) indicates the linearity condition found.

The next step was to compare the system to a standard source of fast neutrons. The source used was a Po-Be source #PB-168 of about 6 curies strength. The proportional counter was suspended 12 ft. above the floor on a pole. The source, too, was placed 12 ft. above the floor and was movable along a horizontal rod, so that the source to counter position could be accurately varied. Various distances from 15 cm. to 130 cm. were then checked (Fig. 2). Using the data thus obtained, the following calculation was made.

Let: R20 be counts per min. at 20 cm. between counter end and source.

Let: R30 be counts per min. at 30 cm. between counter end and source.

Let: x be distance from end of counter to center of detection.

Then:

$$R20 = R30 \times \left(\frac{30 + x}{20 + x}\right)^2$$

For example using the data obtained March 1, 1951

1500 c/m at 20 cm.

732 c/m at 30 cm.

$$1500 = 732 \left(\frac{30 + x}{20 + x}\right)^2$$

$$2.05 = \left(\frac{30 + x}{20 + x}\right)^2 \quad \text{now} \left(\frac{35}{25}\right)^2 = \left(\frac{7}{5}\right)^2 = \frac{49}{25} = 1.96$$

Comparing 2.05 to 1.96 indicates that the center of detection of the counter in air was about 5 cm. from the front end of the counter.

DWG. NO. 11247
NOT CLASSIFIED

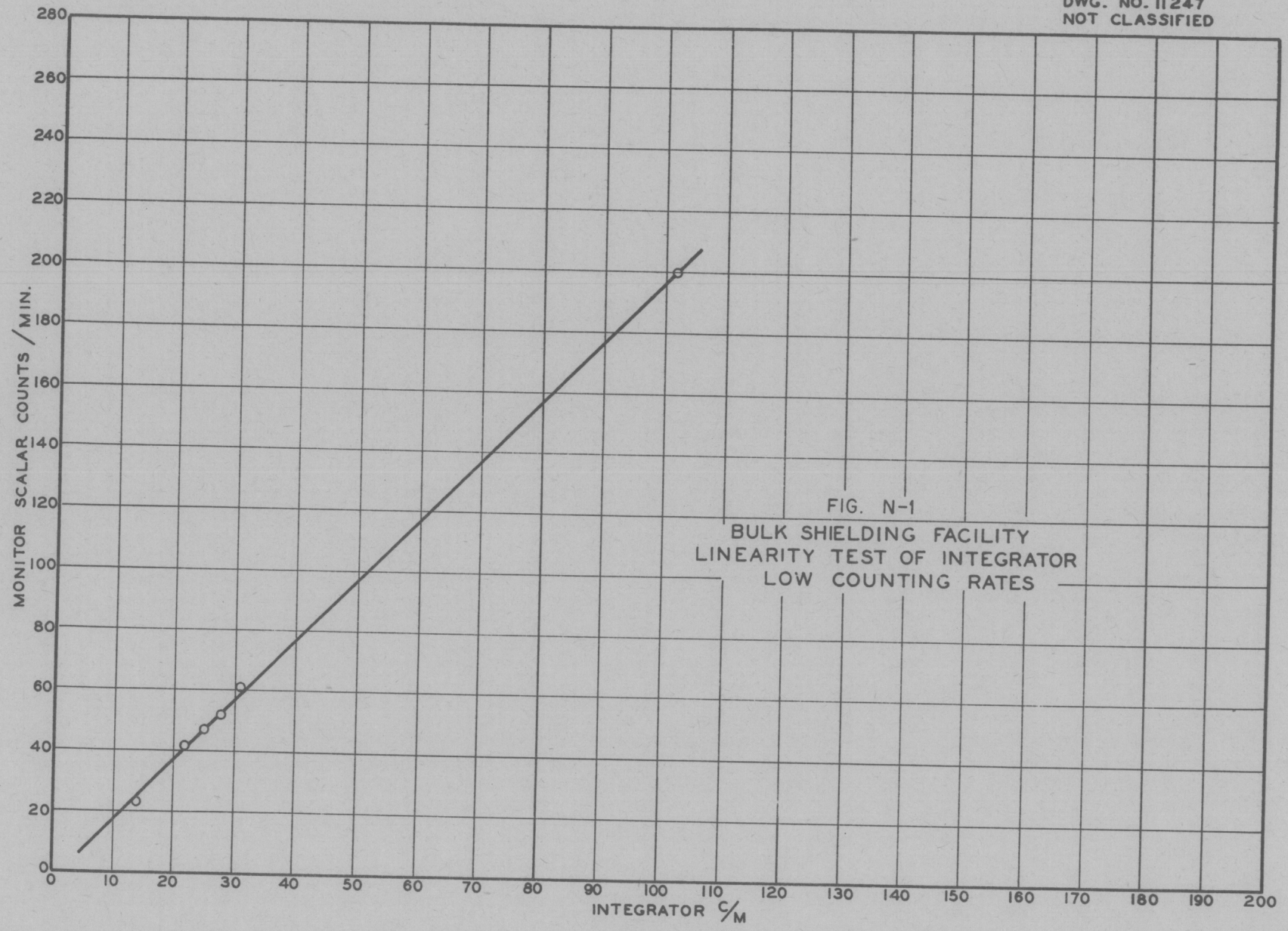

FIG. N-1
BULK SHIELDING FACILITY
LINEARITY TEST OF INTEGRATOR
LOW COUNTING RATES

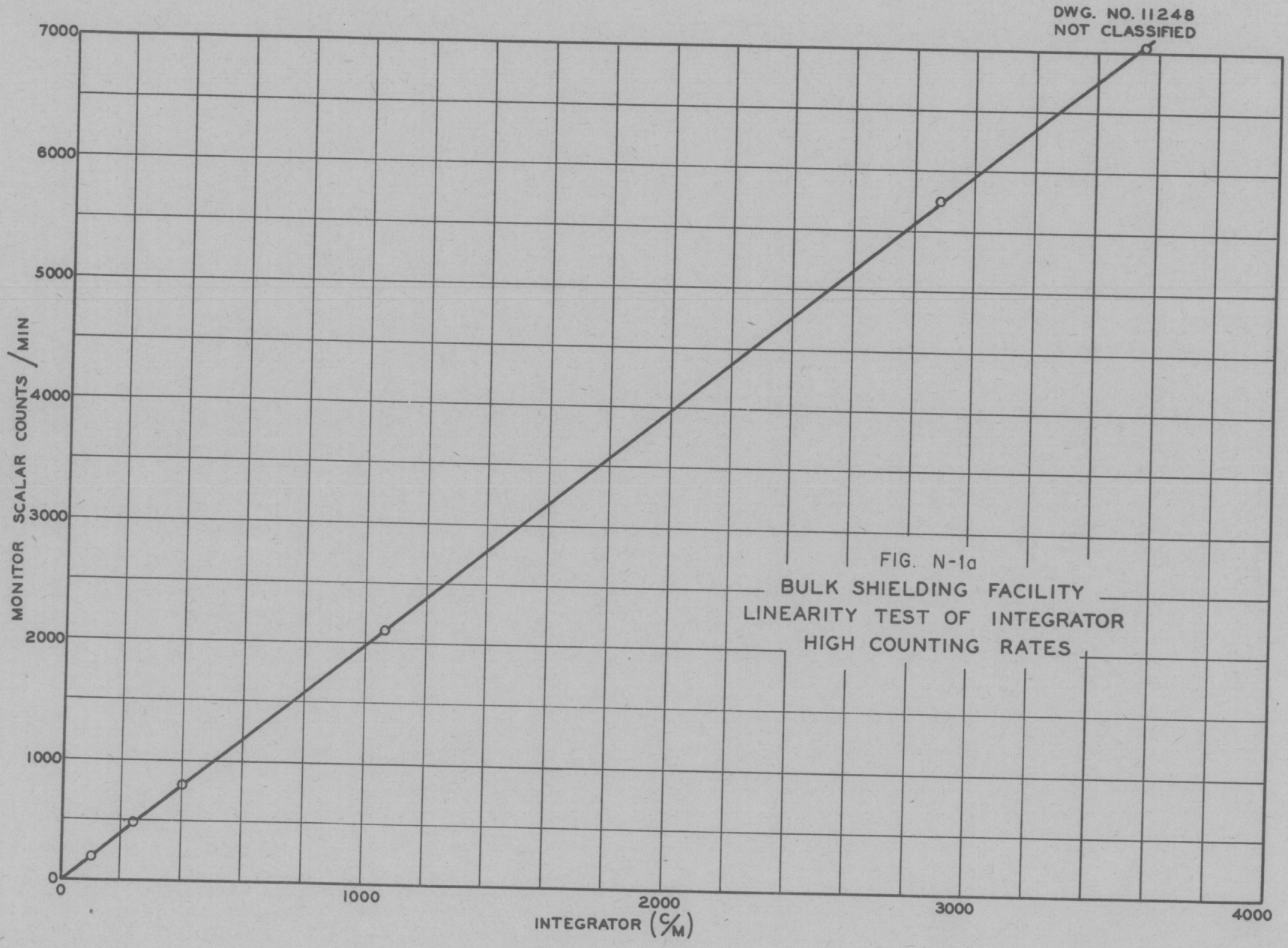

FIG. N-1a
BULK SHIELDING FACILITY
LINEARITY TEST OF INTEGRATOR
HIGH COUNTING RATES

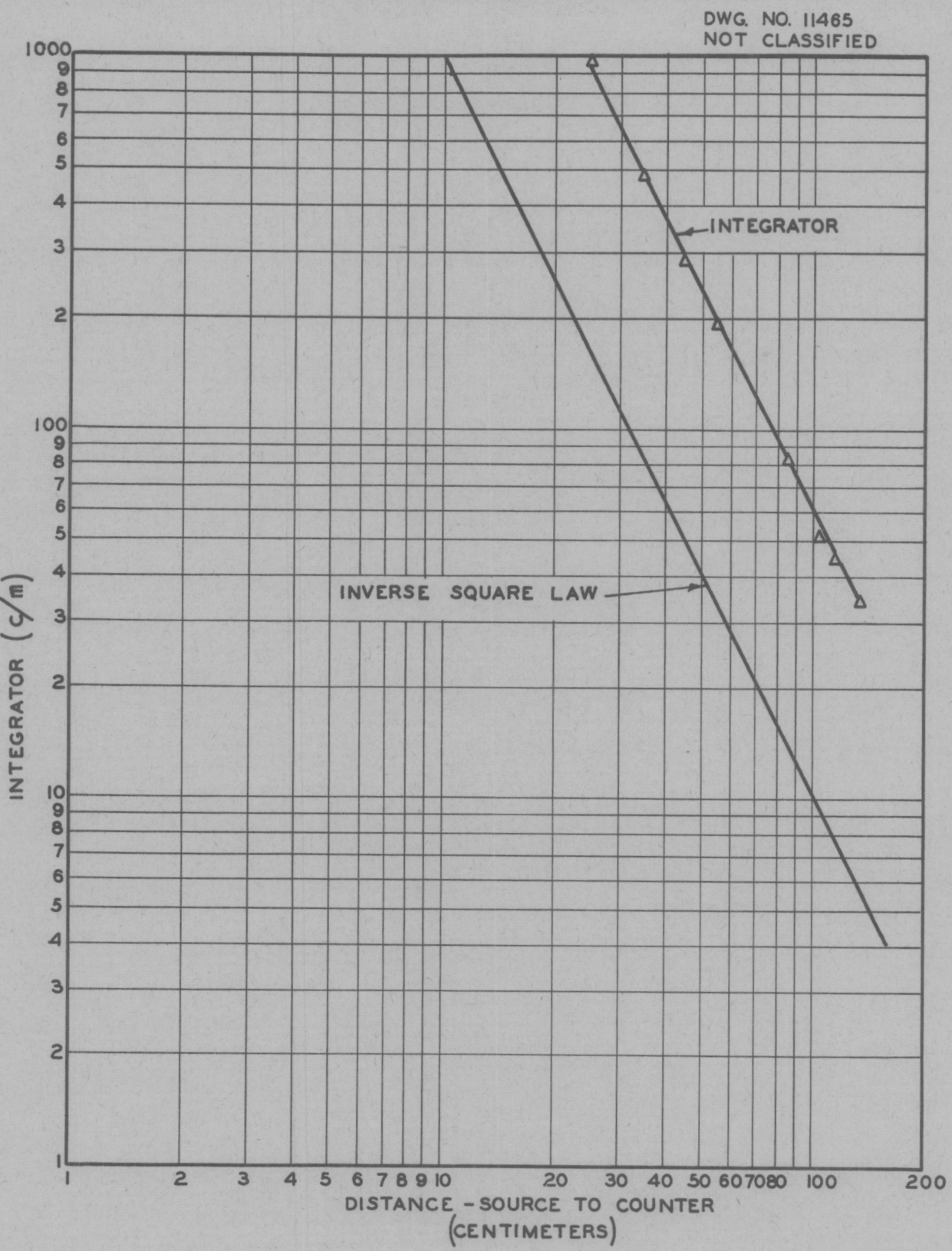

FIG. N-2

AIR CALIBRATION FOR DOSIMETER USING A Po-Be SOURCE

So at 35 cm., we have 730 counts per min. or C/S = 12.1.

According to Central Files letter #50-10-168, the source #PB-168 emitted 3.19×10^7 neutrons per sec. on October 25, 1950.

For example, on March 1, 1951, the source had decayed for 126 days.

$$\text{so n/sec.} = 3.19 \times 10^7 \times e^{-\frac{.693 \times 126}{138}}$$

$$\text{n/sec.} = 1.69 \times 10^7 \text{ neutrons/sec.}$$

Now the neutrons per square centimeter per sec. at 35 cm. is:

$$= \frac{1.69 \times 10^7}{4\pi \times (35)^2} = 1.11 \times 10^3 \text{ n/cm}^2\text{/sec.}$$

G. S. Hurst of the Health Physics Division has calculated a figure of 4.0×10^{-6} as the millirep conversion figure for a Po-Be source.

Thus millireps/sec:

$$= 4.0 \times 10^{-6} \times 1.11 \times 10^3 \text{ millirep/sec.}$$

$$= 4.44 \times 10^{-3} \text{ millirep/sec.}$$

and the millireps/count figure is:

$$\frac{4.44 \times 10^{-3}}{12.1} = 3.68 \times 10^{-4} \text{ millireps/count.}$$

Then, using the above millireps per count constant and knowing the reactor power, the data obtained from shielding measurements were plotted as the centimeter distance from the shield vs. the millirep/watt.

According to a letter from Mr. E. S. Reed, ORO, dated June 1, 1951, the standard source E-665, used to calibrate the Po-Be source PB-168, is known to an accuracy of ± 5%. In addition, the techniques were sufficiently good in comparing PB-168 to E-665 that the introduction of an additional error of only about ±2% was possible. Thus the neutron flux from the PB-168 calibrating

source is known to about ± 7%.

By experiment it was found that the dosimeter would repeat points to within an error of ± 2%. The error due to non-linearity of the integrator can be estimated from Fig. 1 and Fig. 1A to be about ± 5% up to 4000 c/m; above this counting rate the error becomes somewhat larger. However, we usually do not obtain usuable counting rates above 4000 counts per minute due to gamma ray pile-up.

Now considering Fig. 2 it can be seen that the integrator follows the inverse square law very well. Another experiment was performed in the shielding facility using the reactor to check the linearity of the dosimeter. At 100 watts the counting rate was 4.6 c/m, at 1000 watts it was 49.6 c/m, and at 10,000 watts, a counting rate of 597 c/m was obtained. Considering the counting rates at 100 watts and at 10,000 watts the 100 watt counting rate was 23% low. So, until the above mentioned errors can be further investigated, it is best to assume a conservative figure for the overall measurement error of the sum of the two largest errors which would be 30%. Thus, we assume our data to be within an error of about 30% for all shielding measurements.

Robert G. Cochran

Robert G. Cochran

RGC/reb

APPENDIX O

Fast Neutron Measurements at the Bulk Shielding Facility

H. E. Hungerford
R. G. Cochran

(This memorandum has appeared as CF 51-11-96)

OAK RIDGE NATIONAL LABORATORY

December 10, 1951

To: J. L. Meem

From: H. E. Hungerford and R. G. Cochran

Subject: FAST NEUTRON MEASUREMENTS AT THE BULK SHIELDING FACILITY

Until recently all of the fast neutron measurements at the BSF were made with a fast neutron dosimeter designed by G. S. Hurst and F. Glass of ORNL. These measurements are of considerable importance to the designers of mobile reactor shields, so it was considered advisable to check the results by other methods.

Accordingly, two other independent sets of measurements of fast neutrons were made, the first by means of a radioactive threshold detector, and the second by means of a U^{238} fast fission chamber. The data were obtained along the centerline in water at various distances from the BSR.

A suitable threshold detector is provided by sulfur through its (n,p) reaction in a beam of fast neutrons:

$$S^{32} + n \longrightarrow P^{32} + p$$

$$P^{32} \longrightarrow S^{32} + \beta^-$$

The actual threshold for the reaction is about .97 Mev, but the effective threshold is much higher, around 3 Mev, with a cross-section of 285 millibarns. The half life of the beta emission is 14.1 days with a maximum beta energy of 1.71 Mev.

In the past the radioactive phosphorous has been separated chemically from the original sulfur salt and counted, a process which is tedious and unsatisfactory at best.(1)

For the present measurements, it was decided to make sulfur foils out of U.S.P. grade sulfur flowers. This eliminated the necessity of chemically separating out the radioactive phosphorous.

---

(1) "The Aircraft Nuclear Propulsion Project Quarterly Progress Report for Period Ending August 31, 1950", p. 35, ORNL-858

Sample plates to hold the sulfur foils were made so that after exposure they could be placed directly in the shelves of a mica-window counter. They consisted of aluminum plates about 3-5/16" x 2-7/16" x 1/16" with a 2 in diameter slot 1/32" deep counter-sunk into one face.

Sulfur powder was pressed into the shallow molds thus formed by means of a heat press designed for the purpose. Each sample was pressed at a temperature of 95° C at a pressure of around 10,000 psi. for a period of 10 minutes, and allowed to cool in an air stream under pressure until the temperature reached 60°C. Then the pressure was released and the sample cooled quickly to room temperature by immersing the press in cold water. Since sulfur reacts with steel at high pressure, a highly polished 20 mil tantalum disk had to be used between the pressing cylinder and the sulfur to prevent sticking.

The samples were placed between two 40-mil thicknesses of cadmium to prevent thermal reactions during exposure.

The U^{238} fission chamber consisted of 14 plates with about 6 grams total of U^{238} plated on them. The U^{238} was pure to about 1 part in 100,000. The fission chamber with an A-1-A preamp was enclosed in a water tight housing and kept at about 10 lbs/in^2 pressure of argon. The preamp was connected to an A-1 amplifier through 50 ft of cable. An Atomic scaler was connected to the P.H.S. of the amplifier. Fig. 2 shows a plot of P.H.S. vs. counting rate for various voltages on the chamber. The chamber did not seem to be very sensitive to voltage, so a voltage of 247 volts was selected as the operating point. Fig. 3 gives curves of P.H.S. vs. counting rate for a Po-Be source. This curve also shows that the chamber was unaffected by γ-rays from a Co^{60} source.

When instruments are exposed to the BSR, neutron measurements are made in a high gamma radiation field. Thus the effects of γ-rays on the performance of the neutron detecting instruments is an important consideration.

The data obtained from these measurements is given in Tables 1 through 4. Included are the dosimeter measurements given in terms of $n/sec/cm^2/watt$, and in millirep/hr/watt as in previous memoranda.

Conclusion

The results of these experiments are summarized in Fig. 1. The thresholds of the various instruments are 200 kv. for the dosimeter, 1.5 Mev for the U^{238} fission chamber, and 3 Mev for the sulfur threshold detector. The dosimeter was calibrated against PB-168 Po-Be source. The U^{238} fission chamber and the sulfur were calibrated against Po-Be source, PB-217. Experiments indicate that there is a discrepancy in calibration between these two sources since there is some difference in their spectra.

The dosimeter is usually run behind 3 in of lead for γ-ray shielding. It was found advisable to do the same thing for the U^{238} fission counter. The curves in Fig. 1 indicate what effect the lead has on the U^{238}.

At large distances the U^{238} fission chamber curve changes slope. This change in slope is probably due to photofission in the U^{238}. The photofission threshold is about 5.76 Mev from γ-ray spectral measurements. There is a peak at 6 or 7 Mev in the gamma ray spectrum from the reactor. This may explain the change in slope of the curve for the U^{238} counter. Considering all the uncertainties involved, the agreement of the three curves is fairly good, both in magnitude and slope.

TABLE 1

U^{238} Fission Chamber

No Pb or B-Cd Liner

Distance from Reactor cm.	Reactor Average Power	Cts/Min/Watt	Fast Flux N/Sec/Cm^2/Watt
6.7	1 watt	21,586	2.74×10^5
11.7	1 watt	8,018	1.02×10^5
21.7	1 "	1,297	1.65×10^4
21.7	10 "	1,342	1.70×10^4
31.7	10 "	254	3.23×10^3
41.7	10 "	59.0	7.49×10^2
41.7	100 "	64.4	8.18×10^2
51.7	100 "	17.0	2.16×10^2
61.7	100 "	5.53	7.02×10^1
61.7	1000 "	5.96	7.57×10^1
71.7	1000 "	2.44	3.10×10^1
81.7	1000 "	1.17	1.49×10^1
81.7	10,000 "	1.53	1.94×10^1
91.7	10 KW	.797	1.01×10^1
101.7	"	.482	6.12×10^0
111.7	"	.289	3.67×10^0
121.7	"	.188	2.39×10^0
141.7	"	.0867	1.10×10^0
161.7	"	.042	5.33×10^{-1}
181.7	"	.0219	2.78×10^{-1}
201.7	"	.011	1.40×10^{-1}

TABLE 2

U^{238} Fission Chamber

B - Cd Liner in Chamber

3" Pb 10 cm. from front of Counter

Distance from Reactor Cm.	Reactor Power	Average Cts/Min/Watt	Fast Flux N/Sec/Cm^2/Watt
25.0	1 watt	939	1.19×10^4
31.7	10 watts	299.4	3.80×10^3
41.7	10 watts	64.0	8.13×10^2
51.7	100 watts	14.8	1.88×10^2
61.7	100 watts	3.65	4.64×10^1
71.7	1000 watts	1.014	1.29×10^1
91.7	1000 watts	.110	1.40×10^0
101.7	10,000 watts	.035	4.44×10^{-1}
121.7	10,000 watts	.0071	9.02×10^{-2}
151.7	10,000 watts	.00159	2.02×10^{-2}
181.7	10,000 watts	.00055	6.98×10^{-3}

TABLE 3

Dosimeter Measurements

Distance from Reactor	Millirep/Hr/Watt	Fast Flux N/Sec/Cm^2/Watt
2.4	1.34×10^{4}	9.30×10^{5}
7.4	6.66×10^{3}	4.62×10^{5}
17.4	1.08×10^{3}	7.50×10^{4}
21.7	5.22×10^{2}	3.62×10^{4}
28.7	1.60×10^{2}	1.11×10^{4}
32.5	8.91×10^{1}	6.18×10^{3}
41.7	2.13×10^{1}	1.48×10^{3}
50.2	5.64×10^{0}	3.91×10^{2}
60.2	1.55×10^{0}	1.08×10^{2}
70.2	4.48×10^{-1}	3.11×10^{1}
80.2	1.27×10^{-1}	8.10×10^{0}
90.2	3.44×10^{-2}	2.39×10^{0}
100.2	1.09×10^{-2}	7.56×10^{-1}
110.2	3.44×10^{-3}	2.39×10^{-1}
120.2	1.20×10^{-3}	8.33×10^{-2}
130.2	3.92×10^{-4}	2.72×10^{-2}
140.2	1.38×10^{-4}	9.58×10^{-3}
160.2	1.82×10^{-5}	1.26×10^{-3}
165.2	1.18×10^{-5}	8.19×10^{-4}

TABLE 4

Sulfur Threshold Detector Measurements

3 Mev. Neutrons

Distance from Source, Cm.	Fast Flux $N/Sec/Cm^2$ (= nv)
14.7	5.48×10^4
19.7	2.43×10^4
24.7	1.02×10^4
29.7	5.11×10^3
30.0	4.88×10^3
34.7	2.46×10^3
35.0	2.49×10^3
40.0	1.33×10^3
50.0	2.87×10^2
60.0	1.14×10^2
70.0	3.23×10^1
80.0	6.82×10^0

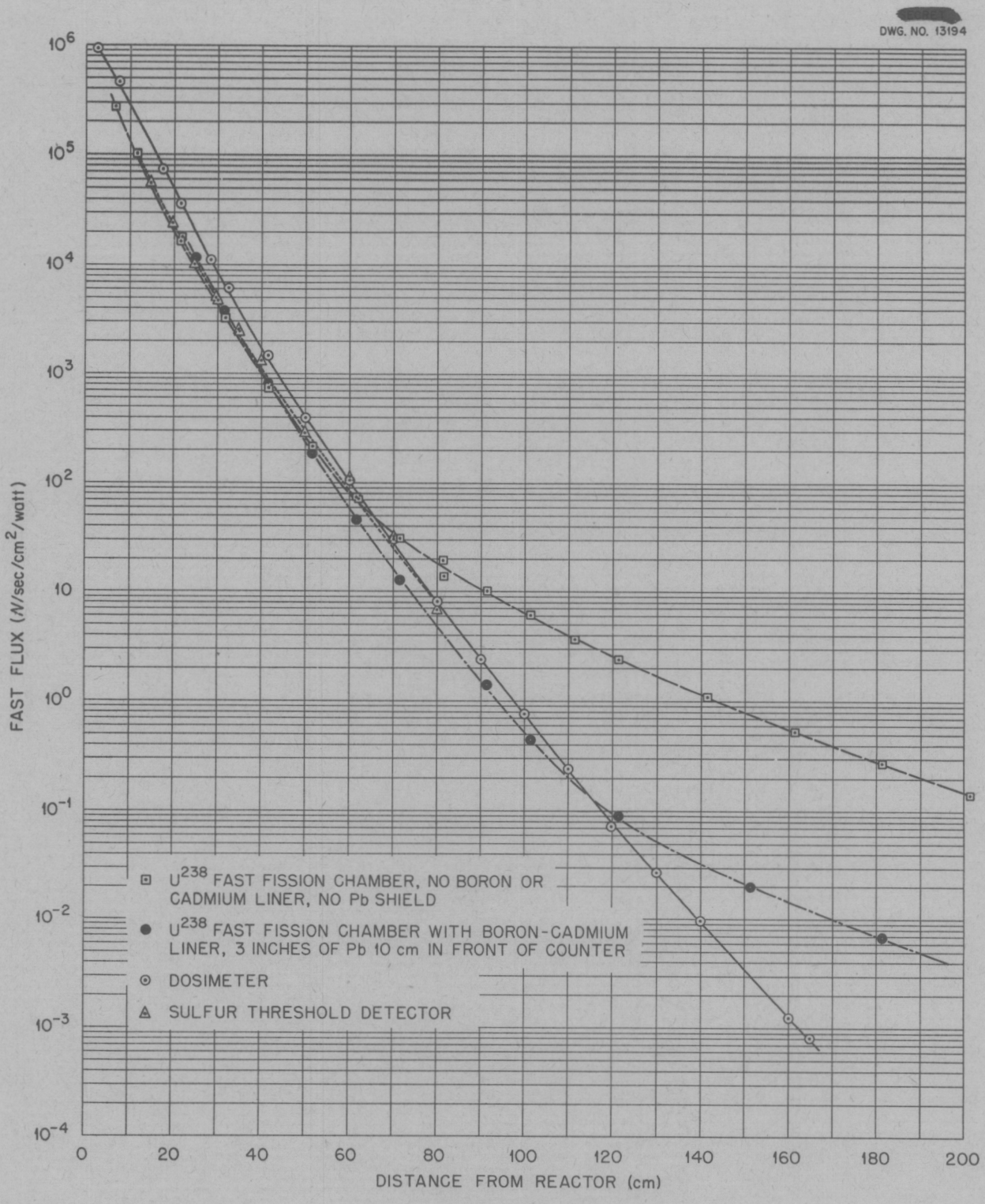

FIG. 0-1 - BULK SHIELDING FACILITY
FAST NEUTRON DATA

SECRET

DWG. 13261

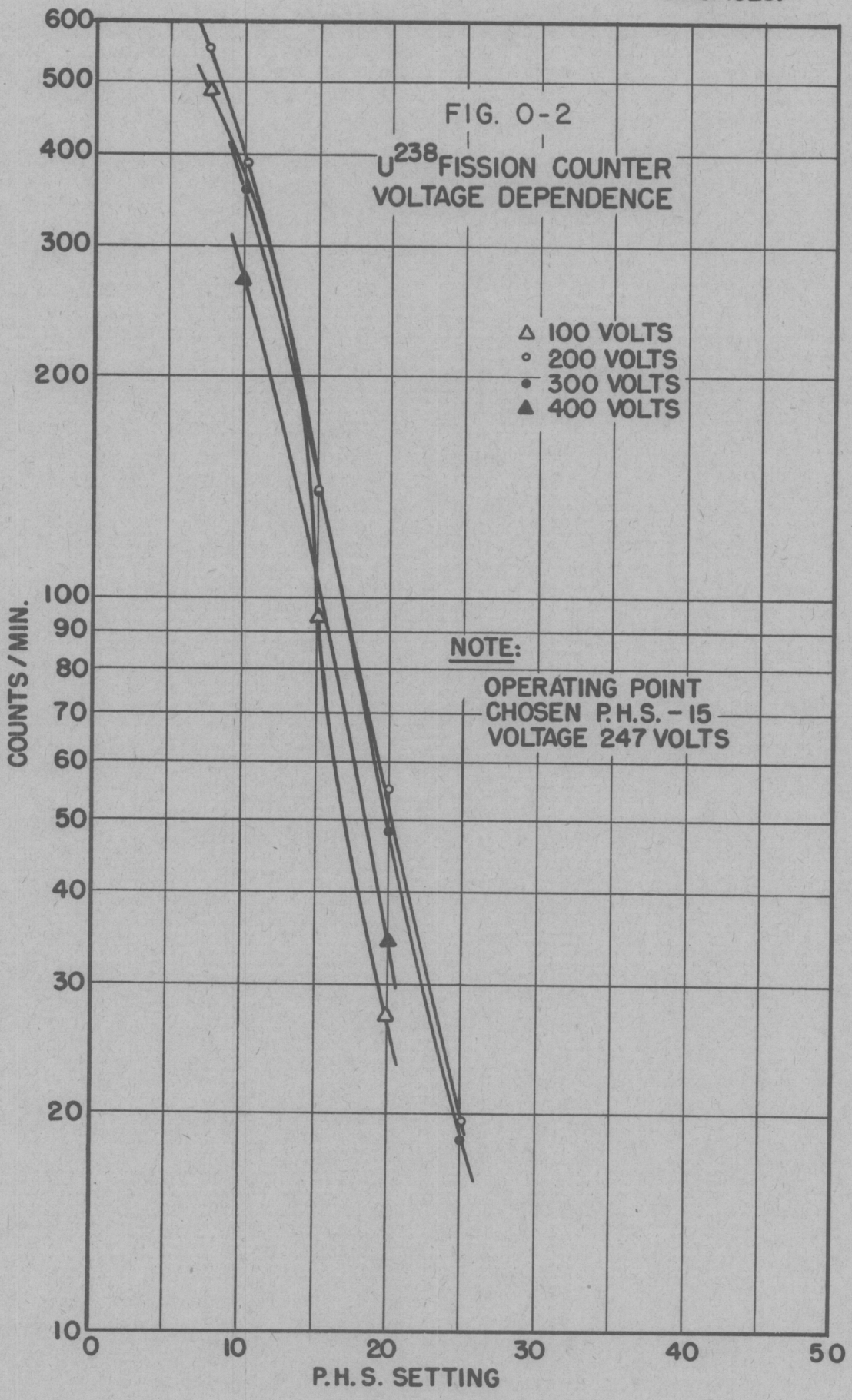

SECRET

DWG. 13260

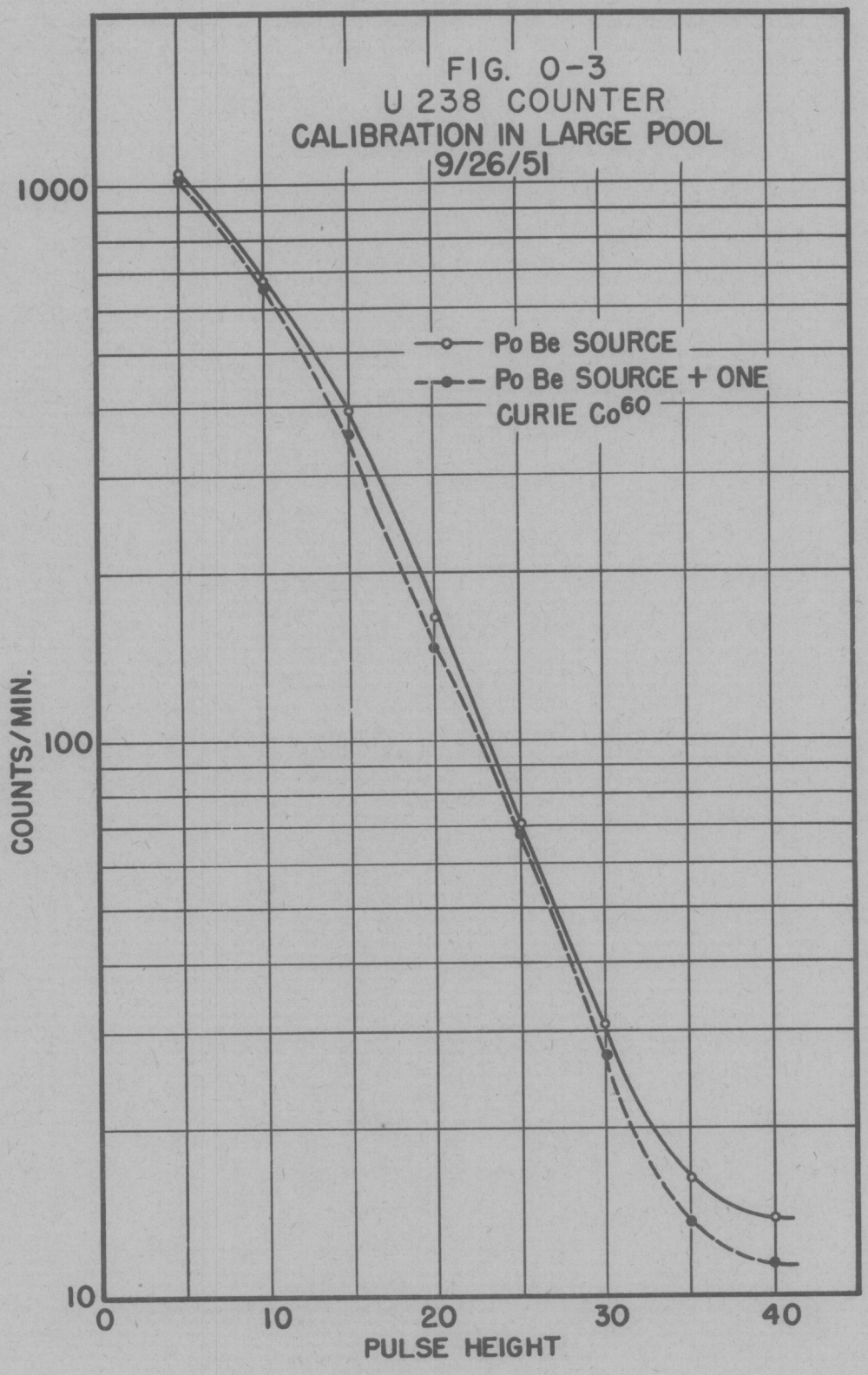

APPENDIX P

Center of Detection Calculations for Neutron Counters and Ion Chambers

H. E. Hungerford

APPENDIX P

CENTER OF DETECTION CALCULATIONS FOR NEUTRON COUNTERS AND ION CHAMBERS

This appendix contains a brief summary of the contents of ORNL CF 51-5-177, a memorandum describing the calculations on the center of detection for each of the Bulk Shielding Facility radiation measuring instruments. Because of space limitations no mathematical theory or detailed calculations involved are given here.

1. General

For measurements of neutrons and gamma rays in air, the distance from source to counter can be approximated rather closely by taking the geometric center of the chamber as the point of measurement of the radiation. It is then necessary only to apply corrections for attenuation of the radiation through the outer case and walls of the chamber, if required. However, if measurements are being made in a highly attenuating medium, such as water, then an entirely different picture is presented. Since there is no appreciable attenuation within the counter itself, after wall corrections, etc. have been made, the counter sees radiation of greater intensity entering from its periphery nearer the source than radiation entering from the rear. Hence, for a collimated beam the point of measurement of the radiation moves forward to the interface between the attenuating medium and the counter, and for non-collimated radiation the point of measurement is shifted from the geometric center slightly near the source due to the effects of attenuation. This point is defined as the center of detection.

2. List of Calculated Centers of Detection for the Bulk Shielding Facility Instruments

Instrument	Radiation Detected	Center of Detection Distance from Front of Counter
8" BF_3 Counter	Thermal neutrons	2.1 cm.
12" BF_3 Single-Chamber Counter	Thermal neutrons	3.55 cm.
12" BF_3 Double-Chamber Counter	Thermal neutrons	3.3 cm.
Dosimeter	Fast neutrons	1.7 cm.
50-cc Ion Chambers	Gamma radiation	2.0 cm.
900-cc Ion Chambers	Gamma radiation	2.95 cm.
G-M Tube	Gamma radiation	0.9 cm.

LIST OF REFERENCES

1. Report of the Shielding Board for the Aircraft Nuclear Propulsion Program, ANP-53, Oct. 15, 1950.

2. Breazeale, W. M., "The New Bulk Shielding Facility at Oak Ridge National Laboratory," ORNL-991, May 8, 1951.

3. Meem, J. L. and Johnson, E. B., "Determination of the Power of the Shield Testing Reactor - I. Neutron Flux Measurements in the Water-Reflected Reactor," ORNL-1027, Aug. 13, 1951.

4. Meem, J. L. and Ballweg, L. H., "A Standard Gamma Ray Ionization Chamber for Shielding Measurements," ORNL-1028, July 9, 1951.

5. Aircraft Nuclear Propulsion Project Quarterly Progress Report for Period Ending August 31, 1950, ORNL-858.